II. NUCLEAR STRUCTURE AND DYNAMICS

CONTENTS

2

INTRODUCTION

The development of particle theory at BLTP in the years 2011-2012 continued the earlier tendencies and established the established new lines of investigations, following modern theoretical and experimental trends. About 300 papers were published and about 50 conference talks were presented. The investigations combined the responses to the challenges raised by current or planned experiment problems as well as the development and improvement of theory methods.

The latter is the subject of the contribution of A.V.Bednyakov and A.F.Pikelner who performed consistent three-loop calculations of all Standard Model beta-functions which allowed one to confirm the calculations of other groups2 and obtain for the first time the results for Yukawa couplings.

The contribution of D.I. Kazakov in collaboration with W.de Boer, C.Beskidt, F.Ratnikov deals with the constraints for Supersymmetry exploring the most complete set of experimental data. Combining the limits from the direct searches at the LHC, heavy flavor constraints, WMAP and XENON100 one can exclude values of $m_{1/2}$ below 525GeV in the CMSSM for $m_0 < 1500$GeV, which implies a lower limit on the WIMP mass of 230 GeV and a gluino mass of 1370GeV, respectively.

The contribution of V.A. Naumov contains a brief review of solar neutrino physics with special emphasis on the Sun and Solar system chemical composition.

The contribution of A.V. Kotikov in collaboration with P. Bolzoni and B.A. Kniehl describes the new approach to the description of gluon and quark jet multiplicities in QCD. Inclusion of all the corrections up to the order s3/2, allowed explaining the discrepancy of the results with the data obtained earlier.

The contribution of A.B. Arbuzov, A. I. Ahmadov, Yu. M. Bystritskiy, V. V. Bytev and E. A. Kuraev describes the calculations of a new process and radiative corrections for the modern and planned collider experiments and Dark Matter searches, with special emphasis on peripheral processes at the LHC, physics at BESIII and PANDA, and two-loop radiative corrections to Moller scattering.

The contribution of H.P. Pavel is dedicated to the formulation of the Hamiltonian approach to QCD in terms of gauge invariant observables. The energy spectra of gluonium and hybrid states are calculated using the variational approach.

The contribution of Ya.N.Klopot, A.G. Oganesian, S.V. Mikhailov and O.V. Teryaev is dedicated to the description of recent data for pion transition form factor within various approaches. While QCD factorization clearly supports the BELLE data, the Anomaly Sum Rule method allows for non-perturbative QCD correction supported by BaBaR data and not excluded by the BELLE ones.

The contribution of S.V. Goloskokov is devoted to the description of spin effects in exclusive meson production in the framework of the Generalized Parton Distributions. It is stressed that a special role is played by the non-forward generalization of transversity parton distribution, describing the transverse polarized quarks in a transverse polatized proton.

The contribution of I.V. Anikin and O.V. Teryaev compares the manifestations of twist 3 in inclusive (Drell-Yan) and exclusive (Deeply Virtual Compton Scattering off deuteron) processes with special emphasis on the electromagnetic gauge invariance. The

expressions for hadronic tensors were obtained and the factor 2 correction for the Drell-Yan process was found.

The hadronic light-by-light scattering contribution to muon Anomalous Magnetic Moment is considered by A.E. Dorokhov in collaboration with A.E. Radzhabov and A.S. Zhevlakov . The pseudoscalar meson contributions within the non-local quark model with full kinematic dependence are systematically lower than the results obtained in other works.

The contribution of M.K. Volkov is dedicated to the applications of the Nambu-Iona-Lasiniio (NJL) model in the fields of hadronic and heavy ion physics. The systematic calculation of the tau-lepton decay rates to various hadronic states was performed. Also, it was shown that the Polyakov loop effect may significantly change the influence of hadronic medium on the mesonic properties.

Another application of the NJL model to the physics of heavy-ion collisions is represented in the analysis of the properties of quantum liquids in the contribution of S.V. Molodtsov in collaboration with G.M. Zinovjev.

The advances in heavy quarkonia spectroscopy are considered in the contribution of M.A. Ivanov, where the analysis in the covariant quark confinement model allowed one to identify X(3872) meson as a tetraquark bound state.

The hadron spectroscopy is also the subject of the contribution of Yu.S. Surovtsev and M. Nagy who performed the extensive model-independent analysis of the scalar-isoscalar meson states which provided complete information on their nature compatible with other theoretical and experimental works.

The contribution of V.I. Korobov is dedicated to the high-precision atomic spectroscopy being a necessary ingredient of the processing of CERN new very accurate data on antiproton-to-electron mass ratio. The new procedure of evaluating the non-relativistic Bethe logarithm was developed and more accurate data were obtained.

<div style="text-align: right">

D. I. Kazakov

O. V. Teryaev

</div>

Twist three in inclusive (DY) and exclusive (DVCS) processes

I.V. Anikin, O.V. Teryaev

Bogoliubov Laboratory of Theoretical Physics, JINR, 141980 Dubna, Russia

Abstract

We study the effects of twist three in the Drell-Yan and deeply virtual Compton scattering processes. As the first item, we explore the electromagnetic gauge invariance of the hadron tensor of the Drell-Yan process with one transversely polarized hadron. Due to the special role of the contour gauge for gluon fields, the prescription for the gluonic pole in the twist 3 correlator can be related to the causality prescriptions for exclusive hard processes. Because of this, we find extra contributions which naively do not have an imaginary phase. The single spin asymmetry for the Drell-Yan process is accordingly enhanced by the factor of two. Then, we study the deeply virtual Compton scattering off a spin-one particle, as the case for the coherent scattering off a deuteron target. We extend our approach, formulated initially for a spinless case, and discuss the role of twist three contributions for restoring the gauge invariance of the amplitude. Using twist three contributions and relations, which emanate from the QCD equations of motion, we derive the gauge invariant amplitude for the deeply virtual Compton scattering (DVCS) off hadrons with spin 1. Using the derived gauge invariant amplitude, the single spin asymmetry is discussed.

1 Introduction

The problem of the electromagnetic gauge invariance in the deeply virtual Compton scattering (DVCS) and similar exclusive processes has intensively been discussed during last few years, see for example, see e.g. [1]. Here we combine the different approaches [1, 2] to apply them in the relevant case of the Drell-Yan (DY) process where one of hadrons is the transversally polarized nucleon. The source of the imaginary part, when one calculates the single spin asymmetry associated with the DY process, is the quark propagator in the diagrams with quark-gluon (twist three) correlators. This leads to the gluonic pole contribution to SSA. The reason is that these boundary conditions provide the purely real quark-gluon function $B^V(x_1, x_2)$ which parameterizes $\langle \bar{\psi} \gamma^+ A_\alpha^T \psi \rangle$ matrix element. By this fact the diagrams with two-particle correlators do not contribute to the imaginary part of the hadron tensor related to SSA. In our paper, we perform a thorough analysis of the transverse polarized DY hadron tensor in the light of the QED gauge invariance, the causality and gluonic pole contributions. We show that, in contrast to the naive assumption, our new-found additional contribution is directly related to a certain complex prescription in the gluonic pole $1/(x_1 - x_2)$ of the quark-gluon function $B^V(x_1, x_2)$. Finally, the account for these extra contributions corrects the SSA formula for the transverse polarized Drell-Yan process by a factor of 2. Note that our analysis is also important in view of the recent investigation of DY process within both the collinear and the transverse-momentum factorization schemes with hadrons replaced by on-shell parton states.

Deeply virtual Compton scattering (DVCS) off the deuteron target has recently attracted much attention from the experimental point of view. One of the main reasons of this interest is the fact that the DVCS process gives information about the generalized parton distributions (GPDs). From the theoretical point of view, the leading twist-2 GPDs for the deuteron were studied in. However, the leading twist-2 accuracy for the DVCS amplitude, calculated in the case where the final deuteron gets a significant transverse momentum, is not sufficient for the study of these processes. This is due to the fact that in the essential case of sizable transverse transfer momentum, $\Delta_T \neq 0$, the leading twist-2 approximation, in the Bjorken limit, is not sufficient for the photon gauge invariance of the DVCS amplitude. Besides, the relevant terms are proportional to the transverse component of the momentum transfer and provide the leading contribution to some observables.

Extending the Ellis-Furmanski-Petronzio-Efremov-Teryaev (EFPET) approach to the non-forward case, this problem was first solved in [1] where it was demonstrated how the inclusion of twist-3 contributions related to the matrix elements of quark-antiquark-gluon operators, can restore the gauge invariance of the DVCS amplitude off a (pseudo)scalar particle (e.g. pion, He^4). Then, the main ideas of [1] were used and generalized to the nucleon target. In our papers, we adhere to the approach [1, 2] and make comprehensive analysis of the twist three contributions to the DVCS amplitude off a spin-1 hadron.

2 Asymmetries associated with higher twists: gauge invariance, gluonic poles and twist three

Causality and contour gauge for the gluonic pole. We study the contribution to the hadron tensor which is related to the single spin (left-right) asymmetry measured in the Drell-Yan process with the transversely polarized nucleon. The DY process with the transversely polarized target manifests the gluonic pole contributions. Since we perform our calculations within a *collinear* factorization, it is convenient to fix the dominant light-cone directions for the DY process shown in Fig. 1 $p_1 \approx Qn^{*+}/(x_B\sqrt{2})$, $p_2 \approx Qn^-/(y_B\sqrt{2})$. Focusing on the Dirac vector projection, containing the gluonic pole, let us start with the standard hadron tensor generated by the diagram depicted on Fig. 1(a):

$$\mathcal{W}_{\mu\nu}^{(1)} = \int d^4k_1\, d^4k_2\, \delta^{(4)}(k_1 + k_2 - q) \int d^4\ell\, \Phi_\alpha^{(A)\,[\gamma^+]}\, \bar{\Phi}^{[\gamma^-]} \text{tr}\left[\gamma_\mu \gamma^- \gamma_\nu \gamma^+ \gamma_\alpha \frac{\ell^+\gamma^- - k_2^-\gamma^+ - \ell_T\gamma_T}{-2\ell^+k_2^- - \ell_T^2 + i\epsilon}\right], \quad (1)$$

where $\Phi_\alpha^{(A)\,[\gamma^+]}$ and $\bar{\Phi}^{[\gamma^-]}$ are defined as in [3, 4, 5]. Analyzing the γ-structure, *i.e* $\gamma^+\gamma^\alpha\gamma^\pm$ in the trace, we may conclude that (i) the $\ell^+\gamma^-$ term singles out $\gamma^+\gamma^\alpha\gamma^-$ with $\alpha = T$ which will lead to $\langle\bar\psi\gamma^+A_\alpha^T\psi\rangle$ giving the contribution to SSA; (ii) the $k_2^-\gamma^+$ term separates out $\gamma^+\gamma^\alpha\gamma^+$ with $\alpha = -$. Therefore, this term will give $\langle\bar\psi\,\gamma^+A^+\psi\rangle$ which will be exponentiated in the Wilson line $[-\infty^-,\, 0^-]$; (iii) the $\ell_T\gamma_T$ term separates out $\gamma^+\gamma^\alpha\gamma_T$ with $\alpha = T$ and, then, will be exponentiated in the Wilson line $[-\infty^-, -\infty_T\,;\, -\infty^-, 0_T]$.

To eliminate the unphysical gluons from our consideration and use the factorization scheme, we may choose a *contour* gauge $[-\infty^-,\, 0^-] = 1$ which actually implies also the axial gauge $A^+ = 0$ used in. Imposing this gauge one arrives at the following representation

of the gluon field in terms of the strength tensor:

$$A^\mu(z) = \int\limits_{-\infty}^{\infty} d\omega^- \theta(z^- - \omega^-) G^{+\mu}(\omega^-) + A^\mu(-\infty) \,. \tag{2}$$

Moreover, if we choose instead an alternative representation for the gluon in the form with $A^\mu(\infty)$, keeping the causal prescription $+i\epsilon$ in (1), the cost of this will be the breaking of the electromagnetic gauge invariance for the DY tensor. Consider now the term with $\ell^+ \gamma^-$ in (1) which gives us finally the matrix element of the twist 3 operator with the transverse gluon field. The parametrization of the relevant matrix elements is

$$\langle p_1, S^T | \bar\psi(\lambda_1 \tilde n) \, \gamma_\beta \, g A_\alpha^T(\lambda_2 \tilde n) \, \psi(0) | S^T, p_1 \rangle \overset{\mathcal{F}_2^{-1}}{=} i\varepsilon_{\beta\alpha S^T p_1} \, B^V(x_1, x_2) \,. \tag{3}$$

Using the representation (2), this function can be expressed as

$$B^V(x_1, x_2) = \frac{T(x_1, x_2)}{x_1 - x_2 + i\epsilon} + \delta(x_1 - x_2) B_{A(-\infty)}^V(x_1) \,, \tag{4}$$

where the real regular function $T(x_1, x_2)$ ($T(x, x) \neq 0$) parametrizes the vector matrix element of the operator involving the tensor $G_{\mu\nu}$:

$$\langle p_1, S^T | \bar\psi(\lambda_1 \tilde n) \, \gamma_\beta \, g \tilde n_\nu G_{\nu\alpha}(\lambda_2 \tilde n) \, \psi(0) | S^T, p_1 \rangle \overset{\mathcal{F}_2^{-1}}{=} \varepsilon_{\beta\alpha S^T p_1} \, T(x_1, x_2) \,. \tag{5}$$

Owing to the time-reversal invariance, the function $B_{A(-\infty)}^V(x_1)$,

$$i\varepsilon_{\beta\alpha S^T p_1} \delta(x_1 - x_2) B_{A(\pm\infty)}^V(x_1) \overset{\mathcal{F}}{=} \langle p_1, S^T | \bar\psi(\lambda_1 \tilde n) \, \gamma_\beta \, g A_\alpha^T(\pm\infty) \, \psi(0) | S^T, p_1 \rangle \,, \tag{6}$$

can be chosen as $B_{A(-\infty)}^V(x) = 0$. Indeed, the function $B^V(x_1, x_2)$ is an antisymmetric function of its arguments, while the anti-symmetrization of the additional term with $B_{A(-\infty)}^V(x_1)$ gives zero. If the only source of the imaginary part of the hadron tensor is the quark propagator, one may realize this property by assumption: $B^V(x_1, x_2) = T(x_1, x_2)\mathcal{P}/(x_1 - x_2)$ corresponding to the asymmetric boundary condition for gluons: $B_{A(\infty)}^V(x) = -B_{A(-\infty)}^V(x)$. Here we suggest another way of reasoning. The causal prescription for the quark propagator, generating its imaginary part, simultaneously leads to the imaginary part of the gluonic pole. We emphasize that this does not mean the appearance of the imaginary part of the matrix element but rather the prescription of its convolution with the hard part. Note that the fixed complex prescription $+i\epsilon$ in the gluonic pole of $B^V(x_1, x_2)$ is one of our main results and is very crucial for an extra contribution to hadron tensor we are now ready to explore. Indeed, the gauge condition must be the same for all the diagrams, and it leads to the appearance of an imaginary phase of the diagram (see, Fig. 1(b)) which naively does not have it. Let us confirm this by explicit calculation.

Hadron tensor and gauge invariance. We now return to the hadron tensor and calculate the part involving $\ell^+ \gamma^-$, obtaining the following expression for the standard hadron tensor (see, the diagram on Fig. 1(a)):

$$\overline{\mathcal{W}}_{\mu\nu}^{(1)\,[\ell^+]} = -\bar q(y_B) \mathrm{Imm} \int dx_2 \, \mathrm{tr}\left[\gamma_\mu \gamma_\beta \gamma_\nu \hat p_2 \gamma_\alpha^T \frac{(x_B - x_2)\hat p_1}{(x_B - x_2)ys + i\epsilon} \right] B^V(x_B, x_2) \, \varepsilon_{\beta\alpha S^T p_1} \,. \tag{7}$$
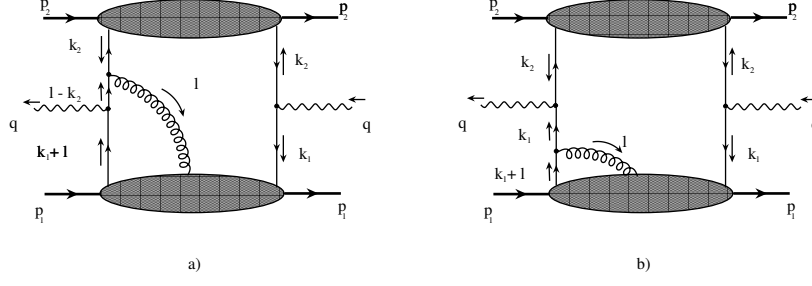
Figure 1: The Feynman diagrams which contribute to the polarized Drell-Yan hadron tensor.

We are now in position to check the QED gauge invariance by contraction with the photon momentum q_μ. Calculating the trace, one gets $q_\mu \overline{\mathcal{W}}_{\mu\nu}^{(1)} \neq 0$ if the gluonic pole is present. We now focus on the contribution from the diagram depicted on Fig. 1(b). Performing the collinear factorization, we derive the expression for the factorized hadron tensor which corresponds to the diagram on Fig. 1(b):

$$\overline{\mathcal{W}}_{\mu\nu}^{(2)} = \int dx_1\, dy \left[\delta(x_1 - x_B)\delta(y - y_B) \right] \bar{q}(y) \operatorname{tr}\left[\gamma_\mu \left(\int d^4k_1\, \delta(x_1 p_1^+ - k_1^+) \mathcal{F}(k_1) \right) \gamma_\nu \hat{p}_2 \right], \quad (8)$$

where the function $\mathcal{F}(k_1)$ reads

$$\mathcal{F}(k_1) = S(k_1)\gamma_\alpha \int d^4\eta_1\, e^{-ik_1 \cdot \eta_1} \langle p_1, S^T | \bar{\psi}(\eta_1)\, g A_\alpha^T(0)\, \psi(0) | S^T, p_1 \rangle. \quad (9)$$

After some algebra we obtain

$$q_\mu \overline{\mathcal{W}}_{\mu\nu}^{(2)} = \int dx_1\, dy \left[\delta(x_1 - x_B)\delta(y - y_B) \right] \bar{q}(y)\, \varepsilon_{\nu p_2 S^T p_1} \int_{-1}^{1} dx_2\, \operatorname{Im}m\, B^V(x_1, x_2). \quad (10)$$

If the function $B^V(x_1, x_2)$ is the purely real one, this part of the hadron tensor does not contribute to the imaginary part. We now study the $\overline{\mathcal{W}}_{\mu\nu}^{(1)}$ and $\overline{\mathcal{W}}_{\mu\nu}^{(2)}$ contributions and their role for the QED gauge invariance. One can easily obtain:

$$q_\mu \overline{\mathcal{W}}_{\mu\nu}^{(1)} + q_\mu \overline{\mathcal{W}}_{\mu\nu}^{(2)} = \varepsilon_{\nu p_2 S^T p_1}\, \bar{q}(y_B)\, \operatorname{Im}m \int_{-1}^{1} dx_2\, B^V(x_B, x_2) \left[\frac{x_B - x_2}{x_B - x_2 + i\epsilon} - 1 \right]. \quad (11)$$

Assuming that the gluonic pole in $B^V(x_1, x_2)$ exists, after inserting (4) into (11), one gets $q_\mu \overline{\mathcal{W}}_{\mu\nu}^{(1)} + q_\mu \overline{\mathcal{W}}_{\mu\nu}^{(2)} = 0$. This is nothing else than the QED gauge invariance for the imaginary part of the hadron tensor. We can see that the gauge invariance takes place only if the prescriptions in the gluonic pole and in the quark propagator of the hard part coincide. As we have shown, only the sum of two contributions represented by the diagrams on Fig. 1(a) and (b) can ensure the electromagnetic gauge invariance. We now inspect the influence of a "new" contribution 1(b) on the single spin asymmetry

8

and obtain the QED gauge invariant expression for the hadron tensor. It reads $\overline{\mathcal{W}}_{\mu\nu}^{GI} = \overline{\mathcal{W}}_{\mu\nu}^{(1)} + \overline{\mathcal{W}}_{\mu\nu}^{(2)} = -\frac{2}{q^2}\,\varepsilon_{\nu S^T p_1 p_2}\left[x_B\,p_{1\,\mu} - y_B\,p_{2\,\mu}\right]\bar{q}(y_B)\,T(x_B, x_B)$. Within the lepton c.m. system, the SSA related to the gauge invariant hadron tensor reads

$$\mathcal{A}^{SSA} = 2\,\frac{\cos\phi\,\sin 2\theta\,T(x_B, x_B)}{M(1 + \cos^2\theta)q(x_B)}, \tag{12}$$

where M is the dilepton mass. We want to emphasize that this differs by a factor of 2 in comparison with the case where only one diagram, presented on Fig. 1(a), has been included in the (gauge non-invariant) hadron tensor. Therefore, from a practical point of view, the neglect of the diagram on Fig. 1(b) or, in other words, the use of the QED gauge non-invariant hadron tensor yields the error of a factor of two.

3   Gauge invariance of DVCS off an arbitrary spin hadron: the deuteron target case

Kinematics and Approximations Let us start with the discussion of the kinematics and approximations which we use in this paper. The process we consider is $\gamma^*(q) + D(p_1) \to \gamma(q') + D(p_2)$. Here, we mainly focus on the deuteron as a target but all our approach is suitable for any spin-one hadron target. This process is a hard exclusive reaction for which a QCD factorization theorem applies. In this case, the virtuality of the initial off-shell photon is used as the large scale, i.e. $q^2 = -Q^2 \to \infty$, while the final photon is on-shell with $q'^2 = 0$. Besides, this asymptotic regime is identical to the light-cone formalism. Therefore, we first introduce a light-cone basis which is constructed by the "plus" and "minus" vectors: $n^\star = \Lambda(1,\,0,\,0,\,1)\,, n = \frac{1}{2\Lambda}(1,\,0,\,0,\,-1)\,, n^\star \cdot n = 1$, where Λ is an arbitrary and dimensionful constant which can be expressed via the Lorentz invariants. The exact form of Λ as a function of invariants depends on the frame which one works in.

In the present paper, we consider the DVCS amplitude up to the twist three accuracy, discarding the contributions associated with the twist four and higher. Such a constraint imposes the following relations for the hadron average and transfer momenta : $P = \frac{p_1 + p_2}{2} = n^\star + \frac{\bar{M}^2}{2}n \approx n^\star$, $\Delta = p_2 - p_1 \approx -2\xi P + \Delta^T$. Notice that keeping the $\bar{M}^2$-term in the Sudakov decomposition of the relative momentum P leads to the necessity to include the twist four contributions as well, which goes beyond the scope of the present paper. Since corrections of the order $O(\Delta_T^2/Q^2)$ demand a special care, at this moment, we postpone their study until a forthcoming paper. It is also instructive to introduce the photon average momentum: $Q = (q + q')/2$. One has to emphasize that the approximations discussed in this section do not affect the generality of our study and can be applied to a study of arbitrary spin hadrons.

Factorization and the gauge invariant amplitude The factorization procedure, which we follow, is presented in detail in [1, 2, 6]. Within this approach, we derive the gauge invariant DVCS amplitude for the deuteron target:

$$T_{\mu\nu}^{(\lambda_1, \lambda_2)} = \frac{1}{2P \cdot \bar{Q}} \int dx \frac{1}{x - \xi + i\epsilon}\left(\mathcal{T}_{\mu\nu}^{(1)} + \mathcal{T}_{\mu\nu}^{(2)} + \mathcal{T}_{\mu\nu}^{(3)} + \mathcal{T}_{\mu\nu}^{(4)}\right)^{(\lambda_1, \lambda_2)} + O(\Delta_T^2; \bar{M}^2) + \text{"crossed"}, \tag{13}$$

where the structure amplitudes $\mathcal{T}_{\mu\nu}^{(k)}$ read

$$\mathcal{T}_{\mu\nu}^{(1)} = H_{1,..,4}^{V}(x; e_1, e_2^*) \left(2\xi P_\mu P_\nu + P_\mu \bar{Q}_\nu + P_\nu \bar{Q}_\mu - g_{\mu\nu}(P \cdot \bar{Q}) + \frac{1}{2} P_\mu \Delta_\nu^T - \frac{1}{2} P_\nu \Delta_\mu^T \right) +$$

$$G_{1,..,4}^{V}(x; e_1, e_2^*) \left(\xi P_\nu \Delta_\mu^T + 3\xi P_\mu \Delta_\nu^T + \Delta_\mu^T \bar{Q}_\nu + \Delta_\nu^T \bar{Q}_\mu \right)$$

$$-\left(\frac{(e_2^* \cdot P)(e_1 \cdot P)}{M^2} G_5^A(x) + (e_2^* \cdot P)(e_1 \cdot n) G_6^A(x) + (e_1 \cdot P)(e_2^* \cdot n) \left(G_7^A(x) - G_8^A(x) \right) \right)$$

$$\left(3\xi P_\mu \Delta_\nu^T - \xi P_\nu \Delta_\mu^T - \Delta_\mu^T \bar{Q}_\nu + \Delta_\nu^T \bar{Q}_\mu \right), \tag{14}$$

and

$$\mathcal{T}_{\mu\nu}^{(2)} = (e_1 \cdot P) G_6^V(x) \left(\xi P_\nu e_{2\,\mu}^{*T} + 3\xi P_\mu e_{2\,\nu}^{*T} + e_{2\,\mu}^{*T} \bar{Q}_\nu + e_{2\,\nu}^{*T} \bar{Q}_\mu \right) + (e_1 \cdot P) G_2^A(x) \left(3\xi P_\mu e_{2\,\nu}^{*T} - \xi P_\nu e_{2\,\mu}^{*T} \right.$$

$$\left. - e_{2\,\mu}^{*T} \bar{Q}_\nu + e_{2\,\nu}^{*T} \bar{Q}_\mu \right), \tag{15}$$

and

$$\mathcal{T}_{\mu\nu}^{(3)} = (e_2^* \cdot P) G_7^V(x) \left(\xi P_\nu e_{1\,\mu}^{T} + 3\xi P_\mu e_{1\,\nu}^{T} + e_{1\,\mu}^{T} \bar{Q}_\nu + e_{1\,\nu}^{T} \bar{Q}_\mu \right) + (e_2^* \cdot P) G_1^A(x) \left(3\xi P_\mu e_{1\,\nu}^{T} - \xi P_\nu e_{1\,\mu}^{T} \right.$$

$$\left. - e_{1\,\mu}^{T} \bar{Q}_\nu + e_{1\,\nu}^{T} \bar{Q}_\mu \right), \tag{16}$$

and

$$\mathcal{T}_{\mu\nu}^{(4)} = \varepsilon_{\mu\nu Pn} \left(\varepsilon_{nPe_2^*Te_1^T} H_1^A(x, \xi) + \frac{1}{M^2} \varepsilon_{nP\Delta^Te_2^T}(e_1 \cdot P) H_2^A(x, \xi) + \frac{1}{M^2} \varepsilon_{nP\Delta^Te_1^T}(e_2^* \cdot P) H_3^A(x, \xi) \right.$$

$$\left. + \varepsilon_{nP\Delta^Te_2^{*T}}(e_1 \cdot n) H_4^A(x, \xi) \right). \tag{17}$$

This gauge invariant amplitude for the DVCS off deuteron is our main result. For the sake of brevity, in Eqs. (14) – (16), we neglected all terms which are proportional to the square of the hadron mass. The full expressions for all amplitudes will be presented in our forthcoming study.

Single Spin Asymmetry In the preceding section, we have obtained the gauge invariant DVCS amplitude which has a significant meaning for the investigation of any observables. As a phenomenologically important example, we now consider the single (electron) spin asymmetry (SSA), which arises in collision of the longitudinally polarized electron beams with an unpolarized hadron target. The SSA parameter is defined as

$$\mathcal{A}_L = \frac{d\sigma(\rightarrow) - d\sigma(\leftarrow)}{d\sigma(\rightarrow) + d\sigma(\leftarrow)}. \tag{18}$$

The numerator of Eq. (18) can be expressed through the imaginary part, first, of the interference between the twist-2 and twist-3 helicity DVCS amplitudes and, second, of the interference between the Bethe-Heitler (BH) and DVCS amplitudes. For the JLAB kinematics, the $|\mathcal{A}_{\mathrm{DVCS}}|^2$ contribution can be neglected compared to the interference term because of a large contribution of the BH amplitude.

The DVCS amplitude contributing to exclusive real photon production at $Q^2 \gg M^2$ for the real and virtual photon polarizations, i and j, reads

$$\mathcal{A}_{\mathrm{DVCS}}^{(i)} = \frac{e_\ell e_q^2}{q^2} \sum_j L^{(j)} \mathcal{A}_{(j,i)} \,, \ L^{(j)} = \mathcal{L}_{\mu'}(\ell_1, \ell_2) \epsilon_{\mu'}^{*\,(j)} \,,$$

respectively. Here, the helicity amplitude is given by

$$\mathcal{A}_{(j,i)} = \epsilon_\mu^{(j)} T_{\mu\nu} \epsilon_\nu'^{*(i)}, \quad i = \pm 1, \quad j = 0, \pm 1 \,. \tag{19}$$

The Bethe-Heitler amplitude reads

$$\mathcal{A}_{BH}^{(i)} = \frac{e_\ell e_q^2}{\Delta^2} \sum_j \Lambda^{(j,i)} \mathcal{T}_{(j)}, \quad \mathcal{T}_{(j)} = \epsilon_\mu^{(j)} F_\mu \,, \Lambda^{(j,i)} = L_{\mu'\nu'}(\ell_1, \ell_2) \epsilon_{\mu'}^{*\,(j)} \epsilon_{\nu'}'^{*(i)} \,,$$

where $\Delta^2 = -4\xi^2 \bar{M}^2 + \Delta_T^2 \equiv t$ with a negative t. The explicit and very cumbersome expression for the contribution of $\mathcal{A}_{\mathrm{BH}}^* \mathcal{A}_{\mathrm{DVCS}}$ coming from the interference between Eqs. (19) and (20) can be found in [6]. Notice that the only surviving contributions in the forward limit are related to the Compton form factors $\mathcal{H}_{1,5}$ and $\mathcal{G}_{8,9}$ terms. Keeping only these contributions one can write

$$\frac{1}{q^2 \Delta^2} \sum_i [L^{(0)} \mathcal{A}_{(0,i)}] \cdot [\Lambda^{(+,i)} \mathcal{T}_{(+)}]^* \sim \frac{1}{\xi(\rho - 4)\rho} \times$$

$$\Big\{ G_1 (16\xi(\xi^2(\rho - 4) - \rho)(\rho - 4)(\xi(\rho - 6) + \rho - 2)\mathcal{G}_8^V + 16\xi(\xi(\rho - 6) - \rho + 2)(\xi^2(\rho - 4) - \rho)(\rho - 4)\mathcal{G}_9^V$$

$$-8(\xi^2(\rho - 4) - \rho)(\rho - 4)((\rho - 4)\rho + 12)\mathcal{H}_1^V - 16((\rho - 6)\xi^2 - \rho - 2)(\xi^2(\rho - 4) - \rho)(\rho - 4)\mathcal{H}_5^V)$$

$$+ G_2(-16\xi(\rho - 4)((\rho - 4)^2\xi^3 + (\rho - 4)(\rho + 2)\xi^2 - (\rho - 8)\rho\xi - (\rho - 2)\rho)\mathcal{G}_8^V - 16\xi(\rho - 4)((\rho - 4)^2\xi^3$$

$$-(\rho - 4)(\rho + 2)\xi^2 - (\rho - 8)\rho\xi + (\rho - 2)\rho)\mathcal{G}_9^V + 8(\xi^2(\rho - 4) - \rho)\rho((\rho - 6)\rho + 8)\mathcal{H}_1^V$$

$$+16(\rho - 4)(\rho - \xi^2(\rho - 4))^2\mathcal{H}_5^V) + G_3(16\xi(\xi^2(\rho - 4) - \rho)(\rho - 4)(\xi(\rho - 4) + \rho)\mathcal{G}_8^V$$

$$+16\xi(\xi(\rho - 4) - \rho)(\xi^2(\rho - 4) - \rho)(\rho - 4)\mathcal{G}_9^V - 8(\xi^2(\rho - 4) - \rho)\rho((\rho - 6)\rho + 8)\mathcal{H}_1^V - 16((\rho - 4)^3\xi^4$$

$$-2\rho((\rho - 6)\rho + 8)\xi^2 + \rho^3)\mathcal{H}_5^V) \Big\} + \ldots \,.$$

If we now calculate the imaginary part of the above-mentioned terms, we will obtain the numerator for experimentally accessible single spin asymmetry parameter.

4   Conclusions

Thus, we showed that it is mandatory to include a contribution of an extra diagram which naively does not have an imaginary part. The account for this extra contribution

leads to the amplification of SSA by a factor of 2. This additional contribution emanates from the complex gluonic pole prescription in the representation of the twist 3 correlator $B^V(x_1, x_2)$ which, in its turn, is directly related to the complex pole prescription in the quark propagator forming the hard part of the corresponding hadron tensor. The causal prescription in the quark propagator, involved in the hard part of the diagram on Fig.1(a), selects from the physical axial gauges the contour gauge. We argued that, in addition to the electromagnetic gauge invariance, the inclusion of new-found contributions corrects by a factor of 2 the expression for SSA in the transverse polarized Drell-Yan process. We proved that the complex prescription in the quark propagator forming the hard part of the hadron tensor, the starting point in the contour gauge, the fixed representation of $B^V(x_1, x_2)$ and the electromagnetic gauge invariance of the hadron tensor must be considered together as deeply related items.

Working with the DVCS process, we have derived the gauge invariant amplitude for the deeply virtual Compton scattering off a spin-1 hadron. As an important phenomenological application of this approach, we have considered the deuteron target and have presented the gauge invariant DVCS amplitude for the deuteron case. We have also discussed the simplest kind of asymmetries – the single spin asymmetry where the initial lepton has longitudinal polarization while all other particles, the initial hadron, the final lepton and the final hadron, are unpolarized.

[1] I. V. Anikin, B. Pire and O. V. Teryaev, "On the gauge invariance of the DVCS amplitude," Phys. Rev. D **62** (2000) 071501;

[2] I. V. Anikin, A. Besse, D. Y. .Ivanov, B. Pire, L. Szymanowski and S. Wallon, "A phenomenological study of helicity amplitudes of high energy exclusive leptoproduction of the rho meson," Phys. Rev. D **84** (2011) 054004;

[3] I. V. Anikin and O. V. Teryaev, "Gauge invariance, gluonic poles and single spin asymmetry in Drell-Yan processes," J. Phys. Conf. Ser. **295** (2011) 012057;

[4] I. V. Anikin and O. V. Teryaev, "Asymmetries associated with higher twists: gauge invariance, gluonic poles and twist three," [arXiv:1201.2569 [hep-ph]];

[5] I. V. Anikin and O. V. Teryaev, "Gauge invariance, causality and gluonic poles," Phys. Lett. B **690** (2010) 519 [arXiv:1003.1482 [hep-ph]];

[6] I. V. Anikin, R. S. Pasechnik, B. Pire and O. V. Teryaev, "Gauge Invariance of DVCS off an Arbitrary Spin Hadron: The Deuteron Target Case," Eur. Phys. J. C **72** (2012) 2055.

The meson-exchange induced light–by–light contribution to $(g-2)_\mu$ within the nonlocal chiral quark model

A. E. Dorokhov[a], A. E. Radzhabov[b], A. S. Zhevlakov[b]

[a]Bogoliubov Laboratory of Theoretical Physics, JINR, 141980 Dubna, Russia

[b]Institute for System Dynamics and Control Theory SB RAS, 664033 Irkutsk, Russia

The anomalous magnetic moment of the muon is known to an unprecedented accuracy. The latest result from the measurements of the Muon $(g-2)$ collaboration at Brookhaven is [1]

$$a_\mu^{\mathrm{BNL}} = 11\ 659\ 208.0\,(6.3) \cdot 10^{-10}, \tag{1}$$

which is a 0.54 ppm uncertainty over combined positive and negative muon measurements. Using e^+e^- annihilation and inclusive hadronic τ decay data the standard model predicts [2]

$$a_\mu^{SM} = \begin{cases} 11\ 659\ 180.2\,(4.9) \cdot 10^{-10}, & [e^+e^-], \\ 11\ 659\ 189.4\,(5.4) \cdot 10^{-10}, & [\tau]. \end{cases} \tag{2}$$

The difference between the experimental determination of a_μ and the standard model using the e^+e^- or τ data for the calculation of the hadronic vacuum polarization (HVP) contribution is 3.6σ and 2.4σ, respectively.

The standard model prediction for a_μ consists of quantum electrodynamics, weak and hadronic contributions. The QED and weak contributions to a_μ were calculated with great accuracy [5]

$$a_\mu^{\mathrm{QED}} = 11\ 658\ 471.8951(0.0080) \cdot 10^{-10} \tag{3}$$

and [6]

$$a_\mu^{\mathrm{EW}} = 15.4(0.2) \cdot 10^{-10}. \tag{4}$$
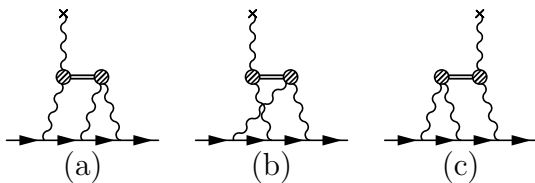
Figure 1: *Hadronic LbL scattering contribution due to quark-antiquark exchanges.*

The theoretical errors in (2) are dominated by the uncertainties induced by the HVP and LbL effects. Thus, to confront usefully theory with the experiment requires a better determination of the hadronic contributions. In the last decade, a substantial improvement in the accuracy of the contribution from the HVP was reached. It uses, essentially, precise determination of the low energy spectrum of the total $e^+e^- \to$ hadrons and inclusive τ lepton decay cross-sections. The HVP contributions at an order of α^2 quoted in the most recent articles on the subject are given in the Table.

Table.

Phenomenological estimates and references for the leading order HVP contribution to the muon anomalous magnetic moment are based on e^+e^- and τ data sets.

	e^+e^-[2]	τ[2]	e^+e^-[3]	e^+e^-[4]
$a_\mu^{\text{HVP (1)}} \cdot 10^{10}$	692.3 ± 4.2	701.5 ± 4.7	681.23 ± 4.51	694.91 ± 4.27

Figure 2: *LbL contribution to the muon AMM from the neutral pion and σ exchanges as a function of the dynamical quar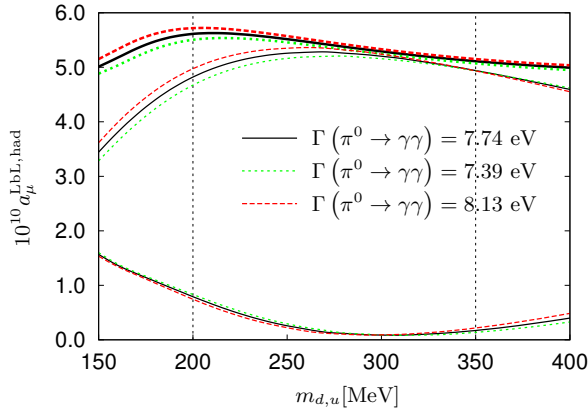k mass. Bunch of three lower lines correspond to the σ contribution, the π^0 contribution is in the middle, and the upper lines are the combined contribution.*

The higher-order contributions at $O(\alpha^3)$ level to $a_\mu^{\text{HVP (2)}}$ was estimated in [4],

$$a_\mu^{\text{HVP (2)}} = -9.84(0.07) \cdot 10^{-10}, \qquad (5)$$

by using analytical kernel functions and experimental data on the $e^+e^- \to$ hadron cross-section. In addition, there exists a $O(\alpha^3)$ contribution to a_μ from the LbL diagram, a_μ^{hLbL}, that cannot be expressed as a convolution of experimentally accessible observables and need to be estimated from theory. In some works [7], the value

$$a_\mu^{\text{hLbL}} = 10.5(2.6) \cdot 10^{-10} \qquad (6)$$

is considered as an estimate of the hadronic LbL contribution to the muon AMM.

Assuming the absence of New Physics effects, a phenomenological estimate of the total hadronic contributions to a_μ^{HVP} has to be compared with the value deduced from the $g-2$ experiment (1) and known electroweak (4) and QED (3) corrections

$$a_\mu^{\text{BNL}} - a_\mu^{\text{QED}} - a_\mu^{\text{EW}} = 721.6\,(6.3) \cdot 10^{-10}. \qquad (7)$$

Two new experiments on measurement of a_μ are proposed at Fermilab (E989)[8] and J-PARC[9] which plan to improve the experimental uncertainty by a factor of 4-5 with respect to the previous BNL experiment. In that respect theoretical predictions of the HVP and LbL contributions to the muon AMM should be at the same level or better than a precision of planed experiments. In the next part we discuss the hadronic LbL contribution as it is calculated within the nonlocal chiral quark model (NχQM) of low energy QCD and show that, within this framework, it might be possible realistically to determine this value to a sufficiently safe accuracy. We want to discuss how well this model does in calculating a_μ^{LbL}.

The uncertainties of the SM value for a_μ are dominated by the uncertainties of the hadronic contributions, a_μ^{Strong}, since their evaluation involve quantum chromodynamics (QCD) at long-distances for which perturbation theory cannot be employed. Below we discuss with some details theoretical status of hadronic LbL contribution to the muon AMM due to exchange by light mesons within NχQM.

Recently, the LbL contribution due to exchange of pseudoscalar (P) and scalar (S) mesons (Fig. 1) was elaborated in [10, 11, 12]. The vertices containing the virtual meson M with momentum p and two photons with momenta $q_{1,2}$ and the polarization vectors $\epsilon_{1,2}$ can be written as [13]

$$\mathcal{A}\left(\gamma^*_{(q_1,\epsilon_1)}\gamma^*_{(q_2,\epsilon_2)} \to M^*_{(p)}\right) = e^2\epsilon_1^\mu \epsilon_2^\nu \Delta_M^{\mu\nu}(p, q_1, q_2) \tag{8}$$

with

$$\Delta_P^{\mu\nu}(p, q_1, q_2) = -i\varepsilon_{\mu\nu\rho\sigma}q_1^\rho q_2^\sigma \mathrm{F}_P\left(p^2; q_1^2, q_2^2\right), \tag{9}$$

and

$$\Delta_S^{\mu\nu}(p, q_1, q_2) = \mathrm{A}_S\left(p^2; q_1^2, q_2^2\right) P_A^{\mu\nu}(q_1, q_2) + \mathrm{B'}_S(p^2; q_1^2, q_2^2) P_{B'}^{\mu\nu}(q_1, q_2), \tag{10}$$

where

$$P_A^{\mu\nu}(q_1, q_2) = \left(g^{\mu\nu}(q_1 q_2) - q_1^\nu q_2^\mu\right),$$
$$P_{B'}^{\mu\nu}(q_1, q_2) = \frac{\left(q_1^2 q_2^\mu - (q_1 q_2)q_1^\mu\right)\left(q_2^2 q_1^\nu - (q_1 q_2)q_2^\nu\right)}{(q_1 q_2)^2 - q_1^2 q_2^2},$$

and $p = q_1 + q_2$. The subject of model calculations are the (P/S)VV vertice functions $\mathrm{F}_P, \mathrm{A}_S, \mathrm{B'}_S$.

The expression for the LbL contribution to the muon AMM from the light meson exchanges can be written as

$$a_\mu^{\mathrm{LbL,M}} = -\frac{4\alpha^3}{3\pi^2}\int_0^\infty dQ_1^2 \int_0^\infty dQ_2^2 \int_{-1}^1 dt\sqrt{1-t^2}\frac{1}{Q_3^2}\sum_M\left[\frac{\mathcal{N}_1^M(Q_1^2, Q_2^2, Q_3^2)}{Q_2^2 + \mathrm{M}_M^2} + \frac{\mathcal{N}_2^M(Q_1^2, Q_3^2, Q_2^2)}{2(Q_3^2 + \mathrm{M}_M^2)}\right],$$
$$\mathcal{N}_{1,2}^P(Q_1^2, Q_2^2, Q_3^2) = \mathrm{F}_P\left(Q_2^2; Q_2^2, 0\right)\mathrm{F}_P\left(Q_2^2; Q_1^2, Q_3^2\right)\mathrm{Tp}_{1,2},$$
$$\mathcal{N}_{1,2}^S(Q_1^2, Q_2^2, Q_3^2) = \left(A\left(Q_2^2; Q_2^2, 0\right) + \frac{1}{2}B'\left(Q_2^2; Q_2^2, 0\right)\right)$$
$$\times\left(A\left(Q_2^2; Q_1^2, Q_3^2\right)\mathrm{Ts}_{1,2}^{\mathrm{AA}} + \frac{1}{2}B\left(Q_2^2; Q_1^2, Q_3^2\right)\mathrm{Ts}_{1,2}^{\mathrm{AB}}\right),$$

where $Q_3 = -(Q_1 + Q_2)$ and $B_S = \mathrm{B'}_S/((q_1 q_2)^2 - q_1^2 q_2^2)$. The kinematic factors Tp_i and Ts_i can be found in [14] and [12], respectively.

The total contribution of pseudoscalar (π^0, η, η') exchanges is estimated as

$$a_\mu^{\mathrm{LbL,PS}} = (5.85 \pm 0.87)\cdot 10^{-10}, \tag{11}$$

and the combined value for the scalar (σ, a_0, f_0) and pseudoscalar contributions is [12]

$$a_\mu^{\mathrm{LbL,PS+S}} = (6.25 \pm 0.83)\cdot 10^{-10}. \tag{12}$$

We found that within the NχQM the pseudoscalar meson contributions to the muon AMM are systematically lower than the results obtained in other works. The full kinematic dependence[1] of the vertices on the pion virtuality diminishes the result by about 20-30%

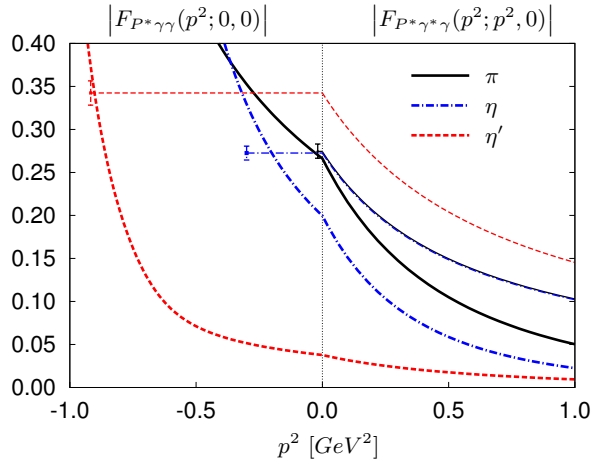[1]This dependence also recently studied in [15].

Figure 3: *Plots of the π^0, η and η' vertices $F_{P^*\gamma\gamma}(p^2; 0, 0)$ in the timelike region and $F_{P^*\gamma^*\gamma}(p^2; p^2, 0)$ in the spacelike region in $N\chi QM$ model (thick lines) and VMD model (thin lines). The points with error bars correspond to the physical points of the meson decays into two photons. The VMD curves for π^0 and η are almost indistinguishable.*

as compared to the case where this dependence is neglected. For η and η' mesons the results are reduced by a factor of about 3 in comparison with the results obtained in other models where the kinematic dependence was neglected (see Fig. 3 and discussion in [11, 12]). The scalar meson contribution is small positive and partially compensates model dependence of the pseudoscalar contribution (Fig. 2).

[1] G.W. Bennett, et al., Phys. Rev. **D73**, 072003 (2006).

[2] M. Davier, A. Hoecker, B. Malaescu and Z. Zhang, Eur. Phys. J. C **71** (2011) 1515 [Erratum-ibid. C **72** (2012) 1874] [arXiv:1010.4180 [hep-ph]].

[3] M. Benayoun, P. David, L. DelBuono and F. Jegerlehner, arXiv:1210.7184 [hep-ph].

[4] K. Hagiwara, R. Liao, A. D. Martin, D. Nomura and T. Teubner, J. Phys. G **38** (2011) 085003 [arXiv:1105.3149 [hep-ph]].

[5] T. Aoyama, M. Hayakawa, T. Kinoshita and M. Nio, Phys. Rev. Lett. **109** (2012) 111808 [arXiv:1205.5370 [hep-ph]].

[6] A. Czarnecki, W. J. Marciano and A. Vainshtein, Phys. Rev. D **67** (2003) 073006 [Erratum-ibid. D **73** (2006) 119901] [hep-ph/0212229].

[7] J. Prades, E. de Rafael and A. Vainshtein, (Advanced series on directions in high energy physics. 20) [arXiv:0901.0306 [hep-ph]].

[8] G. Venanzoni, Frascati Phys. Ser. **54** (2012) 52 [arXiv:1203.1501 [hep-ex]].

[9] N. Saito [J-PARC g-'2/EDM Collaboration], AIP Conf. Proc. **1467** (2012) 45.

[10] A. E. Dorokhov and W. Broniowski, Phys. Rev. D **78** (2008) 073011 [arXiv:0805.0760 [hep-ph]].

[11] A. E. Dorokhov, A. E. Radzhabov and A. S. Zhevlakov, Eur. Phys. J. C **71** (2011) 1702 [arXiv:1103.2042 [hep-ph]].

[12] A. E. Dorokhov, A. E. Radzhabov and A. S. Zhevlakov, Eur. Phys. J. C **72** (2012) 2227 [arXiv:1204.3729 [hep-ph]].

[13] E. Bartos, A. Z. Dubnickova, S. Dubnicka, E. A. Kuraev and E. Zemlyanaya, Nucl. Phys. B **632** (2002) 330 [hep-ph/0106084].

[14] M. Knecht and A. Nyffeler, Phys. Rev. D **65** (2002) 073034 [hep-ph/0111058].

[15] T. Goecke, C. S. Fischer and R. Williams, Phys. Rev. D **83** (2011) 094006 [Erratum-ibid. D **86** (2012) 099901] [arXiv:1012.3886 [hep-ph]].

TRANSVERSITY EFFECTS IN PSEUDOSCALAR MESON LEPTOPTODUCTION AT CLAS ENERGIES

S.V. Goloskokov

We investigate the pseudoscalar meson leptoproduction within the handbag approach where amplitudes factorize into a hard subprocesses and generalized parton distributions (GPDs). At leading-twist accuracy these reactions are only sensitive to the GPDs $\widetilde{H}$ and $\widetilde{E}$ which contribute to the amplitudes for longitudinally polarized virtual photons. Unfortunately, these terms are insufficient to describe experimental data at low Q^2 which require contributions from the transversity GPDs, in particular from H_T and $\bar{E}_T$. We can demonstrate this using the A_{UT} asymmetry in the π^+ leptoproduction [1] as an example. This asymmetry is expressed in terms of $M_{0-,++}$ and proton non-flip amplitude interference – $A_{UT}^{\sin(\phi_s)} \propto \text{Im}[M_{0-,++}^* M_{0+,0+}]$.
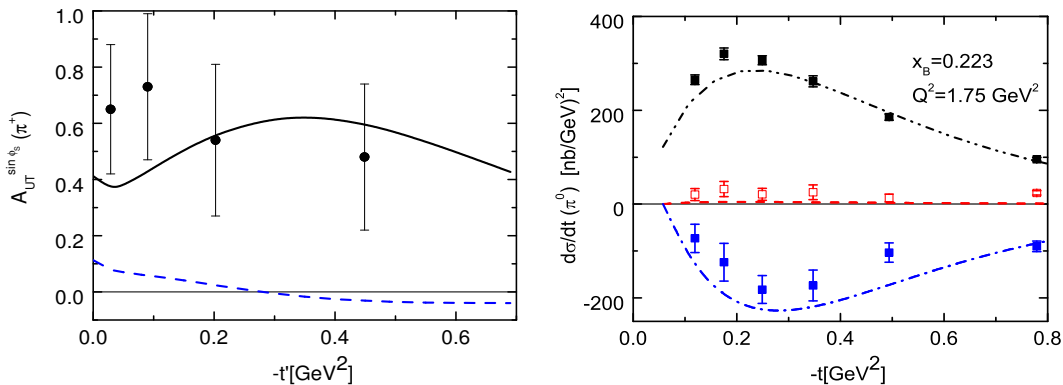

Figure 1: Left: A_{UT} asymmetry of the π^+ production at HERMES energies. Dashed line-results without transversity effects. Right: π^0 production in the CLAS energy range together with the data. Dashed-dot-dotted line- $\sigma = \sigma_T + \epsilon\sigma_L$, dashed line-$\sigma_{LT}$, dashed-dotted- σ_{TT}.

The leading twist contributions cannot explain this asymmetry –see Fig. 1 (left). A new twist-3 contribution to the $M_{0-,++}$ amplitude, which is not small at $t' \sim 0$, is needed. We estimate this contribution by the transversity GPD H_T in conjugation with the twist-3 pion wave function [2]. We have

$$M_{0-,\mu+}^{twist-3} \propto \int_{-1}^{1} d\overline{x} \mathcal{H}_{0-,\mu+}(\overline{x}, ...) H_T. \tag{1}$$

The H_T GPD is connected with transversity PDFs. The $M_{0+,++}$ amplitude is calculated in the same way and expressed in terms of $\bar{E}_T$ GPDs [2]. It is essential in analyses of spin effects in the pseudoscalar meson leptoproduction too.

In Fig 1 (right), we show our predictions for the π^0 production cross section $\sigma \sim \sigma_T$ in the CLAS energy range [3, 4] which is close to the experimental data [5]. We present in this plot the interference cross sections σ_{LT} and σ_{TT} too. The value of σ_{LT} is quite small, compatible with zero. The σ_{TT} cross section is negative and large. The $\bar{E}_T$ contributions to the σ_T and σ_{TT} cross sections are strongly correlated [2]. The fact that we describe

the CLAS data for both cross sections quite well can be an indication of observation of large transversity effects at CLAS. However, the definite conclusion on the importance of transversity effects in the π^0 cross section can be made only if the data on the separated σ_L and σ_T cross section will be available experimentally and σ_T will be much larger than σ_L. Probably, such study can be performed at JLAB12.
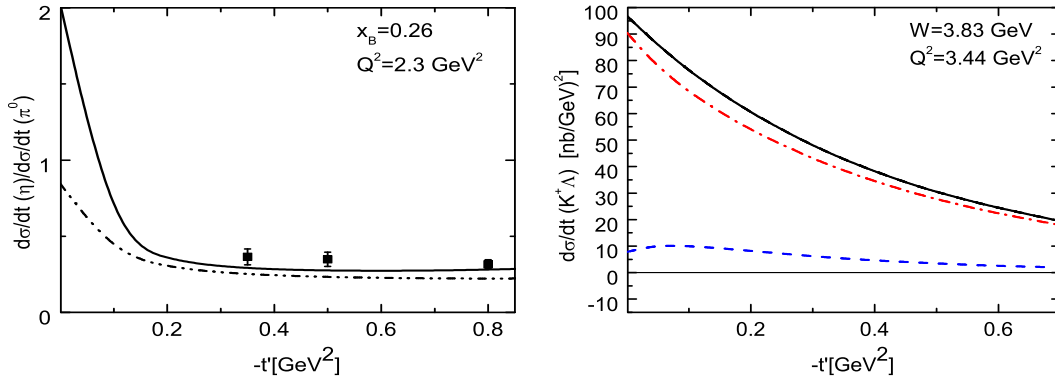

Figure 2: Left: η/π^0 production cross section ratio in the CLAS energy range together with preliminary data. Right: Prediction for the $K^+\Lambda$ production cross sections at HERMES energies. Full line- unseparated cross section, dashed- $d\sigma_L/dt$, dashed-dotted line- $d\sigma_T/dt$.

In Fig. 2 (left), we present the transversity effects in the ratio of the η/π^0 cross section [6] at CLAS energies. Different combinations of the quark contributions to these processes lead to the essential role of H_T effects in this ratio at small $-t < 0.2\text{GeV}^2$. At larger momentum transfer large E_T effects in the π^0 production found in the model lead to a rapid decrease of the η/π^0 cross section ratio with t- growing. At $-t > 0.2\text{GeV}^2$ this ratio becomes close to ~ 0.3, which was confirmed by CLAS.

Using the same model we calculate the cross section and spin asymmetry for the $K^+\Lambda$ production [4]. The large transversity H_T effects in the $K^+\Lambda$ channel provide the large σ_T cross section without a forward dip, which dominated with respect to σ_L at small Q^2, see Fig. 2 (right). The essential contributions to the σ_T cross section are determined by the twist-3 H_T and $\bar{E}_T$ effects and decreases quickly with Q^2 growing. At quite large Q^2 the leading-twist effects will dominate.

Our observation that the transversity contributions provide large transverse cross sections for most of the pseudoscalar meson channels can be checked experimentally.

[1] S.V. Goloskokov, P. Kroll, Euro. Phys. J. **C65**, (2010) 137.

[2] S.V. Goloskokov, P. Kroll, Euro. Phys. J. **A47**, (2011) 112.

[3] S.V. Goloskokov, Nucl.Phys. B (Proc. Suppl.) **219-220**, (2011) 185.

[4] S.V. Goloskokov, arXiv.org:1211.5210[hep-ph] and arXiv.org:1211.5416[hep-ph].

[5] I. Bedlinskiy, et al. (CLAS Collaboration) Phys. Rev. Lett. **109**, (2012) 112001.

[6] S.V. Goloskokov, "Hard Meson Electroproduction And Twist-3 Effects." Proc. of XIV Advanced Res. Workshop on High Energy Spin Phys., Dubna, 2012, P.71-77.

Constraints on Supersymmetry using LHC data

W.de Boer, C.Beskidt, F.Ratnikov (KIT, Karlsruhe) and D.Kazakov (BLTP, JINR)

Introduction

Supersymmetry (SUSY) remains the best candidate for physics beyond the Standard Model because of its exceptional properties, unification paradigm and a plausible DM candidate. Unfortunately, direct searches for the predicted SUSY particles at the LHC running at 7 TeV were unsuccessful. Also, direct DM searches in deep underground experiments were contradictory. Combining all data from the LHC, cosmology and direct DM searches leads to strong constraints on the predicted SUSY masses, as discussed in recent papers. This report is based on the papers [1,2], where a complete set of references can be found. To restrict the number of independent SUSY masses, one usually assumes the universality at the GUT scale and the particles get different masses at lower energies because of radiative corrections. In the constrained Minimal Supersymmetric SM (CMSSM) many parameters of SUSY models are reduced to only four: the two mass parameters $m_0, m_{1/2}$ and two parameters related to the Higgs sector: the trilinear coupling at the GUT scale A_0, and $\tan\beta$, the ratio of the vacuum expectation values of the two neutral components of the two Higgs doublets. Electroweak symmetry breaking (EWSB) fixes the scale of μ, so only its sign is a free parameter. The positive sign is taken, as suggested by the muon anomalous magnetic moment. In this letter we combine the newest data from LHC, WMAP, XENON100, flavor physics and $g - 2$.

Excluded region by direct searches for SUSY at the LHC

In proton-proton collisions, strongly interacting supersymmetric particles can be produced in pairs in strong and weak processes and decay via cascade chains. The cross section for the "strong" production of squarks is large for low values of m_0 and $m_{1/2}$, the production of gluinos is the strongest at small values of $m_{1/2}$, and the electroweak production of gauginos starts to increase at large values of m_0.The reason for the increase of the electroweak production at large m_0 is the decrease of the Higgs mixing parameter μ, as determined from EWSB, which leads to a stronger mixing of the Higgsino component in the gauginos and so the coupling to the weak gauge bosons and Higgs bosons increases, thus increasing the amplitudes. The strong production cross sections are characterized by a large number of jets from long decay chains and missing energy from the escaping neutralino. These characteristics can be used to efficiently suppress the background. For the electroweak production, both the number of jets and the missing transverse energy is low, hence, the electroweak gaugino production needs leptonic decays to reduce the background, so these signatures need more luminosity and cannot compete at present with the sensitivity of the strong production of squarks and gluinos. The total cross-section for the strongly interacting particles are shown in Fig.1 together with the excluded region from direct searches at the LHC for SUSY particles. One observes that the excluded region (below the solid line) follows rather closely the total cross section, indicated by the colour shading. From the colour coding one observes that the excluded region corresponds to a

cross section limit of about 0.1 -0.2 pb. The excluded region was obtained by combining the ATLAS and CMS limits. We only consider limits from LHC data based on jets and missing energy and do not include the less sensitive limits from leptonic data. These limits can be translated to squark and gluino masses and lead to the excluded regions indicated in the right panel of Fig.1. Note that these regions are not specific to the CMSSM and are valid in other models. Squark masses below 1.5 TeV and gluino masses below 0.96 TeV are excluded for the LHC data at 7 TeV. Expected sensitivities for higher integrated luminosities have been indicated as well. One observes that increasing the energy is much more effective than increasing the luminosity.
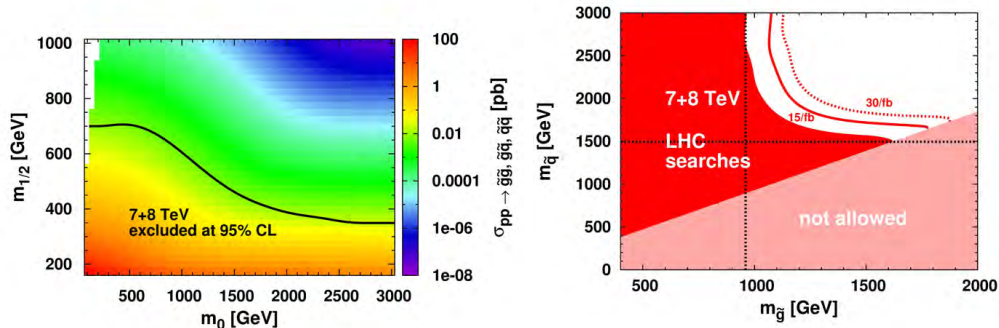

Figure 1: Left: Total production cross section of strongly interacting particles in comparison with the LHC excluded limits for 7 TeV. One observes that a cross section of 0.1 to 0.2 pb is excluded at 95% confidence level. Right: The same but in the m_{sq}, m_{gl} plane. The red area corresponds to excluded regions for an integrated luminosity slightly above 1/fb; the expectations for higher luminosities are indicated as well.

Excluded region by $B_s \to \mu\mu$

The upper limit on the branching ratio of $B_s \to \mu\mu$ can give significant constraints on the SUSY parameter space, since this rate varies as $\tan\beta^6$. In addition, it is sensitive to the stop mixing which is a function of A_0. The $B_s \to \mu\mu$ decay can be suppressed if the stop squarks are degenerate or even get values below SM. The combination with the relic density, which requires a large $\tan\beta$ value in a large region of parameter space causes tension with the $B_s \to \mu\mu$ constraint. This tension can be reduced by large values of A_0, but with the recent upper limit near the SM value from LHCb this tension increased and both constraints cannot be fulfilled at the same time in the whole parameter space. This leads to two excluded regions shown in Fig 2. Compared to the other constraints the $B_s \to \mu\mu$ rate leads only to a tiny increase of the excluded region at small m_0.

Excluded region by direct DM searches

The cross section for direct scattering of WIMPS on nuclei has an experimental upper limit of about 10^{-8} pb, i.e. many orders of magnitude below the annihilation cross section. This is naturally explained in the MSSM by the fact that both cross sections are dominated by Higgs exchange. Due to the smallness of the Yukawa couplings most of the
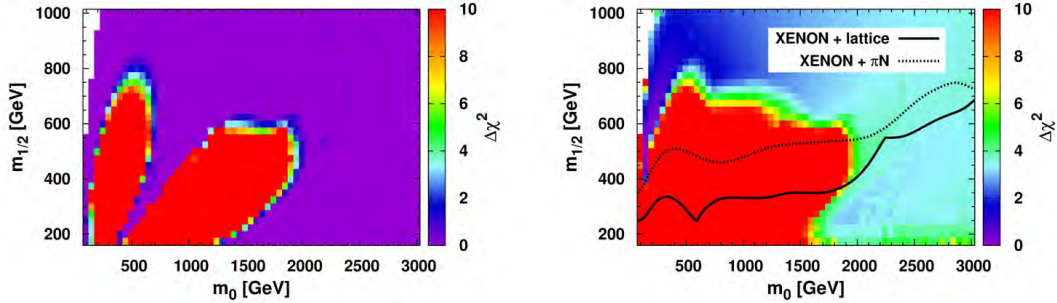
Figure 2: Left: constraints from the $B_s \to \mu\mu$ in the $m_0, m_{1/2}$ plane after optimizing $\tan\beta$ and A_0. The red shaded area is excluded at 95 % C.L. Right: $\Delta\chi^2$ distribution in the $m_0, m_{1/2}$ plane in comparison with the XENON100 limits on the direct WIMP-nucleon cross section for two values of the form factors (dotted line: πN scattering, dashed dotted line: lattice gauge theories).

scattering cross section come from the heavier sea-quarks the density of which inside the nuclei is small. For low momentum transfer, the scattering can be written in terms of an effective coupling, which can be determined either from N scattering or from lattice QCD calculations. The excluded region from the XENON100 cross-section limit is shown on the right panel of Fig.2. At large values of m_0 EWSB forces the higgsino component of the WIMP to increase and consequently the amplitude proportional to the bino-higgsino mixing, starts to increase. This leads to an increase in the excluded region at large m_0 and has here similar sensitivity as the LHC.

Combination of all Constraints

Combining all constraints from the LHC data with data on $B_s \to \mu\mu$, the relic density (WMAP and other cosmological data) and upper limits on the dark matter scattering cross sections on nuclei (XENON100 data) (without 125 GeV Higgs mass) leads to the excluded region below the solid black line in Fig.3 (left). In the fit we use the 95% C.L. LEP limit of 114.4 GeV on the Higgs mass instead of the limits published by CMS and ATLAS with about 5/fb. If a Higgs mass of 125 GeV is included in the fit, the best-fit point moves to higher SUSY masses, but there is a rather strong tension between the relic density constraint, $B_s \to \mu\mu$ and the Higgs mass, so the best-fit point depends strongly on the error assigned to the Higgs mass. We have plotted the best-fit point for Higgs uncertainties of 2 GeV in Fig.3 (right panel). The region below the white line is excluded at 95% C.L. A negative sign of the mixing parameter shows similar results.

Summary

Combining the limits from the direct searches at the LHC, heavy flavor constraints, WMAP and XENON100, we exclude values of $m_{1/2}$ below 525 GeV in the CMSSM for $m_0 < 1500$ GeV, which implies a lower limit on the WIMP mass of 230 GeV and a gluino mass of 1370 GeV, respectively. If a Higgs mass of the lightest Higgs boson of 125 GeV
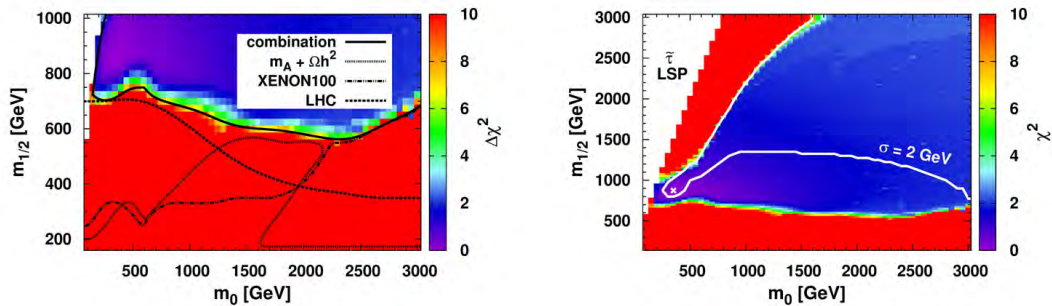
Figure 3: The total $\Delta\chi^2$ distribution without (left) and with (right) account of the 125 GeV Higgs mass

is imposed, the preferred region is well above this excluded region, but the size of the preferred region is strongly dependent on the size of the assumed theoretical uncertainty. However, in models with an extended Higgs sector, like NMSSM, a Higgs mass of 125 GeV can be obtained for lower values of $m_{1/2}$, in which case the regions excluded in the MSSM become viable.

[1] C. Beskidt, W. de Boer, D.I. Kazakov, and F. Ratnikov, *Where is SUSY?*, JHEP 1205 (2012) 094, arXiv:1202.3366 [hep-ph]

[2] C. Beskidt, W. de Boer, D.I. Kazakov, and F. Ratnikov, *Constraints on Supersymmetry from LHC data on SUSY searches and Higgs bosons combined with cosmology and direct dark matter searches*, Eur.Phys.J. C72 (2012) 2166, arXiv:1207.3185 [hep-ph].

Anomaly, mixing and transition form factors of pseudoscalar mesons

Y. N. Klopot[a], A. G. Oganesian[a,b], O. V. Teryaev[a]

[a]Bogoliubov Laboratory of Theoretical Physics, JINR, 141980 Dubna, Russia

[b]Institute of Theoretical and Experimental Physics, Moscow 117218, Russia

The phenomenon of axial anomaly [1] is widely known for its manifestation in two-photon decays of pseudoscalar mesons. The dispersive approach to axial anomaly [2, 3] turns out to be a useful tool for exploration of the processes, which also involve virtual photons, like the photon-meson transitions $\gamma\gamma^* \to \pi^0(\eta, \eta')$ [4, 5, 6, 7].

The axial anomaly is associated with the VVA three-point correlator, which involves two vector currents with momenta k, q and one axial current with momentum $p = k + q$. In what follows, the case with one virtual photon $(-q^2 = Q^2 > 0)$ and one real photon $(k^2 = 0)$ is considered.

The axial anomaly, considered in the dispersive approach, leads to an anomaly sum rule (ASR) [3],

$$\int_{4m^2}^{\infty} A_3^{(a)}(s, Q^2; m^2)ds = \frac{1}{2\pi}N_c C^{(a)}, \ a = 3, 8, \tag{1}$$

where $A_3 = \frac{1}{2}(F_3 - F_6)$, and F_i are the invariant amplitudes at the tensor structures $F_3 k_\nu \varepsilon_{\alpha\mu\rho\sigma}k^\rho q^\sigma, F_6 q_\mu \varepsilon_{\alpha\nu\rho\sigma}k^\rho q^\sigma$ of the decomposition of the VVA correlator, $N_c = 3$ is a number of colors, m is a quark mass and $C^{(a)}$ are the charge factors of components of the axial currents $J_{\alpha5}^{(a)}$. For the isovector $(a = 3, C^{(3)} = \frac{1}{3\sqrt{2}})$ and octet $(a = 8, C^{(8)} = \frac{1}{3\sqrt{6}})$ components of axial current ASR (1) has an important property – both perturbative and nonperturbative corrections to the integral are absent because of the Adler-Bardeen theorem and the 't Hooft's principle.

In the case of *isovector channel*, saturating the lhs of the three-point correlation function with the resonances, singling out the first contribution, given by the pion, and collecting all the other states into the continuum contribution $I_{cont}^{(3)}(s_3, Q^2)$, we get the ASR in the form (in what follows we take $m = 0$):

$$\pi f_\pi F_{\pi\gamma}(Q^2) + I_{cont}^{(3)}(s_3, Q^2) = \frac{1}{2\pi}N_c C^{(3)}, I_{cont}^{(3)} \equiv \int_{s_3}^{\infty} A_3^{(3)}(s, Q^2; m^2)ds, \tag{2}$$

where s_3 is a continuum threshold, and the general definitions of the decay constants f_M^a $(f_\pi^{(3)} \equiv f_\pi = 130.7$ MeV) and the transition form factors (TFFs) of the reactions $\gamma\gamma^* \to M$ are

$$\langle 0|J_{\alpha5}^{(a)}(0)|M(p)\rangle = ip_\alpha f_M^a, \int d^4x e^{ikx}\langle M(p)|T\{J_\mu(x)J_\nu(0)\}|0\rangle = \epsilon_{\mu\nu\rho\sigma}k^\rho q^\sigma F_{M\gamma}. \tag{3}$$

If we employ the one-loop expression for the spectral density, we get [4]

$$F_{\pi\gamma}(Q^2) = \frac{1}{2\sqrt{2}\pi^2 f_\pi}\frac{s_3}{s_3 + Q^2}.\tag{4}$$

At $Q^2 \to \infty$, where the pion TFF acquires its asymptotic value [8] $Q^2 F_{\pi\gamma}^{as}(Q^2) = \sqrt{2}f_\pi$, the continuum threshold s_3 can be determined from (4), $s_3 = 4\pi^2 f_\pi^2 = 0.67$ GeV^2 and then (4) reproduces the well-known Brodsky-Lepage interpolation formula [9].

When compared to the experimental data on pion TFF, equation (4) gives a fairly good description of the data of the CELLO [10], CLEO [11] and BELLE [12] collaborations, while the data of the BABAR collaboration [13] are described much worse.

The BABAR data indicate a log-like growth, and in order to describe them well, one needs to consider a possibility of the correction. Although the integral in ASR does not have any corrections, the spectral density $A_3^{(3)}(s, Q^2)$ can acquire corrections, and therefore, the continuum and the pion contributions can have corrections as well. The exactness of the ASR results in an interplay between corrections to the continuum and pion: they should cancel each other to preserve the ASR, $\delta I_{cont}^{(3)} = -\delta I_\pi$. The form of the correction is not yet known. The α_s correction is shown to be zero, while the OPE corrections cannot provide the desired behaviour, so such a correction should be of non-local OPE origin [7]. Nevertheless, we can propose the form of the correction, relying on general properties of ASR: it should vanish at $s_3 \to \infty$ (the continuum contribution vanishes), at $s_3 \to 0$ (the full integral has no corrections), at $Q^2 \to \infty$ (the perturbative theory works at large Q^2) and at $Q^2 \to 0$ (anomaly perfectly describes pion decay width). Supposing the correction contains rational functions and logarithms of Q^2, the simplest form of the correction satisfying those limits results [7] in

$$F_{\pi\gamma}(Q^2) = \frac{1}{\pi f_\pi}(I_\pi + \delta I_\pi) = \frac{1}{2\sqrt{2}\pi^2 f_\pi}\frac{s_3}{s_3 + Q^2}\left[1 + \frac{\lambda Q^2}{s_3 + Q^2}\left(\ln\frac{Q^2}{s_3} + \sigma\right)\right],\tag{5}$$

where λ and σ are dimensionless parameters.

The fit of the TFF (5) to the combined CELLO+CLEO+BABAR data gives $\lambda = 0.14$, $\sigma = -2.36$, $\chi^2/d.o.f. = 0.94$ $d.o.f. = 35$. The plot of $Q^2 F_{\pi\gamma}$ for these parameters is shown in Fig. 1 as a solid line. The TFF (5) with these parameters λ, σ describes well also the combined CELLO+CLEO+BELLE data with $\chi^2/d.o.f. = 0.84$ $(d.o.f. = 35)$. On the other hand, the TFF without correction (4) (dashed line in Fig. 1) gives $\chi^2/d.o.f. = 2.29$ and $\chi^2/d.o.f. = 1.01$ for CELLO+CLEO+BABAR and CELLO+CLEO+BELLE data sets, respectively. We can conclude that although the BABAR data favour the log-like correction, the newly released BELLE data neither confirm nor exclude the possibility of this correction.

The octet channel of the ASR (in the ciral limit) can be written down as

$$f_\eta^8 F_{\eta\gamma}(Q^2) + f_{\eta'}^8 F_{\eta'\gamma}(Q^2) = \frac{1}{2\sqrt{6}\pi^2}\frac{s_8}{s_8 + Q^2},\tag{6}$$

where s_8 is a continuum threshold which can be determined from the large-Q^2 limit of (6) and the pQCD predicted expression for the η, η' TFFs:

$$s_8 = 4\pi^2((f_\eta^8)^2 + (f_{\eta'}^8)^2 + 2\sqrt{2}[f_\eta^8 f_\eta^0 + f_{\eta'}^8 f_{\eta'}^0]).\tag{7}$$
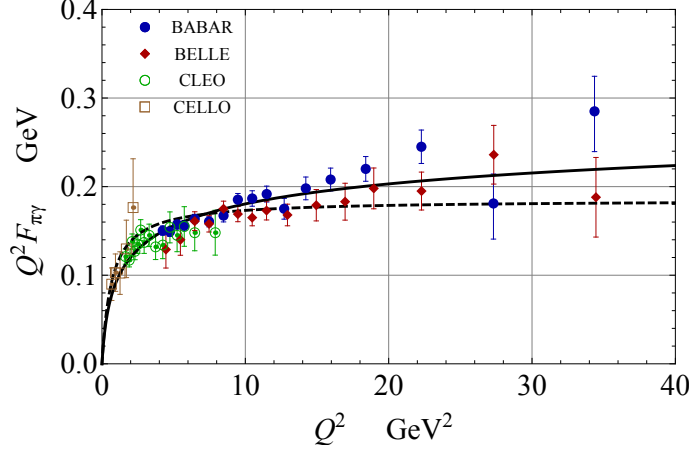
Figure 1: Pion transition form factor: Eqs. (4) (dashed line) and (5) (solid line) compared with experimental data

Let us note that in the octet channel the reliable estimation of $s_0^{(8)}$ from the usual QCD sum rule method meets difficulties (see e.g. discussion in [6]). Fortunately, the ASR approach allows one to determine $s_0^{(8)}$ in the octet channel from high-Q^2 asymptotic, just the same way as in the isovector channel.

The octet channel of ASR is dominated by the mixing states of η and η' mesons. We considered [7] a description of the mixing in the $\eta - \eta'$ system in terms of fields and physical states without introducing the intermediate nonphysical states (when physical states are represented as a linear combination of states with definite $SU(3)_f$ quantum numbers or quark-flavor content). Such a description avoids dealing with the form factors of nonphysical states. It was shown [7] that the widely used mixing schemes, such as quark-flavour and octet singlet schemes lead to the particular constraints on the decay constants,

$$f_\eta^\alpha f_\eta^\beta + f_{\eta'}^\alpha f_{\eta'}^\beta + f_G^\alpha f_G^\beta + ... = 0. \tag{8}$$

We performed the numerical analysis and extracted the decay constants (mixing parameters), using the BABAR data for η and η' TFFs [14] and the ratio of the radiative J/Ψ decays. The values of the decay constants obtained for the considered mixing schemes as well as in the mixing-scheme-independent way.

Naturally, if the log-like correction is present in the isovector channel, it should reveal itself in the octet channel too. A similar correction in the octet channel leads to ASR with the correction term [6, 7]:

$$f_\eta^8 F_{\eta\gamma}(Q^2) + f_{\eta'}^8 F_{\eta'\gamma}(Q^2) = \frac{1}{2\sqrt{6}\pi^2} \frac{s_8}{s_8 + Q^2} \left[1 + \frac{\lambda Q^2}{s_8 + Q^2} \left(\ln \frac{Q^2}{s_8} + \sigma \right) \right]. \tag{9}$$

For the purposes of numerical analysis, we employ the decay constants obtained in a scheme-independent way in Ref. [7]: $f_\eta^8 = 1.11 f_\pi$, $f_{\eta'}^8 = -0.42 f_\pi$, $f_\eta^0 = 0.16 f_\pi$, $f_{\eta'}^8 = 1.04 f_\pi$. Then, the fit of Eq. (9) to the experimental data of the BABAR collaboration [14]
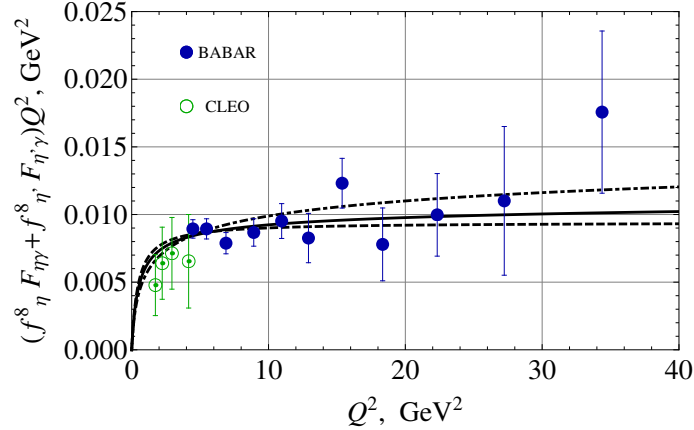
Figure 2: The ASR in the octet channel for different values of fitting parameters compared with the experimental data, see description in the text.

gives $\lambda = 0.05, \sigma = -2.58$ with $\chi^2/d.o.f. = 0.81$ (see the solid line in Fig. 2), while Eq. (6) gives $\chi^2/d.o.f. = 0.85$ (dashed line). At the same time, if the parameters are taken the same as for the pion case $\lambda = 0.14, \sigma = -2.36$, we get $\chi^2/d.o.f. = 1.02$ (dot-dashed line). So the current precision of the experimental data on η, η' TFFs can accommodate the log-like correction in the octet channel, although does not require it.

[1] J. S. Bell, R. Jackiw, Nuovo Cim. **A60**, 47-61 (1969). S. L. Adler, Phys. Rev. **177**, 2426-2438 (1969).

[2] A. D. Dolgov, V. I. Zakharov, Nucl. Phys. **B27**, 525-540 (1971).

[3] J. Horejsi, O. Teryaev, Z. Phys. **C65**, 691-696 (1995).

[4] Y. N. Klopot, A. G. Oganesian and O. V. Teryaev, Phys. Lett. B **695**, 130 (2011) [arXiv:1009.1120 [hep-ph]].

[5] Y. N. Klopot, A. G. Oganesian and O. V. Teryaev, Phys. Rev. D **84**, 051901 (2011) [arXiv:1106.3855 [hep-ph]].

[6] Y. Klopot, A. Oganesian and O. Teryaev, JETP Lett. **94**, 729 (2011) [JETP Lett. **94**, 1 (2012)] [arXiv:1110.0474 [hep-ph]].

[7] Y. Klopot, A. Oganesian and O. Teryaev, Phys. Rev. D **87**, 036013 (2013) [arXiv:1211.0874 [hep-ph]].

[8] G. P. Lepage and S. J. Brodsky, Phys. Rev. **D22**, 2157 (1980).

[9] S. J. Brodsky, G. P. Lepage, Phys. Rev. **D24**, 1808 (1981).

[10] H. J. Behrend *et al.* [CELLO Collaboration], Z. Phys. C **49**, 401 (1991).

[11] J. Gronberg *et al.* [CLEO Collaboration], Phys. Rev. D **57**, 33 (1998)

[12] S. Uehara *et al.* [Belle Collaboration], arXiv:1205.3249 [hep-ex].

[13] B. Aubert *et al.* [BABAR Collaboration], Phys. Rev. D **80**, 052002 (2009)

[14] P. del Amo Sanchez *et al.* [BABAR Collaboration], Phys. Rev. D **84**, 052001 (2011)

New approach for gluon and quark multiplicities

P. Bolzoni, B.A. Kniehl (II. Institut für Theoretische Physik, Universität Hamburg) and A.V. Kotikov (BLTP JINR)

Introduction

Collisions of particles and nuclei at high energies usually produce many hadrons. In Quantum Chromodynamics (QCD) their production is due to the interactions of quarks and gluons and to test it as a theory of strong interactions, the transition from a description based in terms of quarks and gluons to the hadrons observed in experiments is always needed. The production of hadrons is a typical process where non-perturbative phenomena are involved. However, the hypothesis of Local Parton-Hadron Duality assumes that parton distributions are simply renormalized in the hadronization process without changing their shape [1], allowing perturbative QCD to make predictions. The simplest observables of this kind are average gluon and quark multiplicities $\langle n_h \rangle_g$ and $\langle n_h \rangle_s$ which represent the number of hadrons produced in a gluon and a quark jet respectively. In the framework of the generating-functional approach in the modified leading logarithmic approximation [2], several studies of the multiplicities were performed [2,3].

In these studies, the ratio $r = \langle n_h \rangle_g / \langle n_h \rangle_s$ is at least 10% higher than the data (see Fig. 2) or it has a slope too small. Good agreement with the data was achieved in Ref. [4] where recoil effects are included. Nevertheless, in Ref. [5] a constant offset to be fitted to the quark and gluon multiplicities was introduced, while the authors of Ref. [6] suggested that other, better motivated possibilities should be studied.

Results

Recently we studied in Ref. [7] such a possibility inspired by the new formalism that has recently been proposed in Ref. [8]. Thanks to very recent new results in small-x time-like resummation obtained in Refs. [8,9], we are able to reach the next-to-next-to-next-to-leading logarithmic (NNLL) accuracy level in the resummation of double-logarithmic terms at low x.

A purely perturbative and analytic prediction was already attempted in Ref. [6] up to the third order in the expansion parameter $\sqrt{\alpha_s}$ *i.e.* $\alpha_s^{3/2}$ (α_s is strong coupling constant), where paradoxically the quark multiplicity and the ratio are not well described even if the behavior of the perturbative expansion is very good. Our new resummed results in [7] are generalization of what was obtained in Ref. [6] and represent the solution to this apparent paradox.

In Ref. [7], it was shown that our leading order (LO) +NNLL result, which includes all corrections up to an order of $\alpha_s^{3/2}$, solves this problem explaining the discrepancy of the results with the data obtained in Ref. [6] as due to the absence of the so-called singlet "minus" component, which was neglected earlier. In Ref. [7], this component for multiplicities was included for the first time.

Moreover, in [7] we have introduced also a numerical effective approach to perform the resummation of the first Mellin moment of the "plus" component anomalous dimen-
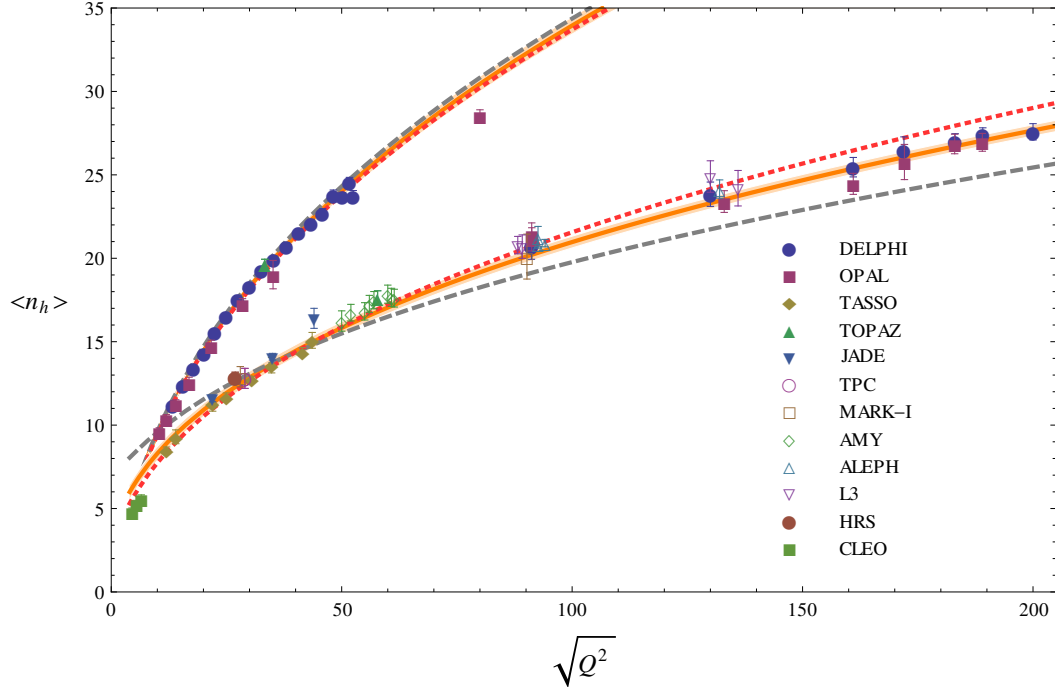
Figure 1: Gluon and quark multiplicities fits compared to the data. The gray dashed line is the $LO + NNLL$ result, the orange solid line is the $NNLL_{\text{approx}}$ result and the red dotted line is the fit without any constraint on the renormalization coefficients of the "plus" and "minus" components. The orange band corresponds to the 90% C.L. fit of the initial conditions for fragmentation functions in the $NNLL_{\text{approx}}$ case.

sion. In that approach, resummation is achieved taking the fixed order "plus" component and substitutes its argument by the effective value $\omega \to \omega_{eff} = \sqrt{6\alpha_s/\pi}$. There we have shown that at order $\sqrt{\alpha_s}$ the approach is exact: we have reproduced exactly the result obtained by Mueller in [10]. We call this approximation $NNLL_{\text{approx}}$. **Analysis** The result of the fits of experimental data is in agreement with the data in both cases: $LO + NNLL$ one and $NNLL_{\text{approx}}$ one. However, in the $NNLL_{\text{approx}}$ case, the 90% C.L. error is much smaller reflecting a much better fit to the data at all energies. Indeed, per degree of freedom we obtain $\chi^2 = 18.09$ in the $LO + NNLL$ case, while we have $\chi^2 = 3.71$ in the $NNLL_{\text{approx}}$ case.

Conclusions

In [7,8], we proposed a solution to the problem of perturbative QCD pointed out in [6] by interpreting their result as corrections to the gluon-quark ratio for the "plus" components and by adding the contributions to the "minus" component of the singlet multiplicity. We showed that the inclusion of these contributions solves the apparent paradox of Ref. [6]: a very good perturbative convergence of QCD but a bad agreement with the experimental data. Our generalized resummed results, which are at the NNLL accuracy level by a good approxiamation, depend on two nonperturbative parameters with a simple physical interpretation because they just represent the gluon and quark multiplicities at a certain reference arbitrary scale Q_0. We obtained them performing a global fit of the gluon and quark multiplicities and comparing the prediction for the
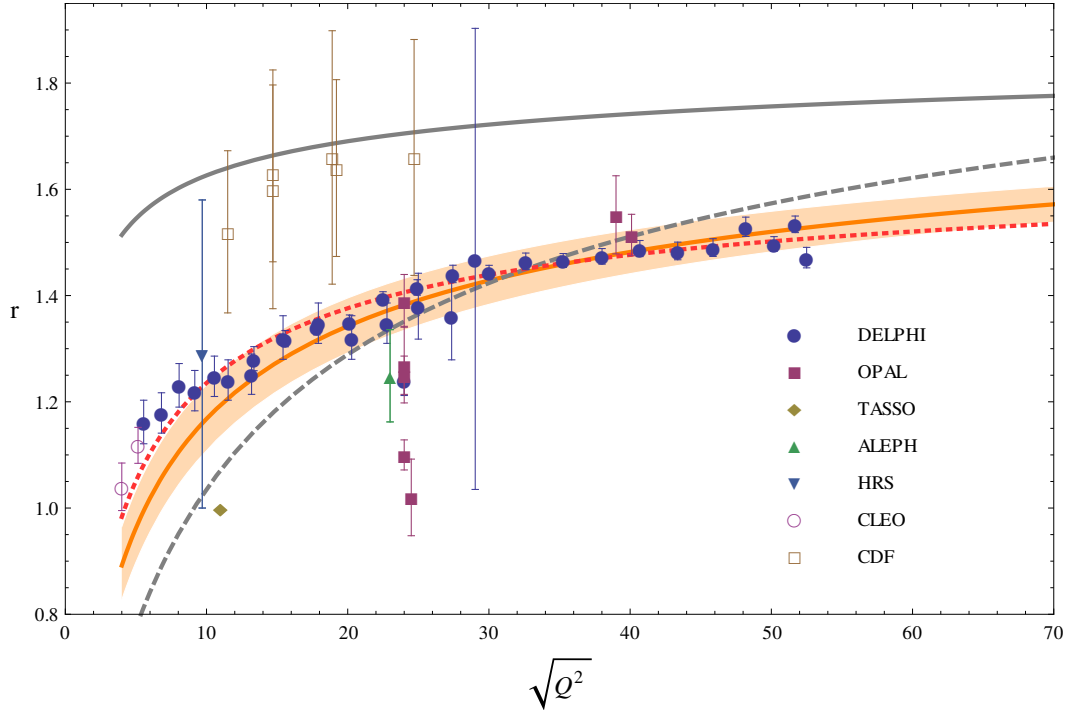
Figure 2: Gluon-quark multiplicity ratio prediction compared to data. The gray solid upper line is the prediction of Ref. [6], the others are as in Fig.1.

gluon-quark multiplicity ratio with the data showing also good consistency of all the data sets.

[1] Y. I. Azimov, Y. L. Dokshitzer, V. A. Khoze, S. I. Troyan, Z. Phys. C **27** (1985) 65.

[2] Y. L. Dokshitzer, V. A. Khoze. Mueller. A. H, S. I. Troian, "Basics of perturbative QCD", 1991, gif-sur-Yvette, France, 274 p.

[3] E. D. Malaza, B. R. Webber, Nucl. Phys. B **267** (1986) 702; S. Catani, Y. L. Dokshitzer, F. Fiorani, B. R. Webber, Nucl. Phys. B **377** (1992) 445.

[4] S. Lupia, W. Ochs, Phys. Lett. B **418** (1998) 214.

[5] P. Eden, G. Gustafson, JHEP **9809** (1998) 015.

[6] A. Capella, I. M. Dremin, J. W. Gary, V. A. Nechitailo, J. Tran Thanh Van, Phys. Rev. D **61** (2000) 074009.

[7] P. Bolzoni, B. A. Kniehl, A. V. Kotikov, Phys. Rev. Lett. **109** (2012) 242002.

[8] S. Albino, P. Bolzoni, B. A. Kniehl, A. V. Kotikov, Nucl. Phys. B **855** (2012) 801; Nucl. Phys. B **851** (2011) 86.

[9] C. -H. Kom, A. Vogt, K. Yeats, JHEP **1210** (2012) 033; S. Moch, A. Vogt, Phys. Lett. B **659** (2008) 290; A. A. Almasy, S. Moch, A. Vogt, Nucl. Phys. B **854** (2012) 133; A. Vogt, JHEP **1110** (2011) 025.

[10] A.H. Mueller, Phys. Lett. B **104** (1981) 161.

ELEMENTARY PARTICLE PROCESSES

A. I. Ahmadov, Yu. M. Bystritskiy,V. V. Bytev, E. A. Kuraev

Bogoliubov Laboratory of Theoretical Physics, JINR

1 LHC related topics

We studied some peripheral processes in proton–proton (proton–antiproton) collisions with the production of different final states. In paper [1], we considered the differential cross sections of processes with high-energy proton–proton and proton–antiproton collisions with the creation of a scalar (Higgs-like), pseudoscalar particles and a lepton pair (see Fig. 1).

The calculations were performed in Weizsäcker–Williams approximation which is well applicable in peripheral kinematics. Besides, the effects of Reggeization were taken into account in the framework of the effective Reggion action of Lipatov's theory.

In paper [2], we considered the effect of azimuthal correlation in production of gluon jets which are separated by a rapidity gap. Strong azimuthal correlation is revealed for two gluonic jets effectively created in the same plane, i.e. the cross section of two gluon jet production $d\sigma^{(2)(\phi)}$ as a function of the azimuthal angle ϕ gives rise to a sharp peak in the azimuthal distribution function $A(\phi)$:

$$A(\phi) = \frac{d\sigma^{(2)(\phi)}}{\int\limits_{-\pi}^{\pi} d\sigma^{(2)}(\phi)d\phi}. \tag{1}$$

This distribution is shown in Fig. 2. The production of one or two vector mesons in high–energy heavy–ion collisions (see Fig. 3) with peripheral kinematics in a similar framework was considered in [3]. The explicit dependence on the virtuality of the intermediate vector meson is obtained within a quark model. The effect of reggeization of the intermediate vector meson state in the case of the production of two vector mesons is taken into account.

2 Standard Model related topics

One of the main subjects of investigation was the Standard Model radiative corrections to Møller scattering within two–loops approximation. This task was induced by the experimental need for precise description of Møller scattering, since this process is of interest for parity violation sources investigated by E-158 experiment at SLAC, and besides the polarized Møller scattering is used to the high-precision determination of the electron–beam polarization at many experimental programs, such as SLC, SLAC, JLab and MIT-Bates. A Møller polarimeter may also be useful in future experiments planned at the ILC.
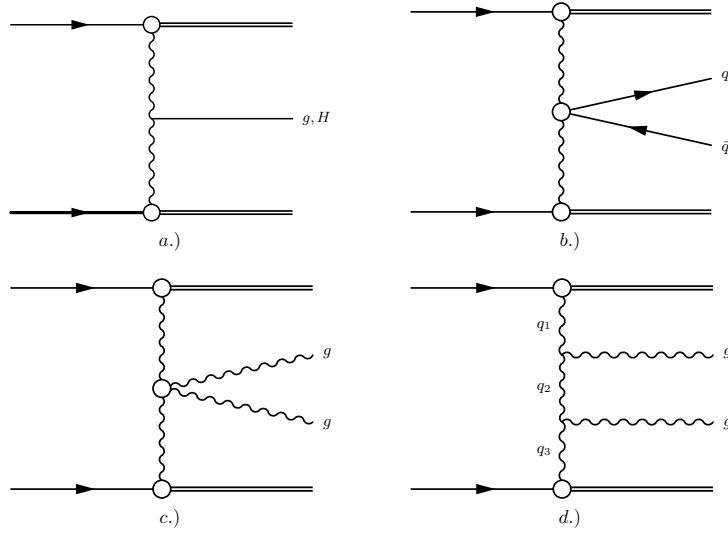
Figure 1: The processes of Higgs boson and two-jets final states production in proton–proton collisions at peripheral kinematics.
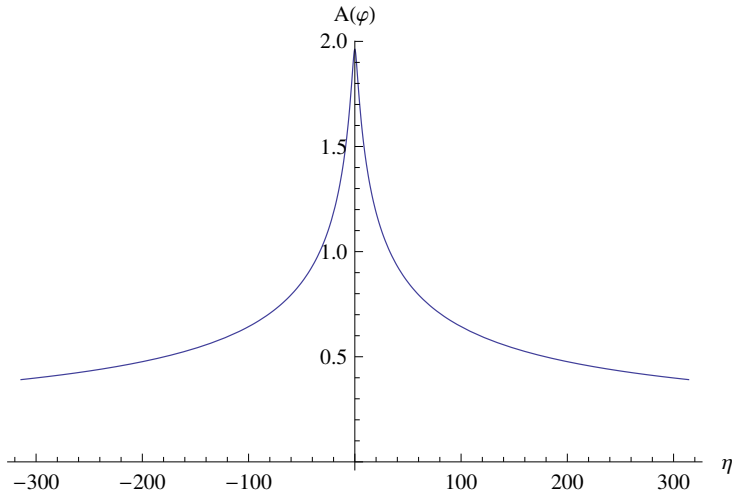

Figure 2: The azimuthal distribution function $A(\phi)$ for $m^2/s = 10^{-4}$, where m is the proton mass and $\phi = \eta\sqrt{m^2/s}$ is presented.
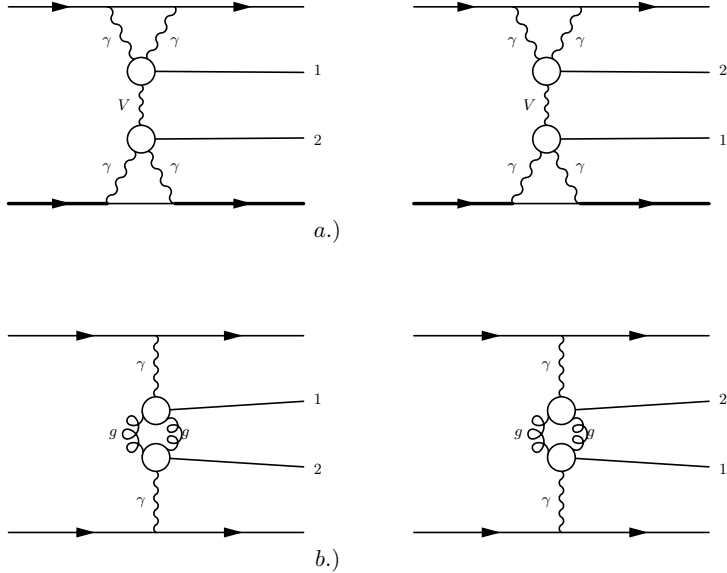
Figure 3: Two vector meson production in heavy–ion collisions with peripheral kinematics.

At the moment, this task is still in progress but a few steps of it have already been done. First, we participated in the analysis of one–loop radiative corrections to Møller scattering in [4, 5] and finally, performed a complete revision of this contribution in [6] where we used the chiral basis at the Born and one–loop QED level. Taking into account as well the contribution from the emission of soft real photons the compact relations free from infrared divergences were obtained. The expressions for separate chiral amplitude contribution to the cross section are in agreement with renormalization group predictions. Second, we considered the sub-class of double-box diagrams in the two–loops approximation in [7].

We also calculated the radiative corrections to the annihilation of the Dark Matter particles into leptons [8]. For the Dark Matter particles we consider both Dirac and Majorana fermions. We sum up all the leading logarithmic contributions where it is possible. We investigate the mass dependence of the resulting cross sections and show that quantitatively the answer is very sensitive to the lepton mass due to the leading logarithm singularity.

3 Proton form factors

The problem of discrepancy of the proton electromagnetic form factor measurement is still the case. The Rosenbluth method based on the unpolarized electron–proton scattering gives a sufficiently different result for the proton form factor in comparison with polarization transfer experiment results. We proposed some model of proton formfactor in [9] which confirms the polarization transfer method result of electric form factor decreasing faster than the magnetic one at high Q^2 (see Fig. 4, 7).

Besides, in [10] we considered the hard scattering mechanism in the leading approxi-
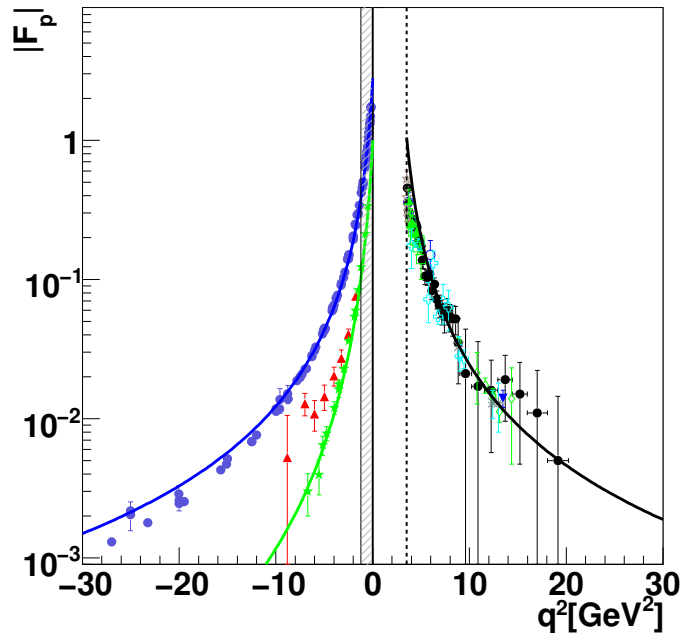
Figure 4: World data on proton form factors as a function of q^2. **Space-like region:** G_M data (blue circles), dipole function (blue line); electric form factor, G_E, from unpolarized measurements (red triangles) and from polarization measurements (green stars). The green line is the model prediction. **Time-like region:** world data for $|G_E| = |G_M|$ (various symbols for $q^2 > 4M_p^2$ and model prediction (black line)).
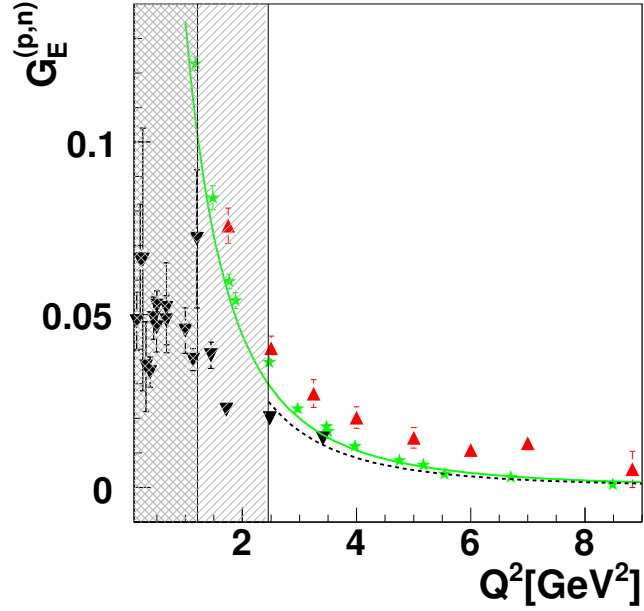
Figure 5: World data on neutron electric form factor (black, triangle down), in space–like region, as functions of $|q^2|$. For comparison, the proton form factor from polarization data (green, stars) and from Rosenbluth method (red,triangles) is shown. The prediction of our model is shown for the proton form factor (solid, green line) and for the neutron (black, dashed line). The shaded area shows the region where the model is not applicable neutron ($q^2 < 2.43$ GeV^2) and the double shaded area shows the region where the model is not applicable for proton ($q^2 < 1.21$ GeV^2).
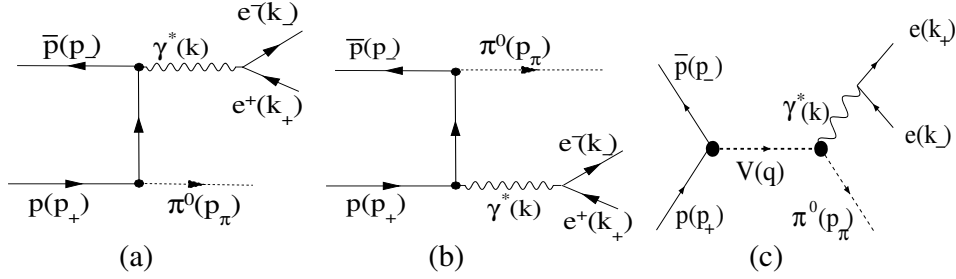
Figure 6: Feynman diagram for the process $\bar{p} + p \to e^+ + e^- + \pi^0$ (a) and (b) in t-channel ('scattering'); (c) in s-channel ('annihilation').

mation and calculated the matrix elements of the proton current $J_p^{\pm\delta,\delta}$ for a full set of spin combinations corresponding to the number of the spin-flipped quarks, which contribute to the proton transition without spin-flip ($J_p^{\delta,\delta}$) and with the spin-flip ($J_p^{-\delta,\delta}$). This allows us to suppose that: 1) at the lower boundary of the experimental measurements of the ratio G_E/G_M not dipole dependence appears but the law of $G_E, G_M \sim 1/Q^6$; 2) the conditions for the observation of the dipole dependence in the experiments have not yet been achieved; 3) since for quarks $J_q^{\delta,\delta} \sim 1$ and $J_q^{-\delta,\delta} \sim \sqrt{\tau}$ (where $\tau = Q^2/(4M_p^2)$), then the dipole dependence is realized when $\tau \gg 1$ in the case when the quark transitions with spin-flip dominate.

We also participated in the program of proton form factor measurement in the time-like region at the PANDA facility (FAIR). In [11], the s-channel annihilation of a proton and an antiproton into a neutral pion and a real or virtual photon followed by lepton pair emission was studied (see Fig. 6). This mechanism is expected to play a role at moderate values of the total energy $\sqrt{s}$ when the pion is emitted around 90° in the center of mass.

4 Reviews

In 2011, our group made a series of reviews which were published in the JINR journal "Physics of Elementary Particles and Atomic Nuclei" [13, 14, 15, 16, 17, 18] where actual problems related to quantum electrodynamics processes, involving weak and strong interactions were considered as well, in view of improving the accuracy of theoretical predictions.

In the last decades important developments in the calculation of high energy QED processes have been driven by the necessity of a very precise knowledge of the cross sections and the amplitudes for photon and lepton interaction, in different kinematics, peripheral as well as large angle scattering.

We consider the processes in peripherical interaction of photons and leptons which correspond to large distances and small scattering angles and the ones with hard particles propagating at large angles when the interaction at small distances becomes essential.

Two different approaches are alternatively presented in the reviews:

- Chiral amplitudes and ultrarelativistic expansions: it is possible to obtain compact expressions for the differential cross sections, providing an accuracy of the theoretical formulas at the level of several thousand.
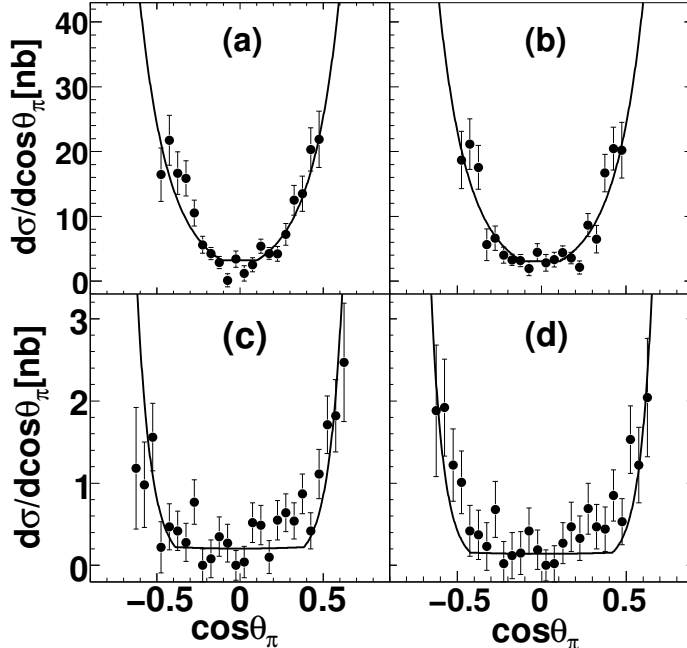
Figure 7: Angular distributions for different values of the center-of-mass energy: a) $\sqrt{s} = 2.975$ GeV, (b) $\sqrt{s} = 2.985$ GeV, (c) $\sqrt{s} = 3.591$ GeV, (d) $\sqrt{s} = 3.686$ GeV. The data are from [12], the line is the result of the model.

- The structure function method based on the renormalization group approach: when combined with exact calculation at the lowest order of perturbation theory it allows one to calculate the differential cross sections to leading and next to leading order approximations, again providing the thousandth accuracy.

The application of the approaches was demonstrated on special and most interested cases of the DVCS tensor, muon decay, pie2 and pie3 decays, special kinematics of Bhabha and Møller scattering (with or without hard photon emission, large and small angle scattering, etc).

The reviews will be in particular interesting for present and forthcoming experiments, at the colliders (BES III, Bejing, China) VEPP-3 (Novosibirsk, Russia) as well as for electromagnetic processes at LHC, and for the research plans connected to ILC.

5 Processes within Nambu–Jona-Lasinio model

A few papers were devoted to the calculation of the cross sections of different meson production in electron-positron annihilation within the Nambu–Jona-Lasinio (NJL) model and its extension for radially excited meson description. These works can be applied in the BES facility to evaluate possible meson production channels.

In [19], the process of electron-positron annihilation into a pair of π^0 and ω mesons was considered in the framework of the $SU(2) \times SU(2)$ NJL model. Contributions of intermediate photons, $\rho(770)$ and $\rho'(1450)$ vector mesons was taken into account. In

[20]m the decays of radially excited mesons π_0', ρ_0' and ω' were considered and in [21], the processes of their production at electron–positron colliders were investigated. In [22], the process of $\pi_0\rho_0$ final state production in electron–positron annihilation was considered. And in [23], the differential distributions in the $\pi_0\pi_0\gamma$ system created in the annihilation channel of an electron-positron collision were calculated, and we pointed out that in relevant experiments the generalized polarizability of the neutral pion can be measured.

[1] A. I. Ahmadov, Y. M. Bystritskiy, and E. A. Kuraev, J.Exp.Theor.Phys. **113**, 637 (2011), arXiv:1101.4471.

[2] E. Kuraev, V. Bytev, and E. Kokoulina, Nucl.Phys. **B851**, 551 (2011), arXiv:1102.1868.

[3] A. Ahmadov, B. Kniehl, E. Kuraev, and E. Scherbakova, Phys.Rev. **C86**, 045203 (2012), arXiv:1206.4441.

[4] A. Aleksejevs, S. Barkanova, Y. Kolomensky, E. Kuraev, and V. Zykunov, Phys. Rev. **D85**, 013007 (2012), arXiv:1110.1750.

[5] A. Aleksejevs, S. Barkanova, Y. Kolomensky, E. Kuraev, and V. Zykunov, Nuovo Cim. **C035**, 192 (2012), arXiv:1110.6637.

[6] A. Ahmadov, Y. Bystritskiy, E. Kuraev, A. Ilyichev, and V. Zykunov, Eur.Phys.J. **C72**, 1977 (2012), arXiv:1201.0460.

[7] A. Aleksejevs *et al.*, Eur.Phys.J. **C72**, 2249 (2012).

[8] A. A. Radovskaya and E. A. Kuraev, (2009), arXiv:0904.3309.

[9] E. Kuraev, E. Tomasi-Gustafsson, and A. Dbeyssi, Phys. Lett. **B712**, 240 (2012), arXiv:1106.1670.

[10] M. V. Galynsky and E. A. Kuraev, JETP Lett. **96**, 6 (2012), arXiv:1210.0634.

[11] E. Kuraev *et al.*, J.Exp.Theor.Phys. **115**, 93 (2012), arXiv:1012.5720.

[12] Fermilab E760, T. A. Armstrong *et al.*, Phys. Rev. **D56**, 2509 (1997).

[13] A. B. Arbuzov, V. V. Bytev, E. A. Kuraev, E. Tomasi-Gustafsson, and Y. M. Bystritskiy, Phys. Part. Nucl. **41**, 394 (2010).

[14] A. B. Arbuzov, V. V. Bytev, E. A. Kuraev, E. Tomasi-Gustafsson, and Y. M. Bystritskiy, Phys. Part. Nucl. **41**, 636 (2010).

[15] A. B. Arbuzov, V. V. Bytev, E. A. Kuraev, E. Tomasi-Gustafsson, and Y. M. Bystritskiy, Phys. Part. Nucl. **41**, 593 (2010).

[16] A. Arbuzov, V. Bytev, E. Kuraev, E. Tomasi-Gustafsson, and Y. Bystritskiy, Phys.Part.Nucl. **42**, 79 (2011).

[17] A. B. Arbuzov, V. V. Bytev, E. A. Kuraev, E. Tomasi-Gustafsson, and Y. M. Bystritskiy, Phys. Part. Nucl. **42**, 55 (2011).

[18] A. Arbuzov, V. Bytev, E. Kuraev, E. Tomasi-Gustafsson, and Y. Bystritskiy, Phys.Part.Nucl. **42**, 1 (2011).

[19] A. B. Arbuzov, E. A. Kuraev, and M. K. Volkov, Phys. Rev. **C83**, 048201 (2011), arXiv:1012.2455.

[20] A. Arbuzov, E. Kuraev, and M. Volkov, Phys. Atom. Nucl. **74**, 726 (2011).

[21] A. Arbuzov, E. Kuraev, and M. Volkov, Eur. Phys. J. **A47**, 103 (2011).

[22] A. Ahmadov, E. Kuraev, and M. Volkov, Phys. Part. Nucl. Lett. **9**, 461 (2012), arXiv:1111.2124.

[23] A. Ahmadov, E. Kuraev, and M. Volkov, Int. J. Mod. Phys. **26**, 3337 (2011), arXiv:1105.5011.

QUANTUM LIQUIDS STUDY

BASED ON MODELS WITH FOUR-FERMION INTERACTION

S. V. Molodtsov[1,2], G. M. Zinovjev[3],

[1]Joint Institute for Nuclear Research, Dubna

[2]Institute of Theoretical and Experimental Physics, Moscow

[3]Bogolyubov ITP National Academy of Sciences of Ukraine, Kiev

A (nearly) perfect liquid discovered in the experements with ultrarelativistic heavy ion collisions is investigated by studying the quark ensembles with four-fermion interaction as a fundamental theoretical approach. Being adapted to the Nambu-Jona-Lasinio (NJL) model this approach allows us to accommodate a phase transition similar to the nuclear liquid-gas one at the proper scale and to argue the existence of the mixed phase of vacuum and normal baryonic matter as a plausible scenario of chiral symmetry (partial) restoration. Analyzing the transition layer between two phases we estimate the surface tension coefficient and discuss the possibility of quark droplet formation. The comparative analysis of several quantum liquid models is performed and it results in the conclusion that the presence of gas—liquid phase transition is their characteristic feature. The problem of instability of the quark droplets with a small quark number is discussed to be rooted in the chiral soliton formation and the existence of a mixed phase of the vacuum and baryon matter is argued as a possible scenario of its stability. Some aspects of the color superconductivity are considered. Besides, nontrivial thermodynamical state—fermion condensate recently proposed is studied. The analysis of unexpected possibility to relate the bare and effective coupling constants is performed in the framework of a simple model. It is pointed out that a simple subtraction procedure leads to the final result without typical logarithmic singularity for observable coupling constant as a function of transmitting energy [1], [2].

These and some related items were considered, inspired by the well-known and fruitful idea about the specific role of surface degrees of freedom in the finite fermi-liquid systems and to a considerable extent by our previous works [3] and [4] in which the quarks were treated as the quasi-particles of the model Hamiltonian and the problem of filling up the Fermi sphere was studied in detail. Under such a treatment an unexpected singularity (discontinuity) of the mean energy functional as a function of the current quark mass was found. In the particular case of the NJL model the existence of new solution branches of the equation for dynamical quark mass as a function of the chemical potential have been demonstrated and the appearance of state filled up with quarks which is almost degenerate with the vacuum state both in the quasi-particle chemical potential and in the ensemble pressure has been discovered. We studied the quark ensemble features at

finite temperature and fixed baryonic chemical potential and analysed the first order phase transition which takes place in this system of free quasi-particles. Analysis was performed within the framework of two approaches which are supplementary, in a sense, albeit giving the identical results. One of those approaches, based on the Bogoliubov transformations, is especially informative to study the process of filling uo the Fermi sphere because at this point the density of a quark ensemble develops a continuous dependence on the Fermi momentum. It allows us to reveal an additional structure in the solution of the gap equation for dynamical quark mass just in the proper interval of parameters characteristic for phase transition and to trace its evolution. The result is that a quark ensemble might be found in two aggregate states, gas and liquid, and the chiral condensate is partially restored in a liquid phase. In order to make these conclusions easily perceptible, we deal with the simplest version of the NJL model (with one flavor and one of the standard parameter sets) and, actually, do not aim to adjust the result obtained with the well-known nuclear liquid-gas phase transition. Besides, it seems that our approach might be treated as a sort of microscopic ground of the conventional bag model and those states filled up with quarks are conceivable as a natural 'construction material' for baryons.

The corresponding Hamiltonian including the interaction term taken in the form of a product of two coloured currents located at the spatial points $\mathbf{x}$ and $\mathbf{y}$ which are connected by the form-factor and its density reads as

$$\mathcal{H} = -\bar{q}(i\gamma\nabla + im)q - \bar{q}t^a\gamma_\mu q \int d\mathbf{y}\bar{q}'t^b\gamma_\nu q'\langle A_\mu^a A_\nu'^b\rangle, \tag{1}$$

where $q = q(\mathbf{x})$, $\bar{q} = \bar{q}(\mathbf{x})$, $q' = q(\mathbf{y})$, $\bar{q}' = \bar{q}(\mathbf{y})$ are the quark and anti-quark operators,

$$q_{\alpha i}(\mathbf{x}) = \int \frac{d\mathbf{p}}{(2\pi)^3} \frac{1}{(2|p_4|)^{1/2}} \left[a(\mathbf{p}, s, c)u_{\alpha i}(\mathbf{p}, s, c)e^{i\mathbf{px}} + b^+(\mathbf{p}, s, c)v_{\alpha i}(\mathbf{p}, s, c)e^{-i\mathbf{px}} \right],$$

$p_4^2 = -\mathbf{p}^2 - m^2$, i–is the colour index, α is the spinor index in the coordinate space, a^+, a and b^+, b are the creation and annihilation operators of quarks and anti-quarks, $a|0\rangle = 0$, $b|0\rangle = 0$, $|0\rangle$ is the vacuum state of free Hamiltonian and m is a current quark mass, index s describes two spin polarizations of quark and the index c plays a similar role for a colour; $t^a = \lambda^a/2$ are the generators of $SU(N_c)$ colour gauge group, the Hamiltonian density is considered in the Euclidean space and γ_μ denote the Hermitian Dirac matrices, $\mu, \nu = 1, 2, 3, 4$. $\langle A_\mu^a A_\nu'^b\rangle = G\delta^{ab}\delta_{\mu\nu}I(\mathbf{x} - \mathbf{y})$ stands for the form-factor. The ground state of the system is searched as the Bogoliubov trial function composed of the quark-anti-quark pairs with opposite momenta and with vacuum quantum numbers, i.e. $|\sigma\rangle = \mathcal{T}|0\rangle$, $\mathcal{T} = \Pi_{p,s}\exp\{\varphi\ [a^+(\mathbf{p}, s)b^+(-\mathbf{p}, s) + a(\mathbf{p}, s)b(-\mathbf{p}, s)]\}$. The parameter $\varphi(\mathbf{p})$ which describes the pairing strength is determined by the minimum of mean energy $E = \langle\sigma|H|\sigma\rangle$. By introducing the 'dressing transformation' we define the creation and annihilation operators of quasi-particles as $A = \mathcal{T}a\mathcal{T}^{-1}$, $B^+ = \mathcal{T}b^+\mathcal{T}^{-1}$ and for fermions $\mathcal{T}^{-1} = \mathcal{T}^\dagger$.

In Ref. [4], the process of filling in the Fermi sphere with the quasi-particles of quarks was studied by constructing the state of the Sletter determinant type $|N\rangle = \Pi_{|\mathbf{P}|<P_F;S} A^+(\mathbf{P}; S)|\sigma\rangle$ which possesses the minimal mean energy over the state $|N\rangle$. The ensemble state at finite temperature T is described by the equilibrium statistical operator ρ. We have used the Bogolyubov-Hartree-Fock approximation for the corresponding

statistical operator

$$\rho = \frac{e^{-\beta \; \hat{H}_{\text{app}}}}{Z_0} \;, \quad Z_0 = \text{Tr}\; \{e^{-\beta \; \hat{H}_{\text{app}}}\} \;, \tag{2}$$

where an approximating effective Hamiltonian H_{app} is quadratic in the creation and annihilation operators of quark and anti-quark quasiparticles. All the quantities of our interest in the Bogoliubov-Hartree-Fock approximation are expressed by the corresponding averages (a density matrix) $n(P) = \text{Tr}\{\rho \, A^+ A\}$, $\bar{n}(Q) = \text{Tr}\{\rho \, B^+ B\}$. The statistical operator ρ is determined in such a form in order to have at the fixed mean charge $\bar{Q}_4 = \text{Tr}\{\rho \, Q_4\}$ and fixed mean entropy $\bar{S} = -\text{Tr}\{\rho \ln \rho\}$ ($S = -\ln \rho$) the minimal value of mean energy of the quark ensemble $E = \text{Tr}\{\rho H\}$. Calculating the corresponding matrix elements leads to the following result for the mean energy density per one quark degree of freedom (see [5]) $w = \mathcal{E}/2N_c$, $\mathcal{E} = E/V$ where E is the total ensemble energy

$$\begin{aligned}
w &= \int \frac{d\mathbf{p}}{(2\pi)^3} |p_4| + \int \frac{d\mathbf{p}}{(2\pi)^3} |p_4| \cos\theta [n(p) + \bar{n}(p) - 1] - \\
&\quad - G \int \frac{d\mathbf{p}}{(2\pi)^3} \sin(\theta - \theta_m) [n(p) + \bar{n}(p) - 1] \int \frac{d\mathbf{q}}{(2\pi)^3} \sin(\theta' - \theta'_m) [n(q) + \bar{n}(q) - 1] \, I \;.
\end{aligned} \tag{3}$$

(up to the constant unessential for our consideration). Here $\theta = 2\varphi$, $\theta' = \theta(q)$, $I = I(\mathbf{p+q})$ and the angle $\theta_m(p)$ is determined by $\sin\theta_m = m/|p_4|$. It is of importance to notice that the existence of such an angle stipulates the discontinuity of mean energy functional mentioned above and found out in [3].

We are interested in minimizing the following functional $\Omega = E - \mu \, \bar{Q}_4 - T \, \bar{S}$ where μ and T are the Lagrange factors for the chemical potential and temperature, respectively. The optimal values of parameters are determined by solving the following system of equations $dw/d\theta = 0$, $dw/dn = 0$, $dw/d\bar{n} = 0$. The induced quark mass is $M(\mathbf{p}) = 2G \int \frac{d\mathbf{q}}{(2\pi)^3} (1 - n' - \bar{n}') \sin(\theta' - \theta'_m) I(\mathbf{p} + \mathbf{q})$. Turning to the presentation in the form customary for mean field approximation we introduce a dynamical quark mass M_q parameterized as: $\sin(\theta - \theta_m) = \frac{M_q}{|P_4|}$, $|P_4| = (\mathbf{p}^2 + M_q^2(\mathbf{p}))^{1/2}$ and ascertain the interrelation between induced and dynamical quark masses $M_q(\mathbf{p}) = M(\mathbf{p}) - m$. The equation for the dynamical quark mass is getting the form characteristic for the mean field approximation $M = 2G \int \frac{d\mathbf{q}}{(2\pi)^3} (1 - n' - \bar{n}') \frac{M'_q}{|P'_4|} I(\mathbf{p} + \mathbf{q})$. From functional (3) we can find the equilibrium densities of quarks and anti-quarks $n = [e^{\beta \, (|P_4| - \mu)} + 1]^{-1}$, $\bar{n} = [e^{\beta \, (|P_4| + \mu)} + 1]^{-1}$ and, hence, the thermodynamic properties of our system as well and, in particular, the pressure of the quark ensemble $P = -dE/dV = -\frac{E}{V} + \frac{\bar{S} \, T}{V} + \frac{\bar{Q}_4 \, \mu}{V}$ (of course, the thermodynamic potential is $\Omega = -PV$).

For example, we consider the NJL model, i.e. the correlation function behaves as the δ-function in the coordinate space. We adjust the standard set of parameters here with $|\mathbf{p}| < \Lambda$, $\Lambda = 631$ MeV, $m = 5.5$ MeV and $G\Lambda^2/(2\pi^2) = 1.3$. This set of parameters at $n = 0$, $\bar{n} = 0$, $T = 0$ gives for the dynamical quark mass $M_q = 335$ MeV. Thus, we determine the density of quark n and anti-quark $\bar{n}$ quasiparticles at given parameters μ and T. As it was found in Ref. [4], the chemical potential at zero temperature first increases first with the charge density, reaches its maximal value, then decreases and at the densities of an order of normal nuclear matter density, $\rho_q \sim 0.16/fm^3$, becomes almost equal to its
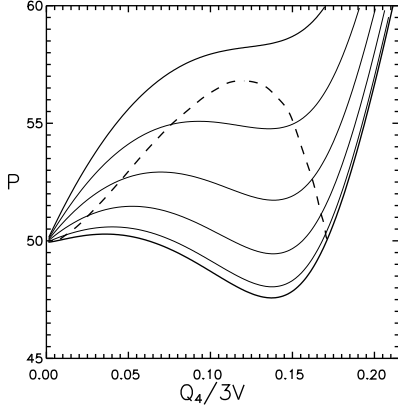
Figure 1: The ensemble pressure P (MeV/fm^3) as a function of charge density $\mathcal{Q}_4$ at temperatures $T = 0$ MeV, ... , $T = 50$ MeV with spacing $T = 10$ MeV. The lowest curve corresponds to zero temperature. The dashed curve shows the boundary of phase transition liquid–gas, see the text.
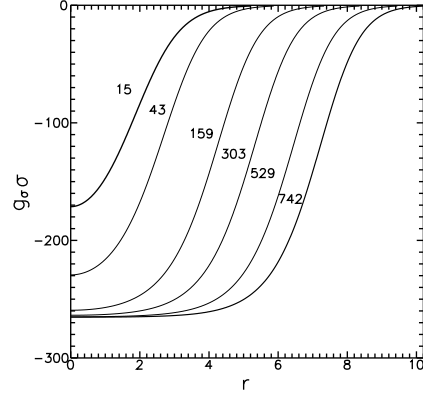
Figure 2: σ-field (MeV) as a function of the distance r (fm) for several solutions of the equation system which are characterized by the net quark number N_q written to the left of each curve.

vacuum value. This a behaviour of the chemical potential results from the fast decrease of dynamical quark mass with the Fermi momentum increase. The charge density occurs in a multivalued function of chemical potential at the temperature slightly below 50 MeV. Figure 1 shows the ensemble pressure P (MeV/fm^3) as the function of charge density $\mathcal{Q}_4$ at several temperatures. The lowest curve corresponds to the zero temperature. The other curves following up correspond to the temperatures $T = 10$ MeV, ... , $T = 50$ MeV (the top curve) with spacing $T = 10$ MeV. In Ref. [4], the vacuum pressure estimate for the NJL model was received as 40—50 MeV/fm^3 which is entirely compatible with the results of the conventional bag model. Besides, some hints on instability presence (rooted in the anomalous behavior of pressure $dP/dn < 0$) in an interval of Fermi momenta were found. The calculated equilibrium points are shown in Fig. 1 by the dashed curve. The intersection points of the dashed curve with an isotherm fix the boundary of gas —liquid phase transition. The corresponding straight line $P = $ const which obeys the Maxwell rule separates the non-equilibrium and unstable fragments of isotherm and describes a mixed phase and appropriate critical temperature for the parameter we use in this paper turns out to be $T_c \sim 45.7$ MeV with the critical charge density as $\bar{Q}_4 \sim 0.12$ charge/fm^3. It was argued in Ref. [4] that the states filled up with quarks and separated from the instability region look like a 'natural construction material' to compose the baryons and to understand the existing fact of equilibrium between vacuum and octet of stable (in strong interaction) baryons.

Apparently, our study of the quark ensemble thermodynamics produces quite reasonable arguments to propound the hypothesis that the phase transition of chiral symmetry

(partial) restoration has already been realized as the mixed phase of physical vacuum and baryonic matter. However, it is clear that our quantitative estimates should not be taken as ones to be compared with, for example, the critical temperature of nuclear matter which has been experimentally measured and equals to 15 – 20 MeV. Besides, the gas component (at $T = 0$) has nonzero density (as 0.01 of the normal nuclear density) but in reality this branch should correspond to the physical vacuum, i.e. zero baryonic density. In principle, the idea of global equilibrium of gas and liquid phases makes it possible to formulate the adequate boundary conditions at describing the transitional layer arising between the vacuum and filled state and to calculate the surface tension effects.

The advanced idea is to obtain substantial confirmation if it becomes possible to claim the existence of the transition layer at which the ensemble transformation from one aggregate state to another takes place. The practical parameter for describing uniform phase (at a given temperature) is the mean charge (density) of ensemble. Thus, one can reconstruct all other characteristics, for example, a chiral condensate, dynamical quark mass, etc. Analyzing the transition layer at zero temperature we assume that the parameters in the gas phase are approximately the same as at zero charge $\rho_g = 0$, i.e. as in the vacuum (ignoring the negligible distinctions in the pressure, chemical potential and quark condensate). Then the dynamical quark mass obtained has maximal value and for the parameter choice of the NJL model it is $M = 335$ MeV. From the corresponding Van der Waals diagram one may draw out that the second (liquid) phase being in equilibrium with the gas phase develops the density $\rho_l = 3 \times 0.185$ ch/fm^3. The detached factor 3 here relates the magnitudes of quark and baryon densities. The quark mass in this phase is approximately $\overset{*}{M} \approx 70$ MeV (we are dealing further with the simple one-dimensional picture).

Usually an adequate description of heterogeneous states can be developed basing on the mean field approximation [6], specifically for our case, by dealing with the corresponding effective quark-meson Lagrangian (a sort of the Ginzburg-Landau functional)

$$\mathcal{L} = -\bar{q}\,(\hat{\partial} + M)\,q - \frac{1}{2}\,(\partial_\mu \sigma)^2 - U(\sigma) - \frac{1}{4}\,F_{\mu\nu}F_{\mu\nu} - \frac{m_v^2}{2}\,V_\mu V_\mu - g_\sigma\,\bar{q}q\,\sigma + ig_v\,\bar{q}\,\gamma_\mu\,q\,V_\mu \ , \ (4)$$

where $F_{\mu\nu} = \partial_\mu V_\nu - \partial_\nu V_\mu$, $U(\sigma) = \frac{m_\sigma^2}{2}\sigma^2 + \frac{b}{3}\sigma^3 + \frac{c}{4}\sigma^4$, σ is the scalar field, V_μ is the field of vector mesons, m_σ, m_v are the masses of scalar and vector mesons and g_σ, g_v are the coupling constants of quark-meson interaction. The $U(\sigma)$ potential includes the nonlinear terms of sigma-field interactions up to the fourth order, for example. We are not going beyond the well-elaborated one loop approximation (4), although recently considerable progress was reached in scrutinizing the nonuniform quark condensates by utilizing the powerful methods of exact integration [7]. We believe that it is more practical to adjust phenomenologically the parameters of effective Lagrangian being guided also by transparent physical picture. It is easy to see that handling one loop approximation actually we have the Walecka model [8] but applied to quarks. In the context of our deliberation Eq. (4) can be interpreted in the following way. Each phase, to some extent, might be considered as an excited state as to its relation with another phase which requires an additional (besides a charge density) set of parameters just as the meson fields for describing and those fields characterize the measure of deviation from the equilibrium state. Then the key question becomes whether it is possible to adjust the effective Lagrangian parameters

of (4) in order to obtain the solutions in which the quark field interpolates between the quasi-particles in the gas (vacuum) phase and in the quasiparticles of the filled up state. The density of the ensemble of the filled up states should asymptotically approach an equilibrium value of ρ_l and turn to zero value in the gas phase (vacuum).

Taking the parameterization of the potential $U(\sigma)$ as $b_\sigma = 1.5\ m_\sigma^2\ (g_\sigma/M)$, $c_\sigma = 0.5\ m_\sigma^2\ (g_\sigma/M)^2$ we come to the sigma model and the choice $b = 0$, $c = 0$ results in the Walecka model. As to the application to nuclear matter, the parameters b and c demonstrate essentially the model dependent character and are different from the parameter values of the sigma model. They are phenomenologically adjusted with requiring an accurate description of the saturation property. On the contrary, for the quark Lagrangian (4) we could intuitively anticipate some resemblance with the sigma model and, hence, introduce two dimensionless parameters η, ζ as $b = \eta\ b_\sigma$, $c = \zeta^2\ c_\sigma$ which characterize some fluctuations of the effective potential. Then the scalar field potential is presented by the following form $U(\sigma) = \frac{m_\sigma^2}{8}\frac{g_\sigma^2}{M^2}\left(4\frac{M^2}{g_\sigma^2} + 4\frac{M}{g_\sigma}\eta\sigma + \zeta^2\sigma^2\right)\sigma^2$. The meson and quark fields are defined by the corresponding equations. The density matrix describing the quark ensemble at $T = 0$ has the form $\xi(x) = \int^{P_F}\frac{d\mathbf{p}}{(2\pi)^3}q_\mathbf{p}(x)\bar{q}_\mathbf{p}(x)$ where $\mathbf{p}$ is the quasiparticle momentum and the Fermi momentum P_F is defined by the ensemble chemical potential. The densities ρ_s, ρ are equal (by definition) to $\rho_s(x) = Tr\{\xi(x), 1\}$, $\rho(x) = Tr\{\xi(x), \gamma_4\}$. Here we confine ourselves to the Thomas–Fermi approximation while describing the quark ensemble. Then the densities in which we are interested in are given with some local Fermi momentum $P_F(x)$ as $\rho = \gamma\int^{P_F}\frac{d\mathbf{p}}{(2\pi)^3} = \frac{\gamma}{6\pi^2}P_F^3$ $\rho_s = \gamma\int^{P_F}\frac{d\mathbf{p}}{(2\pi)^3}\frac{\overset{*}{M}}{E}$ where $\gamma = 2N_cN_f$, $E = (\mathbf{p}^2 + \overset{*}{M}^2)^{1/2}$. By definition, the ensemble chemical potential does not change and it leads to the situation in which the local value of Fermi momentum is defined by the running value of the dynamical quark mass and vector field as $\mu = M = g_v\ V + (P_F^2 + \overset{*}{M}^2)^{1/2}$. The details of tuning the Lagrangian parameters (4) can be found in [9]. The point of our attraction here is the surface tension coefficient: $u_s = 4\pi\ r_o^2\ \int_{-\infty}^{\infty}dx\ \left[\mathcal{E}(x) - \frac{\mathcal{E}_l}{\rho_l}\ \rho(x)\right]$, here $\mathcal{E}_l$ is the energy density in the liquid phase. In the Thomas–Fermi approximation $\mathcal{E}(x) = \gamma\int^{P_F(x)}\frac{d\mathbf{p}}{(2\pi)^3}[\mathbf{p}^2 + \overset{*}{M}(x)]^{1/2} + \frac{1}{2}g_v\rho(x)V(x) - \frac{1}{2}g_\sigma\rho_s(x)\sigma(x)$. The surface tension coefficient u_s was found about some tens of MeV.

The above results lead us to puting the challenging question about the properties of finite quark systems or droplets of quark liquid which are in equilibrium with the vacuum state. As a droplet here we imply the spherically-symmetric solution of the equation system for $\sigma(r)$ and $V(r)$ with the obvious boundary conditions $\sigma'(0) = 0$ and $V'(0) = 0$ in the origin (the primed variables denote the first derivatives over r) and rapidly decreasing at the large distances $\sigma \to 0$, $V \to 0$ when $r \to \infty$. Figure 2 shows the set of solutions (σ-field (MeV)) of the system of equations with a number of flavors $N_f = 1$. The curves plotted in Fig. 2 and results obtained [9] allows us to conclude that the density distributions at $N_q \geq 50$ correspond quite well to the data typical for the nuclear medium. The thicknesses of transition layers are similar. The coefficient r_0 with the factor $3^{1/3}$ included is in full correspondence with the nuclear one. The values of the σ-meson mass turn out to be quite reasonable as well, although at small quark numbers in the droplet the corresponding behaviors become essentially different. We know experimentally that in the nuclear matter one can observe some increase of the

ensemble density which is quite considerable for the Helium and is much higher than the normal nuclear matter density for the Hydrogen. One may criticize us in this point because working within the Thomas–Fermi approximations becomes hardly justified at the small number of quarks and it is necessary to handle the solution of the system of equations. However, fortunately, the exploration we are interested in was performed in the chiral soliton model of nucleon [10]. It was demonstrated there that reasonably good description of nucleon and Δ can be made. The interesting remark here is that the soliton solutions obtained in [10] could be interpreted as a "confluence" of two kinks we have discussed above. Each of those kinks develops the restoration of chiral symmetry in a sense that the scalar field is approaching its zero value at the distance ~ 0.5 fm from the kink center. Actually, one branch corresponds to the solution with the positive value of the dynamical quark mass and another branch presents the solution with the negative dynamical quark mass.

[1] S. V. Molodtsov and G. M. Zinovjev, PEPAN **44**, N 3 (2013).

[2] G. M. Zinovjev, S. V. Molodtsov, Yad. Fiz. **75**, 1387 (2012)

[3] S. V. Molodtsov and G. M. Zinovjev, Teor. Mat. Fiz. **160**, 244 (2009);
Phys. Rev. D **80**, 076001 (2009).

[4] S. V. Molodtsov, A. N. Sissakian and G. M. Zinovjev, Europhys. Lett. **87**, 61001 (2009);
Phys. of Atomic Nucl. **73** 1245 (2010).

[5] S. V. Molodtsov, G. M. Zinovjev, Europhys. Lett. **93**, 11001 (2011).

[6] A. I. Larkin and Yu. N. Ovchinnikov, JETF, **47**, 1136 (1964).

[7] T. Kunihiro, Y. Minami and Z. Zhang, arXiv:1009.4534 [nucl-th];
S. Carignano, D. Nickel and M. Buballa, arXiv:1007.1397 [hep-ph];
D. Nickel, Phys. Rev. Lett. **103**, 072301 (2009);
G. Basar and G. V. Dunne, Phys. Rev. Lett. **100**, 200404 (2008).

[8] J. D. Walecka, Annals of Phys. **83**, 491 (1974).

[9] S. V. Molodtsov, G. M. Zinovjev, Phys. Rev. **D 84**, 036011 (2011);
G. M. Zinovjev, S. V. Molodtsov, Yad. Fiz. **75**, 262 (2012)

[10] W. Broniowski and M. K. Banerjee, Phys. Lett. B **158**, 335 (1978).

SOLAR NEUTRINOS: ASTROPHYSICAL ASPECTS

V.A. Naumov

In this summary of the review paper [1] we'll omit the description of the thermonuclear fusion theory, standard solar models (SSM) and helioseismology (the main subjects of the review) and will take a quick look at the only particular but important and yet unresolved problem of the solar neutrino physics – the problem of chemical composition of the Sun. The elemental abundances in the solar interior is one of the key ingredients in understanding the formation and evolution of the Sun. The chemical elements involved into the *pp* and CNO reactions directly affect the reaction rates and thus the solar neutrino fluxes. The heavy elements on the whole are important as they govern radiative opacities, which in turn affect[1] the density distribution in the outer convection zone and energy transport by the radiative transfer.

The elements up to and beyond ^{56}Fe are discovered in the heliosphere and in the pristine meteorites like CI-chondrites and ureilites (assumed to have the same composition as the Sun, excluding volatile elements) [2, 3, 4, 5, 6, 7, 8, 9]. About twenty years ago astrophysicists believed they knew the solar composition on the level sufficient for an accurate modelling of its evolution and inner structure. However, new analyses of absorption lines in the solar spectrum are essentially downward the photospheric abundances of metals, compared to the previously used values. This is in particular true for the most abundant elements C, N, O, and Ne which participate in the CNO poly-cycle. The trend is illustrated in Fig. 1, which shows the mass fractions of hydrogen, helium, and metals (conventionally abbreviated as, respectively, X, Y, and $Z = 1 - X - Y$) as well as the metal-to-hydrogen ratio (Z/X). The data are taken from the comprehensive compilations [2] (AG89), [3] (GN93), [4] (GS98), [5] (L03), [6] (AGS05), [7] (AGSS09), and [8, 9] (L10) and plotted as a function of the year of publication. Figure shows the mass fractions for both the present-day photosphere and protosolar values, necessary as inputs of the solar models. The current and protosolar chemical compositions are slightly different owing to the combined effects of thermal diffusion, gravitational settling, and radiative acceleration over the past 4.56 Gyr. Comparatively small changes are due to the decay of radioactive isotopes that contribute to the overall atomic abundance of an element. Most of the differences seen in Fig. 1 are due to essential changes in modeling the solar atmosphere, upgrade of atomic and molecular data and better solar observations.[2] The new solar chemical composition is supported by a high degree of internal consistency between available abundance indicators, and by agreement with values obtained in the Solar Neighborhood and from the most pristine meteorites. The SSM predictions based on the old GS98 metallicity were in fantastically good agreement (within 0.1 to 0.3% for most sophisticated SSM calculations) with the sound speed profiles precisely measured by helioseismic methods. The new AGS05 result completely destroyed this agreement. The relative sound speed discrepancy for the AGS05 based solar models reaches about

---

[1]Like the ozone molecules in a trace concentration in the atmosphere govern the ultraviolet radiation level on the Earth's surface.

[2]To recognize the gravity of this deceptively marginal change for the life of the Sun, one can, for example, imagine the climatic consequences from a 50 per cent decrease of the global ozone concentration in the Earth atmosphere.
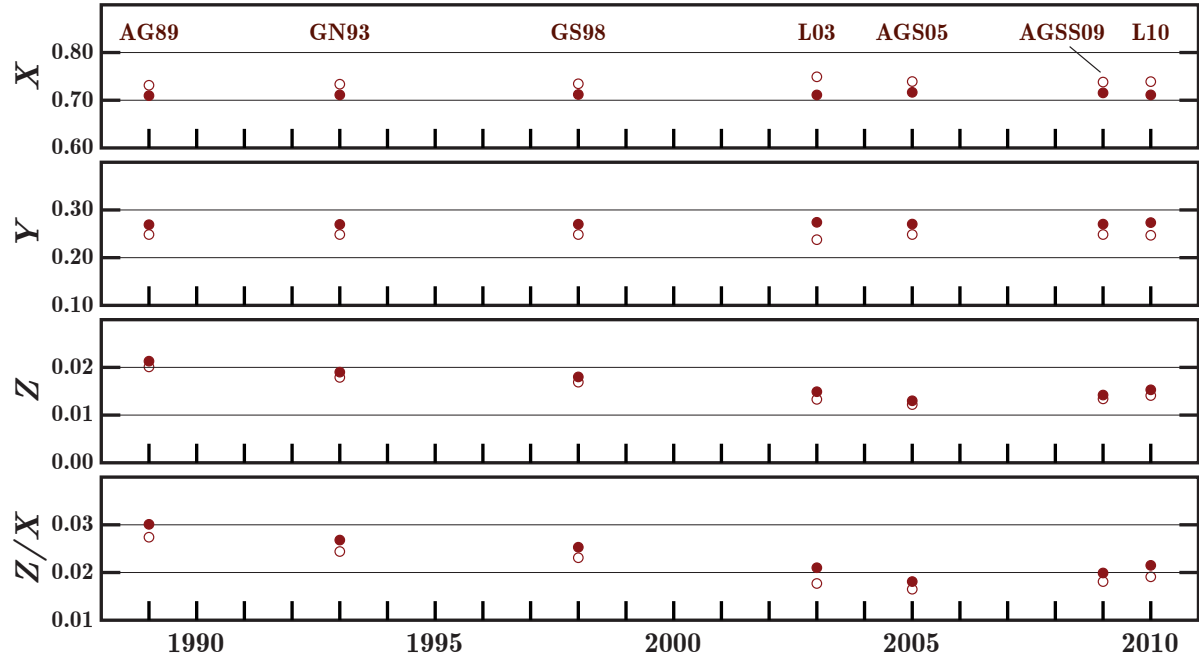
Figure 1: Present-day photospheric (open circles) and protosolar (filled circles) mass fractions of hydrogen (X), helium (Y), and metals (Z) and metals to hydrogen ratio (Z/X). The data are taken from [2, 3, 4, 5, 6, 7, 8, 9]. Horizontal axis indicates the publication years. See text for the abbreviations in the top panel.

1.2% immediately below the bottom of the convection zone. To date, there has been no fully convincing solution put forward. In most up-to-date analyses L10 and AGSS09, the discordance was alleviated somewhat relative to the AGS05 model, but it nevertheless remains a significant discrepancy in urgent need of resolution.

One of the modern versions of the present-day elemental abundance curve in the solar system is shown in Fig. 2, constructed from [4, 6, 8]. The data presented in Fig. 2 are almost similar to those recommended in [7], but differ in details. The data of [8] are based on CI-chondrites, photospheric data, and theoretical calculations. In the cases where solar and meteorite data have comparable accuracy for a given element, the recommended abundance is the average of these values. For other elements, meteoritic data seem more reliable. The general trend of the abundance curve is towards ever decreasing abundance as the atomic number increases. For example, there is a decrease between carbon and oxygen (the element is nitrogen), between neon and magnesium (sodium), oxygen and neon (fluorine). The distinct up-down zig-zag pattern is because the elements with odd numbers of nucleons (e.g., nitrogen, sodium, fluorine) are less stable, resulting in one unpaired (odd) proton or neutron. The huge drop in abundance for the Li-Be-B triplet results from two factors:

(i) at the Big Bang, nuclear processes that could fuse the proper H or He isotopes into Li and/or the other two were statistically very rare and hence inefficient, and

(ii) some of the Li-Be-B nuclei that were formed and survived were destroyed later on by reactions in stars.
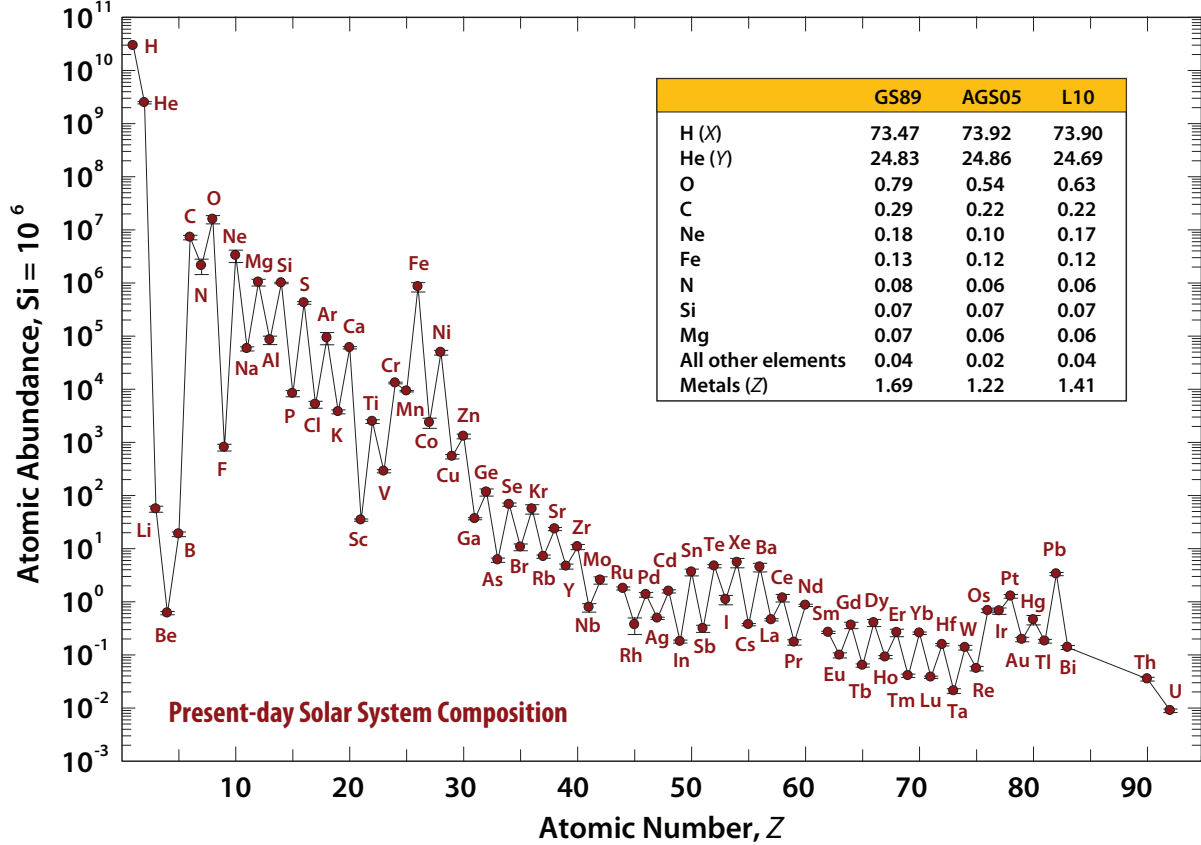
Figure 2: Present-day solar system elemental abundances as function of atomic number normalized to 10^6 Si atoms [8]. The insert shows the present-day solar composition (mass %) according to [4] (GS98), [6] (AGS05) and [8] (L10).

Table 1 summarizes the predicted solar neutrino capture rates for the chlorine and gallium detectors published during the last 20 years. It is seen that the predictions of different models for the gallium target are more robust than those for the chlorine one: the former vary from model to model within 22% (9% for the most recent models [34, 35, 37], that is within the quoted model uncertainties), while the disagreement between the chlorine predictions is as large as 78% (29% for the models [34, 35, 37]). Essentially, all these models are based on the same physical principles and the disagreement between the output values is mainly due to the input nuclear-physics and astrophysical parameters and main source of uncertainties in the modern solar models is the choice of the input chemical composition of the Sun. The "terms-of-trade" between the low, high, or medium metallicities is not a matter of majority vote and in any case, today, there is no generally accepted proposals for resolving the disagreements between the current SSM predictions and helioseismic data. For the most recent discussions of the solar abundance problem and efforts for its solution (published after [1]) see [38] and reference therein.

Table 1: Predicted neutrino capture rates for chlorine and gallium targets. The quoted errors are combinations of (usually 3σ) uncertainties from all known sources added quadratically. The recent SSM calculations [34, 35] use the two solar abundances determinations with high and low metallicity (CS98 and AGS05, respectively). The SSM and seismic model (SeSM) of [37] use the most recent abundances from [7].

Year	Authors	Ref.	^{37}Cl (SNU)	^{71}Ga (SNU)
1990	Sackmann et al.	[10]	7.68	125.0
1992	Bahcall & Pinsonneault	[11]	8.0 ± 3.0	131.5^{+21}_{-17}
1993	Turck-Chièze & Lopes	[12]	6.4 ± 1.4	122.5 ± 7
1993	Schramm & Shi	[13]^a	4.7	117
1994	Shi et al.	[14]	7.3	129
1994	Castellani et al.	[16]	7.8	130
1994	Dar & Shaviv	[18]	4.2 ± 1.2	116 ± 6
1995	Bahcall & Pinsonneault	[19]	$9.3^{+1.2}_{-1.4}$	137^{+7}_{-8}
1996	Dar & Shaviv	[20]	4.1 ± 1.2	115 ± 6
1996	Christensen-Dalsgaard et al.	[21]	8.2	132
1997	Morel et al.	[22]^b	8.93	144
1998	Bahcall et al.	[23]	$7.7^{+1.2}_{-1.0}$	129^{+8}_{-6}
1998	Brun et al.	[24]	7.18	127.2
1999	Brunet et al.	[25]^c	7.25 ± 0.94	127.1 ± 8.9
2001	Bahcall et al.	[26]	$8.0^{+1.4}_{-1.1}$	128^{+9}_{-7}
2001	Turck-Chièze et al.	[27]	7.44 ± 0.96	127.8 ± 8.6
2003	Couvidat et al.	[28]^d	6.90 ± 0.90	126.8 ± 8.9
2004	Bahcall & Peña-Garay	[29]^e	8.5 ± 1.8	131^{+12}_{-10}
2004	Turck-Chièze et al.	[30]	7.60 ± 1.10	123.4 ± 8.2
2006	Bahcall et al. (GS98)	[34]	8.12	126.08
2006	Bahcall et al. (AGS05)	[34]	6.58	118.88
2008	Peña-Garay & Serenelli (GS98)	[35]	$8.46^{+0.87}_{-0.88}$	$127.9^{+8.1}_{-8.2}$
2008	Peña-Garay & Serenelli (AGS05)	[35]	$6.86^{+0.69}_{-0.70}$	$120.5^{+6.9}_{-7.1}$
2010	Turck-Chièze & Couvidat (SSM)	[37]	6.315	120.9
2010	Turck-Chièze & Couvidat (SeSM)	[37]	7.67 ± 1.1	123.4 ± 8.2

^{a} The quoted numbers are corrected according to [14].
^{b} Several models; the quoted numbers are for the model "D11" preferred by the authors.
^{c} Several models; the quoted numbers are for the reference model "BTZ" as cited in [28].
^{d} Several models; the quoted numbers are for the model "Seismic$_2$" provided minimal predicted rate.
^{e} Several models; the quoted numbers are for the model "BP04" preferred by the authors.

[1] V.A. Naumov, Phys. Part. Nucl. Lett. **8** (2011) 683.

[2] E. Anders, N. Grevesse, Geochim. Cosmochim. Acta, **53** (1989) 197.

[3] N. Grevesse, A. Noels, in: "Origin and Evolution of the Elements," ed. by N. Pratzo et al. (Cambridge University Press, 1993), p.14.

[4] N. Grevesse, A.J. Sauval, Space Sci. Rev. **85** (1998) 161.

[5] K. Lodders, Astrophys. J. **591** (2003) 1220.

[6] M. Asplund, N. Grevesse, J. Sauval, in: "Cosmic Abundances as Records of Stellar Evolution and Nucleosynthesis," ed. by T.G. Barnes III and F.N. Bash, ASP Conf. Ser. **336** (2005) 25; Nucl. Phys. A **777** (2006) 1; N. Grevesse, M. Asplund, A.J. Sauval, Space Sci. Rev. **130** (2007) 105.

[7] M. Asplund, N. Grevesse, A.J. Sauval, P. Scott, Ann. Rev. Astron. Astrophys. **47** (2009) 481.

[8] K. Lodders, H. Palme, H.P. Gail, in: "SpringerMaterials – The Landolt-Börnstein Database," ed. by J.E. Trumper (Astronomy and Astrophysics, New Series, Springer Verlag, Berlin, 2009), Sect.4.4.

[9] K. Lodders, in: "Principles and Perspectives in Cosmochemistry," Lecture Notes of the Kodai School on "Synthesis of Elements in Stars, Kodaikanal Observatory, India, April 29 – May 13, 2008, ed. by A. Goswami and B.E. Reddy (Astrophysics and Space Science Proceedings, Springer-Verlag Berlin-Heidelberg, 2010), p.379.

[10] I.J. Sackmann, A.I. Boothroyd, W.A. Fowler, Astrophys. J. **360** (1990) 727.

[11] J.N. Bahcall, M.H. Pinsonneault, Rev. Mod. Phys. **64** (1992) 885.

[12] S. Turck-Chièze, I. Lopes, Astrophys. J. **408** (1993) 347.

[13] D.N. Schramm, X.D. Shi, Nucl. Phys. B (Proc. Suppl.) **35** (1994) 321.

[14] X. Shi, D.N. Schramm, D.S.P. Dearborn, Phys. Rev. D **50** (1994) 2414.

[15] V. Castellani, S. Degl'Innocenti, G. Fiorentini, Astron. Astrophys. **271** (1993) 601.

[16] V. Castellani, S. Degl'Innocenti, G. Fiorentini, M. Lissia, B. Ricci, Phys. Lett. B **324** (1994) 425; addendum – *ibid.* **329** (1994) 525.

[17] A. Kovetz, G. Shaviv, Astrophys. J. **426** (1994) 787.

[18] A. Dar, G. Shaviv, astro-ph/9401043; astro-ph/9404035 (unpublished).

[19] J.N. Bahcall, M.H. Pinsonneault, Rev. Mod. Phys. **67** (1995) 781.

[20] A. Dar, G. Shaviv, Astrophys. J. **468** (1996) 933.

[21] J. Christensen-Dalsgaard *et al.* (GONG Collaboration), Science **272** (1996) 1286.

[22] P. Morel, J. Provost, G. Berthomieu, Astron. Astrophys. **327** (1997) 349.

[23] J.N. Bahcall, S. Basu, M.H. Pinsonneault, Phys. Lett. B **433** (1998) 1.

[24] A.S. Brun, S. Turck-Chièze, P. Morel, Astrophys. J. **506** (1998) 913.

[25] A.S. Brun, S. Turck-Chièze, J.P. Zahn, Astrophys. J. **525** (1999) 1032.

[26] J.N. Bahcall, M.H. Pinsonneault, S. Basu, Astrophys. J. **555** (2001) 990.

[27] S. Turck-Chièze *et al.*, Astrophys. J. Lett. **555** (2001) L69.

[28] S. Couvidat, S. Turck-Chièze, A.G. Kosovichev, Astrophys. J. **599** (2003) 1434.

[29] J.N. Bahcall, C. Peña-Garay, New J. Phys. **6** (2004) 63.

[30] S. Turck-Chièze *et al.*, Phys. Rev. Lett. **93** (2004) 211102.

[31] J.N. Bahcall, A.M. Serenelli, Astrophys. J. **626** (2005) 530.

[32] J.N. Bahcall, A.M. Serenelli, S. Basu, Astrophys. J. Lett. **621** (2005) L85.

[33] J.N. Bahcall, S. Basu, A.M. Serenelli, Astrophys. J. **631** (2005) 1281.

[34] J.N. Bahcall, A.M. Serenelli, S. Basu, Astrophys. J. Suppl. Ser. **165** (2006) 400.

[35] C. Peña-Garay, A.M. Serenelli, arXiv:0811.2424 [astro-ph.SR].

[36] S. Turck-Chièze, A. Palacios, J.P. Marques, P.A.P. Nghiem, Astrophys. J. **715** (2010) 1539.

[37] S. Turck-Chièze, S. Couvidat, Rept. Prog. Phys. **74** (2011) 086901.

[38] S. Bi, T. Li, L. Li, W. Yang, arXiv:1104.1032 [astro-ph.SR]; A.M. Serenelli, W.C. Haxton, C. Peña-Garay, Astrophys. J. **743** (2011) 24; W.C. Haxton, R.G. Hamish Robertson, A.M. Serenelli, arXiv:1208.5723 [astro-ph.SR]; W. C. Haxton, arXiv:1210.1320 [nucl-th]; A.C. Vincent, P. Scott, R. Trampedach, arXiv:1206.4315 [astro-ph.SR].

QCD IN TERMS OF GAUGE-INVARIANT DYNAMICAL VARIABLES

H.-P. Pavel

Bogoliubov Laboratory of Theoretical Physics, Joint Institute for Nuclear Research, Dubna

Institut für Kernphysik,Theorie, Darmstadt, Germany

Abstract

For a complete description of the physical properties of low-energy QCD, it might be advantageous to first reformulate QCD in terms of gauge-invariant dynamical variables, before applying any approximation schemes. Using a canonical transformation of the dynamical variables, which Abelianises the non-Abelian Gauss-law constraints to be implemented, such a reformulation can be achieved for QCD. The exact implementation of the Gauss laws reduces the colored spin-1 gluons and spin-1/2 quarks to unconstrained colorless spin-0, spin-1, spin-2 and spin-3 glueball fields and colorless Rarita-Schwinger fields, respectively. The obtained physical Hamiltonian can then be rewritten into a form which separates the rotational from the scalar degrees of freedom, and admits a systematic strong-coupling expansion in powers of $\lambda = g^{-2/3}$, equivalent to an expansion in the number of spatial derivatives. The leading-order term in this expansion corresponds to non-interacting hybrid-glueballs whose low-lying masses can be calculated with high accuracy by solving the Schrödinger-equation of the Dirac-Yang-Mills quantum mechanics of spatially constant physical fields (at the moment only for the 2-color case). Due to the presence of classical zero-energy valleys of the chromomagnetic potential for two arbitrarily large classical glueball fields (the unconstrained analogs of the well-known constant Abelian fields), practically all glueball excitation energy is expected to go into the increase of the strengths of these two fields. Higher-order terms in λ lead to interactions between the hybrid-glueballs and can be taken into account systematically using perturbation theory in λ.

1 Introduction

The QCD action

$$\mathcal{S}[A, \psi, \overline{\psi}] \;=\; \int d^4x \left[-\frac{1}{4} F^a_{\mu\nu} F^{a\mu\nu} + \overline{\psi} \left(i\gamma^\mu D_\mu - m \right) \psi \right] \tag{1}$$

is invariant under the $SU(3)$ gauge transformations $U[\omega(x)] \equiv \exp(i\omega_a \tau_a/2)$

$$\psi^\omega(x) = U[\omega(x)] \, \psi(x), \qquad A^\omega_{a\mu}(x)\tau_a/2 = U[\omega(x)] \left(A_{a\mu}(x)\tau_a/2 + \frac{i}{g}\partial_\mu \right) U^{-1}[\omega(x)]. \tag{2}$$

Exploiting the time dependence of the gauge transformations (2) to put (see e.g. [1])

$$A_{a0} = 0 \;, \qquad a = 1, .., 8 \qquad \text{(Weyl gauge)}, \tag{3}$$

and quantising the dynamical variables A_{ai}, $-E_{ai}$, $\psi_{\alpha r}$ and $\psi_{\alpha r}^*$ in the Schrödinger functional approach by imposing equal-time (anti-) commutation relations (CR) , e.g. $-E_{ai} = -i\partial/\partial A_{ai}$, the physical states Φ have to satisfy both the Schrödinger equation and the Gauss laws

$$H\Phi = \int d^3x \left[\frac{1}{2}E_{ai}^2 + \frac{1}{2}B_{ai}^2[A] - A_{ai}\,j_{ia}(\psi) + \overline{\psi}\,(\gamma_i\partial_i + m)\,\psi \right] \Phi = E\Phi \ , \qquad (4)$$

$$G_a(x)\Phi = \left[D_i(A)_{ab}E_{bi} - \rho_a(\psi) \right]\Phi = 0 \ , \quad a = 1, .., 8 \ . \qquad (5)$$

The Gauss law operators G_a are the generators of the residual time independent gauge transformations in (2), satisfying $[G_a(x), H] = 0$ and $[G_a(x), G_b(y)] = if_{abc}G_c(x)\delta(x-y)$. Furthermore, H commutes with the angular momentum operators

$$J_i = \int d^3x \left[-\epsilon_{ijk}A_{aj}E_{ak} + \Sigma_i(\psi) + \text{orbital parts} \right] \ , \quad i = 1, 2, 3 \ . \qquad (6)$$

The matrix element of an operator O is given in the Cartesian form

$$\langle \Phi'|O|\Phi \rangle \propto \int dA\ d\overline{\psi}\ d\psi\ \Phi'^*(A, \overline{\psi}, \psi)\, O\, \Phi(A, \overline{\psi}, \psi) \ . \qquad (7)$$

The spectrum of Eqs.(4)-(5) for the case of Yang-Mills quantum mechanics of spatially constant gluon fields, was in [2] for $SU(2)$ and in [3] for $SU(3)$, in the context of a weak coupling expansion in $g^{2/3}$, using the variational approach with gauge-invariant wavefunctionals automatically satisfying (5). The corresponding unconstrained approach, a description in terms of gauge-invariant dynamical variables via the exact implementation of the Gaws laws, was considered by many authors (o.a. [1],[4]-[10], and references therein) to obtain a non-perturbative description of QCD at low energy, as an alternative to the lattice QCD.

I shall first discuss in Section 2 the unphysical, but a technically much simpler case of 2-colors, and then show in Section 3 how the results can be generalised to $SU(3)$.

2 Unconstrained Hamiltonian formulation of 2-color QCD

2.1 Canonical transformation to adapted coordinates

Point transformation from A_{ai}, ψ_α to a new set of adapted coordinates, the 3 angles q_j of an orthogonal matrix $O(q)$, the 6 elements of a pos. definite symmetric 3×3 matrix S, and new ψ'_β

$$A_{ai}(q, S) = O_{ak}(q)\,S_{ki} - \frac{1}{2g}\epsilon_{abc}\left(O(q)\,\partial_i O^T(q) \right)_{bc} \ , \quad \psi_\alpha(q, \psi') = U_{\alpha\beta}(q)\,\psi'_\beta \ , \qquad (8)$$

where the orthogonal $O(q)$ and the unitary $U(q)$ are related via $O_{ab}(q) = \frac{1}{2}\text{Tr}\,(U^{-1}(q)\tau_a U(q)\tau_b)$. Equation (8) is the generalisation of the (unique) polar decomposition of A and corresponds to

$$\chi_i(A) = \epsilon_{ijk}A_{jk} = 0 \quad (\text{"symmetric gauge"}). \qquad (9)$$

Preserving the CR, we obtain the old canonical momenta in terms of the new variables

$$-E_{ai}(q, S, p, P) = O_{ak}(q) \left[P_{ki} + \epsilon_{kil} {}^*D_{ls}^{-1}(S) \left(\Omega_{sj}^{-1}(q)p_j + \rho_s(\psi') + D_n(S)_{sm}P_{mn} \right) \right]. \quad (10)$$

In terms of the new canonical variables the Gauss law constraints are Abelianised,

$$G_a \Phi \equiv O_{ak}(q)\Omega_{ki}^{-1}(q)p_i \Phi = 0 \quad \Leftrightarrow \quad \frac{\delta}{\delta q_i}\Phi = 0 \quad \text{(Abelianisation)}, \quad (11)$$

and the angular momenta become

$$J_i = \int d^3x \left[-2\epsilon_{ijk}S_{mj}P_{mk} + \Sigma_i(\psi') + \rho_i(\psi') + \text{orbital parts} \right]. \quad (12)$$

Equation(11) identifies q_i with the gauge angles and S and ψ' as the physical fields. Furthermore, from Eq(12) follows that the S are colorless spin-0 and spin-2 glueball fields, and ψ' colorless reduced quark fields of spin-0 and spin-1. Hence, the gauge reduction corresponds to the conversion "color $\rightarrow$ spin". The obtained unusual spin-statistics relation is specific to SU(2).

2.2 Physical quantum Hamiltonian

According to the general scheme [1], the correctly ordered physical quantum Hamiltonian in terms of the physical variables $S_{ik}(\mathbf{x})$ and the canonically conjugate $P_{ik}(\mathbf{x}) \equiv -i\delta/\delta S_{ik}(\mathbf{x})$ reads [8]

$$H(S, P) = \frac{1}{2}\mathcal{J}^{-1} \int d^3\mathbf{x} \, P_{ai} \, \mathcal{J}P_{ai} + \frac{1}{2} \int d^3\mathbf{x} \left[B_{ai}^2(S) - S_{ai} \, j_{ia}(\psi') + \overline{\psi}' \left(\gamma_i \partial_i + m \right) \psi' \right]$$

$$- \mathcal{J}^{-1} \int d^3\mathbf{x} \int d^3\mathbf{y} \left\{ \left(D_i(S)_{ma}P_{im} + \rho_a(\psi') \right)(\mathbf{x})\mathcal{J} \right.$$

$$\left. \langle \mathbf{x} \, a|^*D^{-2}(S)|\mathbf{y} \, b \rangle \, \left(D_j(S)_{bn}P_{nj} + \rho_b(\psi') \right)(\mathbf{y}) \right\} \quad (13)$$

with the Faddeev-Popov (FP) operator

$$^*D_{kl}(S) \equiv \epsilon_{kmi}D_i(S)_{ml} = \epsilon_{kli}\partial_i - g(S_{kl} - \delta_{kl}\text{tr}S), \quad (14)$$

and the Jacobian $\mathcal{J} \equiv \det|^*D|$. The matrix element of a physical operator O is given by

$$\langle \Psi'|O|\Psi \rangle \propto \int_{S \text{ pos.def.}} \int_{\overline{\psi}',\psi'} \prod_{\mathbf{x}} \left[dS(\mathbf{x})d\overline{\psi}'(\mathbf{x})d\psi'(\mathbf{x}) \right] \mathcal{J}\Psi'^*[S, \overline{\psi}', \psi']O\Psi[S, \overline{\psi}', \psi']. \quad (15)$$

The inverse of the FP operator and hence the physical Hamiltonian can be expanded in the number of spatial derivatives equivalent to a strong coupling expansion in $\lambda = g^{-2/3}$.

2.3 Strong coupling expansion of the physical Hamiltonian in $\lambda = g^{-2/3}$

Introducing an UV cutoff a by considering an infinite spatial lattice of granulas $G(\mathbf{n}, a)$ at $\mathbf{x} = a\mathbf{n}$ ($\mathbf{n} \in Z^3$) and averaged variables

$$S(\mathbf{n}) := \frac{1}{a^3} \int_{G(\mathbf{n},a)} d\mathbf{x} \, S(\mathbf{x}) , \tag{16}$$

and discretised spatial derivatives, the expansion of the Hamiltonian in $\lambda = g^{-2/3}$ can be written

$$H = \frac{g^{2/3}}{a} \left[\mathcal{H}_0 + \lambda \sum_\alpha \mathcal{V}_\alpha^{(\partial)} + \lambda^2 \left(\sum_\beta \mathcal{V}_\beta^{(\Delta)} + \sum_\gamma \mathcal{V}_\gamma^{(\partial\partial \neq \Delta)} \right) + \mathcal{O}(\lambda^3) \right] . \tag{17}$$

The "free" Hamiltonian $H_0 = (g^{2/3}/a)\mathcal{H}_0 + H_m = \sum_\mathbf{n} H_0^{QM}(\mathbf{n})$ is the sum of the Hamiltonians of Dirac-Yang-Mills quantum mechanics of constant fields in each box, and the interaction terms $\mathcal{V}^{(\partial)}, \mathcal{V}^{(\Delta)}, ..$ leading to interactions between the granulas.

2.4 Zeroth-order: Dirac-Yang-Mills quantum mechanics of spatially constant fields

Transforming to the intrinsic system of the symmetric tensor S, with Jacobian $\sin\beta \prod_{i<j}(\phi_i - \phi_j)$,

$$S = R^T(\alpha, \beta, \gamma) \, \text{diag}(\phi_1, \phi_2, \phi_3) \, R(\alpha, \beta, \gamma), \qquad \psi_{L,R}^{\prime(i)} = R_{ij}^T \widetilde{\psi}_{L,R}^{(j)}, \qquad \psi_{L,R}^{\prime(0)} = \widetilde{\psi}_{L,R}^{(0)}, \tag{18}$$

the "free" Hamiltonian in each box (volume V) takes the form [9]

$$H_0^{QM} = \frac{g^{2/3}}{V^{1/3}} \left[\mathcal{H}^G + \mathcal{H}^D + \mathcal{H}^C \right] + \frac{1}{2} m \left[\left(\widetilde{\psi}_L^{(0)\dagger} \widetilde{\psi}_R^{(0)} + \sum_{i=1}^3 \widetilde{\psi}_L^{(i)\dagger} \widetilde{\psi}_R^{(i)} \right) + h.c. \right], \tag{19}$$

with the glueball part $\mathcal{H}^G$, the minimal-coupling $\mathcal{H}^D$, and the Coulomb-potential-type part $\mathcal{H}^C$

$$\mathcal{H}^G = \frac{1}{2} \sum_{ijk}^{\text{cyclic}} \left(-\frac{\partial^2}{\partial\phi_i^2} - \frac{2}{\phi_i^2 - \phi_j^2} \left(\phi_i \frac{\partial}{\partial\phi_i} - \phi_j \frac{\partial}{\partial\phi_j} \right) + (\xi_i - \widetilde{J}_i^Q)^2 \frac{\phi_j^2 + \phi_k^2}{(\phi_j^2 - \phi_k^2)^2} + \phi_j^2\phi_k^2 \right), \tag{20}$$

$$\mathcal{H}^D = \frac{1}{2}(\phi_1 + \phi_2 + \phi_3)\left(\widetilde{N}_L^{(0)} - \widetilde{N}_R^{(0)} \right) + \frac{1}{2} \sum_{ijk}^{\text{cyclic}} (\phi_i - (\phi_j + \phi_k))\left(\widetilde{N}_L^{(i)} - \widetilde{N}_R^{(i)} \right), \tag{21}$$

$$\mathcal{H}^C = \sum_{ijk}^{\text{cyclic}} \frac{\widetilde{\rho}_i(\xi_i - \widetilde{J}_i^Q + \widetilde{\rho}_i)}{(\phi_j + \phi_k)^2} , \tag{22}$$

and the total spin

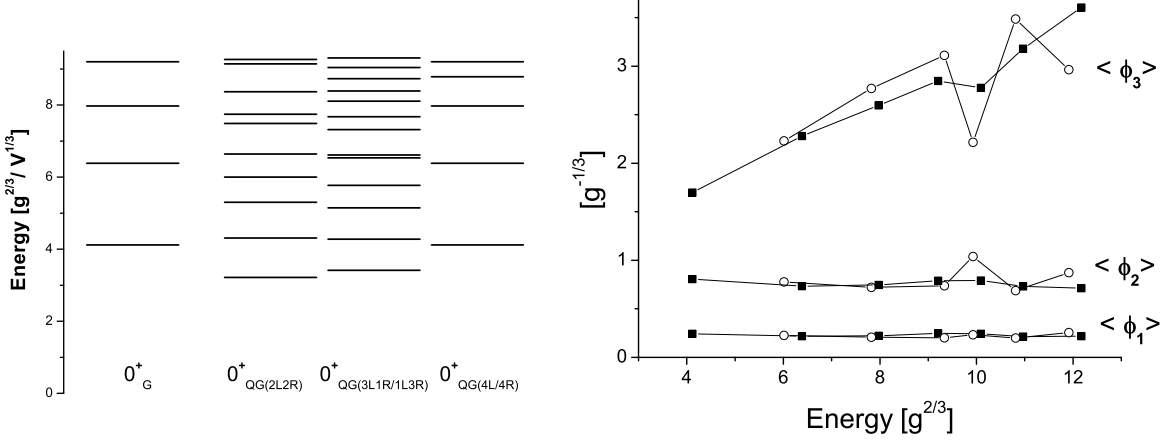$$J_i = R_{ij}(\chi) \, \xi_j , \qquad [J_i, H] = 0 . \tag{23}$$

Figure 1: L.h.s.: Lowest energy levels for the pure-gluon (G) and the quark-gluon case (QG) for 2-colors and one quark flavor. The energies of the quark-gluon ground state and the sigma-antisigma excitation are lower than that of the lowest pure-gluon state. R.h.s. (for pure-gluon case and $V \equiv 1$): $\langle\phi_3\rangle$ is raising with increasing excitation, whereas $\langle\phi_1\rangle$ and $\langle\phi_2\rangle$ are practically constant, independent of whether spin-0 (dark boxes) or spin-2 states (open circles).

The matrix elements become

$$\langle\Phi_1|\mathcal{O}|\Phi_2\rangle = \int d\alpha \sin\beta d\beta d\gamma \int_{0<\phi_1<\phi_2<\phi_3} d\phi_1 d\phi_2 d\phi_3 \ (\phi_1^2-\phi_2^2)(\phi_2^2-\phi_3^2)(\phi_3^2-\phi_1^2) \int d\overline{\psi}' d\psi' \Phi_1^* \mathcal{O}\Phi_2 \ .$$

The l.h.s. of Fig.1 shows the 0^+ energy spectrum of the lowest pure-gluon (G) and quark-gluon (QG) cases for one quark-flavor which can be calculated with high accuracy using the variational approach. The energies of the quark-gluon ground state and the sigma-antisigma excitation are lower than that of the lowest pure-gluon state. This is due to a large negative contribution from $\langle\mathcal{H}^D\rangle$, in addition to the large positive $\langle\mathcal{H}^G\rangle$, while $\langle\mathcal{H}^C\rangle \simeq 0$ (see [9] for details).

Furthermore, as a consequence of the zero-energy valleys "$\phi_1 = \phi_2 = 0, \ \phi_3$ arbitrary" of the classical magnetic potential $B^2 = \phi_2^2\phi_3^2 + \phi_3^2\phi_1^2 + \phi_1^2\phi_2^2$, practically all glueball excitation-energy results from an increase of expectation value of the "constant Abelian field" ϕ_3 as shown for the pure-gluon case on the r.h.s. of Fig.1 (see [7] for details).

2.5 Perturbation theory in λ and coupling constant renormalisation in the IR

Including the interactions $\mathcal{V}^{(\partial)}, \mathcal{V}^{(\Delta)}$ by using the 1st and 2nd order perturbation theory in $\lambda = g^{-2/3}$ give the result [8] (for the pure-gluon case and only including spin-0 fields in the first approximation)

$$E_{\text{vac}}^+ = \mathcal{N}\frac{g^{2/3}}{a}\left[4.1167 + 29.894\lambda^2 + \mathcal{O}(\lambda^3)\right], \tag{24}$$

$$E_1^{(0)+}(k) - E_{\text{vac}}^+ = \left[\ 2.270 + 13.511\lambda^2 + \mathcal{O}(\lambda^3)\right]\frac{g^{2/3}}{a} + 0.488\frac{a}{g^{2/3}}k^2 + \mathcal{O}((a^2k^2)^2) \tag{25}$$

for the energy of the interacting glueball vacuum and the spectrum of the interacting spin-0 glueball. Lorentz invariance demands $E = \sqrt{M^2 + k^2} \simeq M + \frac{1}{2M} k^2$, which is violated in this 1st approximation by a factor of 2. In order to get a Lorentz invariant result, $J = L + S$ states should be considered including also spin-2 states and the general $\mathcal{V}^{(\partial\partial)}$.

Independence of the physical glueball mass

$$M = \frac{g_0^{2/3}}{a} \left[\mu + c g_0^{-4/3} \right]$$

of box size a leads to

$$\gamma(g_0) \equiv a \frac{d}{da} g_0(a) = \frac{3}{2} g_0 \frac{\mu + c g_0^{-4/3}}{\mu - c g_0^{-4/3}} \tag{26}$$

which vanishes for $g_0 = 0$ (pert. fixed point) or $g_0^{4/3} = -c/\mu$ (IR fixed point, if $c < 0$). For $c > 0$

$$\text{for } c > 0 : \qquad g_0^{2/3}(Ma) = \frac{Ma}{2\mu} + \sqrt{\left(\frac{Ma}{2\mu}\right)^2 - \frac{c}{\mu}} , \qquad a > a_c := 2\sqrt{c\mu}/M \tag{27}$$

My (incomplete) result $c_1^{(0)}/\mu_1^{(0)} = 5.95$ suggests that no IR fixed points exist. Critical coupling $g_0^2|_c = 14.52$ and $a_c \sim 1.4$ fm for $M \sim 1.6$ GeV.

Hence, using strong coupling expansion, the difficult questions of Lorentz invariance and coupling constant renormalisation in the IR can be studied in a systematic way.

3 Symmetric gauge for SU(3)

Using the idea of *minimal embedding* of $su(2)$ in $su(3)$ by Kihlberg and Marnelius [4]

$$\tau_1 := \lambda_7 = \begin{pmatrix} 0 & 0 & 0 \\ 0 & 0 & -i \\ 0 & i & 0 \end{pmatrix} \quad \tau_2 := -\lambda_5 = \begin{pmatrix} 0 & 0 & i \\ 0 & 0 & 0 \\ -i & 0 & 0 \end{pmatrix} \quad \tau_3 := \lambda_2 = \begin{pmatrix} 0 & -i & 0 \\ i & 0 & 0 \\ 0 & 0 & 0 \end{pmatrix}$$

$$\tau_4 := \lambda_6 = \begin{pmatrix} 0 & 0 & 0 \\ 0 & 0 & 1 \\ 0 & 1 & 0 \end{pmatrix} \quad \tau_5 := \lambda_4 = \begin{pmatrix} 0 & 0 & 1 \\ 0 & 0 & 0 \\ 1 & 0 & 0 \end{pmatrix} \quad \tau_6 := \lambda_1 = \begin{pmatrix} 0 & 1 & 0 \\ 1 & 0 & 0 \\ 0 & 0 & 0 \end{pmatrix}$$

$$\tau_7 := \lambda_3 = \begin{pmatrix} 1 & 0 & 0 \\ 0 & -1 & 0 \\ 0 & 0 & 0 \end{pmatrix} \quad \tau_8 := \lambda_8 = \frac{1}{\sqrt{3}} \begin{pmatrix} 1 & 0 & 0 \\ 0 & 1 & 0 \\ 0 & 0 & -2 \end{pmatrix} \tag{28}$$

such that the corresponding non-trivial non-vanishing structure constants, $\left[\frac{\tau_a}{2}, \frac{\tau_b}{2}\right] = i c_{abc} \frac{\tau_c}{2}$, have at least one index $\in \{1, 2, 3\}$, the symmetric gauge, Eq.(9), can be generalised to $SU(3)$ [5, 10],

$$\chi_a(A) = \sum_{b=1}^{8} \sum_{i=1}^{3} c_{abi} A_{bi} = 0 , \quad a = 1, ..., 8 \qquad (\text{"symmetric gauge" for SU(3)}). \tag{29}$$

Carrying out the coordinate transformation [10]

$$A_{ak}\left(q_1,..,q_8,\widehat{S}\right) = O_{a\hat{a}}(q)\,\widehat{S}_{\hat{a}k} - \frac{1}{2g}c_{abc}\left(O(q)\,\partial_k O^T(q)\right)_{bc}, \quad \psi_\alpha\left(q_1,..,q_8,\psi^{RS}\right) = U_{\alpha\hat{\beta}}(q)\,\psi_{\hat{\beta}}^{RS}$$

$$\widehat{S}_{\hat{a}k} \equiv \begin{pmatrix} S_{ik} \\ \overline{S}_{Ak} \end{pmatrix} = \begin{pmatrix} \multicolumn{3}{c}{S_{ik} \text{ pos. def.}} \\ \hline W_0 & X_3 - W_3 & X_2 + W_2 \\ X_3 + W_3 & W_0 & X_1 - W_1 \\ X_2 - W_2 & X_1 + W_1 & W_0 \\ -\frac{\sqrt{3}}{2}Y_1 - \frac{1}{2}W_1 & \frac{\sqrt{3}}{2}Y_2 - \frac{1}{2}W_2 & W_3 \\ -\frac{\sqrt{3}}{2}W_1 - \frac{1}{2}Y_1 & \frac{\sqrt{3}}{2}W_2 - \frac{1}{2}Y_2 & Y_3 \end{pmatrix}, \quad c_{\hat{a}\hat{b}k}\widehat{S}_{\hat{b}k} = 0 , \qquad (30)$$

an unconstrained Hamiltonian formulation of QCD can be obtained. The existence and uniqueness of (30) can be investigated by solving 16 equations.

$$\widehat{S}_{\hat{a}i}\widehat{S}_{\hat{a}j} = A_{ai}A_{aj} \text{ (6 equs.)} \quad \wedge \quad d_{\hat{a}\hat{b}\hat{c}}\widehat{S}_{\hat{a}i}\widehat{S}_{\hat{b}j}\widehat{S}_{\hat{c}k} = d_{abc}A_{ai}A_{bj}A_{ck} \text{ (10 equs.)} \qquad (31)$$

for 16 components of $\widehat{S}$ in terms of 24 given components A.

Analysing the Gauss law operators and the unconstrained angular momentum operators in terms of the new variables by analogy to the 2-color case, it can be shown that the original constrained 24 colored spin-1 gluon fields A and 12 colored spin-1/2 quark fields ψ (per flavor) reduce to 16 physical colorless spin-0, spin-1, spin-2, and spin-3 glueball fields (16 components of $\widehat{S}$) and a colorless spin-3/2 Rarita-Schwinger field ψ^{RS} (per flavor), respectively. As for the 2-color case, the gauge reduction converts color $\rightarrow$ spin, which might have important consequences for low energy Spin-Physics. In terms of the colorless Rarita-Schwinger fields $\Delta^{++}(3/2)$ could have the spin content $(+3/2, +1/2, -1/2)$ in accordance with the Spin-Statistics-Theorem.

Transforming to the intrinsic system of the embedded upper part S of $\widehat{S}$ (see [10] for details)

$$S = R^T(\alpha, \beta, \gamma)\,\text{diag}(\phi_1, \phi_2, \phi_3)\,R(\alpha, \beta, \gamma), \quad \wedge \quad X_i \rightarrow x_i, \; Y_i \rightarrow y_i,.., \quad \wedge \quad \psi^{RS} \rightarrow \widetilde{\psi}^{RS}, (32)$$

one finds that the magnetic potential B^2 has the zero-energy valleys ("constant Abelian fields")

$$B^2 = 0 \;\; : \;\; \phi_3 \text{ and } y_3 \text{ arbitrary} \quad \wedge \quad \text{all others zero} \qquad (33)$$

Hence, practically all glueball excitation-energy should result from an increase of expectation values of these two "constant Abelian fields", by analogy to $SU(2)$. Furthermore, at the bottom of the valleys the important minimal-coupling-interaction of $\widetilde{\psi}^{RS}$ (analogous to (21)) becomes diagonal

$$\mathcal{H}_{\text{diag}}^D = \frac{1}{2}\widetilde{\psi}_L^{(1,\frac{1}{2})\dagger}\left[(\phi_3\lambda_3 + y_3\lambda_8) \otimes \sigma_3\right]\widetilde{\psi}_L^{(1,\frac{1}{2})} - \frac{1}{2}\widetilde{\psi}_R^{(\frac{1}{2},1)\dagger}\left[\sigma_3 \otimes (\phi_3\lambda_3 + y_3\lambda_8)\right]\widetilde{\psi}_R^{(\frac{1}{2},1)} . \qquad (34)$$

Due to the difficulty of the FP-determinant (see [10]), precise calculations are not possible yet, but are, in my opinion, a solvable future task.

[1] N.H. Christ and T.D. Lee, Phys. Rev. D **22** (1980) 939.

[2] M. Lüscher and G. Münster, Nucl. Phys. B **232** (1984) 445.

[3] P. Weisz and V. Ziemann, Nucl. Phys. B **284** (1987) 157.

[4] A. Kihlberg and R. Marnelius, Phys. Rev. D **26** (1982) 2003.

[5] B. Dahmen and B. Raabe, Nucl. Phys. B **384** (1992) 352.

[6] A.M. Khvedelidze and H.-P. Pavel, Phys. Rev. D **59** (1999) 105017.
   A.M. Khvedelidze, D. M. Mladenov, H.-P. Pavel, G. Röpke, Phys. Rev. D **67** (2003) 105013.

[7] H.-P. Pavel, Phys. Lett. B **648** (2007) 97.

[8] H.-P. Pavel, Phys. Lett. B **685** (2010) 353.

[9] H.-P. Pavel, Phys. Lett. B **700** (2011) 265.

[10] H.-P. Pavel, *Unconstrained Hamiltonian formulation of low energy SU(3) Yang-Mills quantum theory*, arXiv: 1205.2237 [hep-th] (2012).

PRODUCTION OF MESON IN TAU LEPTON DECAYS AND ELECTRON-POSITRON COLLISIONS AND BEHAVIOR OF MESONS IN HOT DENSE MATTER

M.K. Volkov[a]

[a] Bogoliubov Laboratory of Theoretical Physics, JINR, Dubna 141980, Russia

At the present time, there is a vast amount of experimental data on processes of meson production in electron-positron collisions with an energy up to 2 GeV as well as in τ lepton decays [1]. However, the problem of theoretical description of these processes is still under investigation. Really, fundamental perturbative QCD theory is not applicable in this energy region. So a set of phenomenological models is used based as a rule on the chiral symmetry of strong interactions. The typical drawback of these models is the presence of a rather large number of arbitrary parameters decreasing the predictive ability. Among these models, a special place is occupied by the standard chiral Nambu-Jona-Lasinio (NJL) model [2-4]. It is based on the effective chiral-symmetric four-quark interactions of scalar, pseudoscalar, vector, and axial-vector types.

In the case of the $U(3) \times U(3)$ chiral symmetry, this model contains seven parameters: masses of constituent quarks $m_u = 280$ MeV, $m_d = 284$ MeV, $m_s = 406$ MeV, the cut-off parameter $\Lambda = 1.24$ GeV, the 't Hooft interaction constant and two constants of 4-quark interactions $G_S = G_P = G_1$, $G_V = G = G_2$. These parameters are used to describe the mass spectrum of 4 meson nonets (scalar, pseudoscalar, vector, and axial-vector ones), as well as their strong and electromagnetic interactions such as radii, polarizabilities etc. Note that constants G_1 and G_2 appear only in the calculation of the constituent quarks masses. Other parameters are used to describe meson interactions. In the case of the $SU(2) \times SU(2)$ chiral symmetry, only two parameters remain $m_u = m_d \equiv m$ and Λ. The extended NJL model developed in papers [5,6] allows one to consider apart from the ground meson states also the radial-excited ones. For the description of 4 nonets of excited mesons two additional parameters G_1' and G_2' are used, they are fixed with the help of the first radial excited pion and ρ meson masses. In the series of our studies [7-15], carried out during the last two years, the ability of this extended model to describe various processes in accordance with the existing experimental data was shown. It is important to note that this model is used in the mean field approximation. It means that only quark loops are considered, which corresponds to the lowest order in the $1/N_c$ expansion (N_c is the number of colors). Besides, only the real parts of the corresponding loop amplitudes are taken into account. Photoproduction of pions and eta mesons (the Primakoff effect) in the ground and excited states was considered in [7-12]. Similar processes were studied in the case of colliding e^+e^- beams. In these papers, the processes $e^+e^- \to \pi^0(\pi^{0\prime})\gamma$; $\pi^0\omega$; $\pi^0\rho^0$; $\pi\pi$ and $\pi\pi(1300)$ were investigated. Here, an important role is played by intermediate states of ρ^0, ω, ϕ vector mesons and their excited states. Note that the conversion of a virtual photon into a vector meson of the kind $\gamma \to \rho$, ω, ϕ, ρ', ω' can be unambiguously described in terms of logarithmically divergent quark loop amplitudes using the cut-off parameter Λ.

During 2012 in works [13-15], we continued theoretical description of τ lepton decays with production of $\pi\pi\nu$, $\pi\pi(1300)\nu$, $\pi\omega\nu$, $\pi\eta\nu$, and $\pi\eta'\nu$. The transitions of type $W^- \to \rho^-$ and $\rho^-(1450)$ are similar to the $\gamma \to \rho^0$ one, are also described by means of quark

loops. Note that probabilities of the decay processes $\tau \to \eta(\eta')\nu$ turn out to be suppressed in accordance with experimental data. Such suppression is caused by the difference of light quark mass providing the transitions $W^- \to a_0^-$ and $p^0 \to \eta$ through quark loops. In particular, the branching ratio $\text{Br}(\tau \to \eta\pi\nu) = 4.7 \cdot 10^{-6}$ received in [15] does not exceed the current experimental upper limit [1] being equal to $9.9 \cdot 10^{-5}$.

Besides, in Refs.[17-18] the behavior of mesons in hot dense matter was studied in the frames of an extended NJL model with Polyakov loops. A nonlocal chiral quark model is consistently extended beyond the mean field using a strict $1/N_c$ expansion scheme. The parameters of the nonlocal model are refitted so that the physical values of the pion mass and the weak pion decay constant are obtained. The size of the 1/Nc correction to the quark condensate is carefully studied and compared with the usual local NambuJona-Lasinio model. It is found that even the sign of the corrections can be different. This can be attributed to the mesonic cutoff of the local model. The model is also applied to finite temperature. We find that the $1/N_c$ corrections dominate the melting of the chiral condensate at low temperatures, $T \lesssim 100$ MeV, in agreement with chiral perturbation theory. On the other hand, the relative importance of the 1/Nc corrections in the crossover regime depends on the parameter T0 of the Polyakov-loop potential. For $T_0 = 270$ MeV, corresponding to a fit of lattice data for pure gluodynamics, the correction terms are large and lead to a lowering of the chiral phase-transition temperature in comparison with the mean-field result. Near the phase transition the $1/N_c$ expansion breaks down and a nonperturbative scheme is needed to include mesonic correlations in that regime. Lowering T_0 leads to a more rapid crossover even at the mean-field level and the unstable region for the $1/N_c$ corrections shrinks. For $T_0 \lesssim 220$ MeV the temperatures of deconfinement and chiral restoration are practically synchronized.

Bibliography

[1] J. Beringer et al., [Particle Data Group Coll.], Phys. Rev. D 86, 010001 (2012).

[2] M.K. Volkov, Sov. J. Part. Nucl. 17, 186 (1986).

[3] D. Ebert, H. Reinhardt and M.K. Volkov, Prog. Part. Nucl. Phys. 33, 1 (1994).

[4] M.K. Volkov, A.E. Radzhabov, Phys. Usp. 49, 551 (2006).

[5] M.K. Volkov, C. Weiss, Phys. Rev. D 56, 221 (1997).

[6] M.K. Volkov, Phys. Atom. Nucl. 60, 997 (1997).

[7] E.A. Kuraev, M.K. Volkov, Phys. Lett. B 682, 212 (2009).

[8] A.B. Arbuzov, M.K. Volkov, Phys. Rev. C 84, 058201 (2011).

[9] A.B. Arbuzov, E.A. Kuraev, M.K. Volkov, Eur. Phys. J.A 47, 103 (2011).

[10] A.B. Arbuzov, E.A. Kuraev, M.K. Volkov, Phys. Rev. C 83, 048201 (2011).

[11] A.I. Ahmadov, E.A. Kuraev, M.K. Volkov, Int. J. Mod. Phys. A 26, 3337 (2011).

[12] M.K. Volkov, D.G. Kostunin, Phys. Rev. C 86, 025502 (2012).

[13] M.K. Volkov, D.G. Kostunin, arXiv: 1202.0506 [hep-ph] (2012).

[14] M.K. Volkov, A.B. Arbuzov, D.G. Kostunin, Phys. Rev. D 86, 057301 (2012).

[15] M.K. Volkov, D.G. Kostunin, Phys. Rev. D 86, 013005 (2012).

[16] Yu.P. Ivanov, A.A. Osipov, M.K. Volkov, Phys. Lett. B 242, 498 (1990); Z. Phys. C 49, 563 (1991).

[17] A.E. Radzhabov, D. Blaschke, M. Buballa and M.K. Volkov, Phys. Rev. D **83**,

116004 (2011).

[18] D. Blaschke, M. Buballa, A.E. Radzhabov and M.K. Volkov, Phys. Atom. Nucl. **75**, 738 (2012).

Multiquark states in the covariant quark confinement model.

M.A. Ivanov

The covariant quark model with infrared confinement developed in a series of papers (see Refs. [1]-[5]) is a successful tool for a unified description of the multiquark states: mesons, baryons, tetraquarks, etc. The covariant quark model is an effective quantum field approach to hadronic interactions based on the interaction Lagrangian between hadrons and their constituent quarks. Knowing the corresponding interpolating quark current allows calculating the matrix element of physical processes in a consistent way. A distinctive feature of this approach is that the multiquark states, such as baryons (three quarks), tetraquarks (four quarks), etc., can be considered and described as rigorously as the simplest quark-antiquark systems (mesons). The coupling constants between hadrons and their interpolating quark currents are determined from the compositeness condition $Z_H = 0$. The matrix elements of physical processes are determined by a set of associated quark diagrams, which are constructed according to $1/N_c-$expansion. In the covariant quark model an infrared cutoff is effectively introduced in the space of Fock–Schwinger parameters which are integrated out in the expressions for the matrix elements. Such a procedure allows one to eliminate all the threshold singularities associated with quark production and thereby ensures quark confinement. The model has no ultraviolet divergences due to vertex hadron–quark form factors which describe a nonlocal structure of hadrons. The covariant quark model has a few free parameters: the mass of constituent quarks, the infrared cutoff parameter that characterizes the confinement region, and the parameters that describe an effective size of hadrons.

The last applications of the covariant quark model are devoted to studying the properties of the B_s-meson, the light baryons and tetraquarks. The form factors of the $B(B_s) \to P(V)-$transitions are evaluated in the full kinematic region of momentum transfer squared. As an application of the obtained results, the widths of the B_s-nonleptonic decays are calculated. The modes $D_s^- D_s^+$, $D_s^{*-} D_s^+ + D_s^- D_s^{*+}$ and $D_s^{*-} D_s^{*+}$ give the largest contribution to $\Delta\Gamma$ for the $B_s - \bar{B}_s$ system. The mode $J/\psi\phi$ is suppressed by the color factor but it is interesting for the search of CP-violating New-Physics possible effects in the $B_s - \bar{B}_s$ mixing.

The static properties of the proton, neutron, and the Λ-hyperon (magnetic moments and charge radii) and the behavior of the nucleon form factors at low momentum transfers are described. The conservation of gauge invariance of the electromagnetic transition matrix elements in the presence of a nonlocal coupling of the baryons to the three constituent quark fields is discussed.

The consequences of treating the X(3872) meson as a tetraquark bound state are explored. The decay widths of the observed channels $X \to J/\psi + 2\pi(3\pi)$ and $X \to \bar{D}^0 + D^0 + \pi^0$ via the intermediate off–shell states $X \to J/\psi + \rho(\omega)$ and $X \to \bar{D} + D^*$ are calculated. Its one-photon decay $X \to \gamma + J/\psi$ is also analyzed. The matrix element of the transition $X \to \gamma + J/\psi$ is calculated and its gauge invariance is proved. For reasonable values of the size parameter Λ_X of the X(3872) consistency with the available experimental data is found. The possible impact of X(3872) in a s-channel dominance description of the J/ψ dissociation cross section is clarified.

[1] T. Branz, A. Faessler, T. Gutsche, M. A. Ivanov, J. G. Körner and V. E. Lyubovitskij, Phys. Rev. D **81** (2010) 034010.

[2] S. Dubnicka, A. Z. Dubnickova, M. A. Ivanov and J. G. Körner, Phys. Rev. D **81** (2010) 114007.

[3] S. Dubnicka, A. Z. Dubnickova, M. A. Ivanov, J. G. Körner and G. G. Saidullaeva, AIP Conf. Proc. **1343** (2011) 385.

[4] S. Dubnicka, A. Z. Dubnickova, M. A. Ivanov, J. G. Koerner, P. Santorelli and G. G. Saidullaeva, Phys. Rev. D **84** (2011) 014006.

[5] T. Gutsche, M. A. Ivanov, J. G. Körner, V. E. Lyubovitskij and P. Santorelli, Phys. Rev. D **86** (2012) 074013.

Precision spectroscopy of light atoms and molecules.

V.I. Korobov

Recently, at CERN new data on the antiproton-to-electron mass ratio have been obtained with high precision of 10^{-9} [1]. To this end, the two-photon spectroscopy of the antiprotonic helium was used for the first time.

At present, theoretical precision is at the same level as experimental one and further progress in determination of the antiproton mass (or, assuming validity of CPT invariance, the atomic mass of electron) would require serious improvements in theoretical studies.

One of the bottlenecks in theory is the numerical calculation of the nonrelativistic Bethe logarithm for metastable (resonant) states. This requires new approaches that may use the Complex Coordinate Rotation (CCR) formalism. Such methods should be based on the generalization of the perturbation theory (second order) to be applied to a CCR solution of a resonant state.

In 2011–12, a new general procedure to evaluate the nonrelativistic Bethe logarithm for a general few–body atomic or molecular bound system was suggested by us [2]. The ground states of a helium atom and H_2^+ molecular ion were used as benchmark calculations. The obtained values are: $\beta_{\mathrm{He}} = 4.37016022306(2)$ for the helium atom and $\beta_{H_2^+} = 3.012230335(1)$ for H_2^+. Both the results substantially improve the best known data for these quantities [3].

This method was generalized to the CCR formalism. At present, calculations of the leading order radiative correction for the metastable (resonant) states of antiprotonic helium atoms are being carried out [4] and soon should become available with required precision.

[1] M. Hori *et al.*, Nature **475**, 484 (2011).

[2] V.I. Korobov, Phys. Rev. A **85**, 042514 (2012).

[3] V.I. Korobov and Zhen-Xiang Zhong, Phys. Rev. A **86**, 044501 (2012).

[4] V.I. Korobov, *Nonrelativistic Bethe logarithm for metastable states in antiprotonic helium*, in preparation.

Dynamics of composed systems under action of fast particles and external fields

S.I. Vinitsky[1], A.A. Gusev[2], O. Chuluunbaatar[2], V.V. Serov[3]
[1]Bogoliubov Laboratory of Theoretical Physics and [2]Laboratory of Information Technologies, Joint Institute for Nuclear Research, Dubna
[3]Chair of Theoretical Physics, Physics Department, Saratov State University, Saratov

A review of some recently developed methods of calculating multiple differential cross-sections of photoionization and electron impact ionization of atoms and molecules having two active electrons was presented [1]. The methods imply original approaches to calculating three-particle Coulomb wave functions. The external complex scaling method and the formalism of the Schrödinger equation with a source in the right-hand side was considered. Efficiency of the time-dependent approaches to the scattering problem, such as the paraxial approximation and the time-dependent scaling, was demonstrated. An original numerical method elaborated by the authors for solving the 6D Schrödinger equation for an atom with two active electrons, based on the Chang-Fano transformation and the discrete variable representation, was formulated. By comparison of the results of different authors the preference of using spheroidal coordinates for calculation of ionization diatomic molecules in comparison with spherical ones was shown. Basing on numerical simulations, the threshold behavior of angular distributions of the two-electron photoionization of the negative hydrogen ion and helium atom, and multiple differential cross-sections of electron impact ionization of hydrogen and nitrogen molecules were analyzed and compared with experimental data. The most essential physical results which are obtained by the authors of the present review by means of the methods explained in it are:

1. It was shown that the Wannier law for the angular distribution of double ionization is not correct even at very small energies.

2. Direct connection of a number of peaks in the symmetric double an ionization amplitude with a number of nodes of the initial state wave function was revealed.

3. It was shown that the deviations of angular distribution of ejected electrons in ionization process of atoms and two atomic molecules by electron impact of the intermediate energy, from the results calculated in the first Born approximation are generally caused by interaction of an ejected electron with a scattering electron after ejection.

4. It was shown that contrary to expectations, the bidipole second Born terms, describing sequential double ionization by electron impact of the intermediate energy, does not make an essential contribution to multiple differential cross-section.

5. For hydrogen molecule with a nonequilibrium distance between atoms it was shown that the interference of the electrons which were let out by the different centers at single-pass ionization significantly influences probability of the double ionization and angular distribution of the electrons which were taken off at the double ionization. It opens a possibility for experimental observation of the dependence of a two-center interference from a nuclear distance as double ionization is accompanied by dissociation after which it is possible to determine the initial nuclear distance by the energy of scattered protons.

The adiabatic method for analysis of a quantum tunneling model of a coupled pair of identical and nonidentical ions was developed [2]. Symbolic-numerical algorithms for

solving a boundary value problem (BVP) for the 2D Schrödinger equation with the homogeneous third type boundary conditions were elaborated [3]. The Kantorovich reduction of the above problem with non-symmetric long-range potentials to the BVPs for sets of the second order ordinary differential equations (ODEs) was given by expanding solution over the one-parametric set of basis functions. Symbolic algorithms for evaluation of asymptotics of the basis functions, effective potentials, and linear independent solutions of the ODEs in the form of inverse power series of independent variable at large values are given by using appropriate etalon equations. The elaborated scheme was applied to analyze a quantum tunneling problem of a coupled pair of identical ions through Coulomb-like barrier. It was shown that the total transmission coefficient demonstrates the resonance behavior due to the existence of barrier quasistationary states, imbedded in the continuum. The effect of quantum transparency manifesting itself in the nonmonotonic resonance-type dependence of the transmission coefficient upon the energy of the particles was revealed.

Within the effective mass approximation, an adiabatic description of spheroidal and dumbbell quantum dot models in the regime of strong dimensional quantization was formulated using the expansion of the wave function in appropriate sets of single-parameter basis functions. The comparison was given and the peculiarities were considered for spectral and optical characteristics of the models with axially symmetric confining potentials depending on their geometric size, making use of the complete sets of exact and adiabatic quantum numbers in appropriate analytic approximations[4]. The absorption coefficients for ensembles of spheroidal quantum dots (SQDs) were analyzed using the eigenvalues and eigenfunctions calculated by means of the Kantorovich and adiabatic methods. The comparison of absorption coefficients for oblate and prolate SQDs with random dimensions of the minor semiaxis, and with parabolic and non-parabolic dispersion laws, revealed different behavior depending on the aspect ratio (ratio of minor to major semiaxe) and the external homogeneous electric fields. Such behavior leads to a possibility of verification of the quantum-size Stark effect in the considered models of semiconductor SQDs [5].

The adiabatic method for analysis of the problem describing the impurity states of a quantum wire or a hydrogen-like atom in a strong homogeneous magnetic field was developed [6]. The analytical and numerical scheme for solving of the boundary value problem for the Schrödinger equation in cylindrical coordinates was elaborated. It was solved by applying the Kantorovich method that reduces the problem to the boundary-value problem for a set of ordinary differential equations with respect to the longitudinal variables. The effective potentials of these equations were given by integrals over the transverse variable. The integrands are products of the transverse basis functions depending on the longitudinal variable as a parameter and their first derivatives. To solve the problem at high magnetic quantum numbers $|m|$ and study its solutions, we presented an algorithm implemented in Maple, which allows one to obtain analytic expressions for the effective potentials and for the transverse dipole moment matrix elements. The efficiency and accuracy of the derived algorithm and that of the Kantorovich numerical scheme were confirmed by calculating eigenenergies and eigenfunctions, dipole moments and decay rates of low-excited Rydberg states at high $|m| \sim 200$ of a hydrogen atom in the laboratory homogeneous magnetic field $\gamma \sim 2.35 \cdot 10^{-5}$ ($B \sim 6$T). To analyze the low-excited Rydberg states of a system like this it is useful to have the solution in an an-

alytic form. Indeed, for high $|m|$ we can consider the Coulomb potential as perturbation with respect to the transversal centrifugal potential and the oscillator potential with the frequency $\omega_\rho = \gamma/2$. For the laboratory magnetic field $B = B_0\gamma \sim 6$T, this is true at the adiabatic parameter values $\tilde{m} \sim 5.89$, where $\tilde{m}$ is defined as $\tilde{m} = (\omega_\rho/\omega_z)^{4/3} = |m|\gamma^{1/3}$. The proposed scheme explains not only transition to the adiabatic limit (diagonal representation), but predicts the existence of maximum of the photoionization cross-section of an electron or the capture rate of an electron of the continuous spectrum at a fixed value of a magnetic field B in the region of variation of the magnetic quantum number $|m|$ bounded by value of the adiabatic parameter $\tilde{m} = |m|\gamma^{1/3}$.

[1] V.V. Serov, V.L. Derbov, T.A. Sergeeva, S.I. Vinitsky, arXiv:1210.3046 (2012); Submitted to "Physics of Elementary Particles and Atomic Nuclei".

[2] A.A. Gusev, S.I. Vinitsky, O. Chuluunbaatar, V.P. Gerdt, V.A. Rostovtsev, Lecture Notes in Computer Science, **6885** (2011) 175–191.

[3] A. A. Gusev, O. Chuluunbaatar, S. I. Vinitsky, in "Proceedings of the second international conference the modeling of non-linear processes and systems" (Moscow, Yanus-K, 2011) p. 8-18.

[4] A. A. Gusev, O. Chuluunbaatar, S.I. Vinitsky, K.G. Dvoyan, E.M. Kazaryan, H.A. Sarkisyan, V.L. Derbov, A.S. Klombotskaya and V. V. Serov, Physics of Atomic Nuclei **75** (2012) 1210–1226.

[5] A.A. Gusev, O. Chuluunbaatar, L.L. Hai, S.I. Vinitsky, E.M. Kazaryan, H.A. Sarkisyan and V.L. Derbov, Journal of Physics: conference series **393** (2012) 012011.

[6] A. Gusev, S. Vinitsky, O. Chuluunbaatar, V. Gerdt, L.L. Hai, V. Rostovtsev, Lecture Notes in Computer Science, **7442** (2012) 155-171.

On the nature of scalar-isoscalar mesons in the uniformizing-variable method based on analyticity and unitarity.

Yu.S. Surovtsev and M. Nagy

It was shown [1, 2] that the scalar resonance poles on sheet II, obtained in the one-channel dispersive equations (see PDG tables) and being used in our approach, allow us to describe the $\pi\pi$ data well up to 1.89 GeV (in the dispersive-equations approach it is only up to about 1.15 GeV). However, (1) these resonance poles do not permit an even qualitative description of the $\pi\pi \to K\overline{K}$ data above 1.15 GeV (where the "elastic" two-channel unitarity is violated). Furthermore, (2) the background obtained in our approach with these resonance poles is unsatisfactory. This is an important criterion of the analysis correctness: description of the background must be simple and reasonable. In the combined analysis of data on the $\pi\pi$ scattering and $\pi\pi \to K\overline{K}$, both flaws of the only $\pi\pi$ scattering analysis are cured, obviously changing the $f_0(600)$ pole position of the one-channel analysis which is now near the one of the 3-channel analyse. Moreover, the remaining pseudo-background arising at the $\eta\eta$ threshold indicates clearly that it is necessary to consider explicitly also the $\eta\eta$-threshold branch-point in the 3 -channel analysis. This was made successfully using a new uniformizing variable in which we neglected the $\pi\pi$-threshold branch-point and took into account the $K\overline{K}$- and $\eta\eta$-threshold branch-points and the left-hand branch-point at $s = 0$. The combined analysis of data on $\pi\pi \to \pi\pi, K\overline{K}, \eta\eta$ and on $J/\psi \to \phi\pi\pi, \phi K\overline{K}$ from Mark III, DM2 and BES Collaborations gives: 1) Additional confirmation of $f_0(600)$ with mass about 700 MeV and width 930 MeV. This mass value accords with the prediction ($m_\sigma \approx m_\rho$) on the basis of mended symmetry by S.Weinberg (PRL 65, 1177 (1990)) and with refined analysis using the large-N_c consistency conditions between the unitarization and resonance saturation suggesting $m_\rho - m_\sigma = O(N_c^{-1})$ (J.Nieves, E.Ruiz Arriola, PR D80, 045023 (2009). 2) Indication for $f_0(980)$ to be a non-$q\bar{q}$ state, e.g., the bound $\eta\eta$ state. 3) Indication for the $f_0(1370)$ and $f_0(1710)$ to have the dominant $s\bar{s}$ component. This is in agreement with a number of experiments. 4) Two states in the 1500-MeV region: the $f_0(1500)$ ($m_{res} \approx 1495$ MeV, $\Gamma_{tot} \approx 124$ MeV) and the $f_0'(1500)$ ($m_{res} \approx 1539$ MeV, $\Gamma_{tot} \approx 574$ MeV). The $f_0'(1500)$ is interpreted as a glueball.

[1] Y. S. Surovtsev, P. Bydzovsky and V. E. Lyubovitskij, Phys. Rev. D **85** (2012) 036002.

[2] Yu.S. Surovtsev, P. Bydžovský, R. Kamiński, V.E. Lyubovitskij, M. Nagy, Phys. Rev. D **86**, (2012) 116002.

Determination of the mass spectrum of the bound state in the framework of the relativistic hamiltonian approach.

M. Dineykhan and S. A. Zhaugasheva

We propose[1] one of the versions of calculation of the energy spectrum of bound state systems with relativistic corrections. In the framework of quantum field theory the expression that takes into account relativistic corrections to the mass of the bound state with a known nonrelativistic pair interaction potential is proposed on the basis of calculating the asymptotic behaviour of correlation functions of the corresponding field currents with the necessary quantum numbers. Excluding the time variables allows one to determine nonperturbative corrections to the interaction potential. In the framework of the given approach the following results are obtained. The nonperturbative corrections arising due to the relativistic nature of a system to the interaction Hamiltonian are determined. The dependence of the constituent mass of bound-state forming particles on the free state mass and on the orbital and radial quantum numbers is analytically derived. The energy level shift of muonic hydrogen taking into account relativistic corrections is calculated. The energy spectrum of a wide class of potentials which describe the Coulomb bound state is analytically derived with relativistic corrections. The mass spectrum of the glueballs and the constituent masses of the gluons are analytically calculated taking into account spin-orbit, spin-spin and tensor interactions. Our numerical results have shown very good agreement with the lattice data. Taking into account nonperturbative and nonlocality characters of interactions, the mass spectrum of the mesons consisting of the light-light and light-heavy quarks with orbital and radial excitations is determined. Our results show that good agreement with the experimental data for the slope and the intercept of the Regge trajectory can be obtained only by taking into account the nonperturbative and the nonlocal characters of interactions. The dependence of the constituent masses of constituent particles on the masses of a free state is certain. When quarks are light, the difference of current and valent masses of quarks is greater than valent masses of quarks, and when quarks are heavy the difference of these masses is insignificant. One of the alternative variants for accounting of nonlocality is suggested for the definition of properties of hadrons at large distances. The dependence of the constituent masses of constituent particles on the radius of confinement is determined.

[1] M. Dineykhan and S. A. Zhaugasheva, "*Determination of the mass spectrum of the bound state in the framework of the relativistic hamiltonian approach,*"
Phys. Part. Nucl. **42** (2011) 379-413.

Strong electromagnetic field as a trigger of deconfinement

Sergei N. Nedelko

Bogoliubov Laboratory of Theoretical Physics, JINR

Abstract

Effective Lagrangian for Yang-Mills fields invariant under the standard space-time and local gauge $SU(3)$ transformations is considered. It has been demonstrated that a set of twelve degenerated minima exists as soon as a nonzero gluon condensate is postulated. The minima are connected to each other by the parity transformations and Weyl group transformations associated with the color $su(3)$ algebra. The presence of degenerated discrete minima in the effective potential leads to the solutions of the effective Euclidean equations of motion in the form of the kink-like gauge field configurations interpolating between different minima. Spectrum of charged scalar field in the kink background was estimated. The one-loop quark contribution to the QCD effective potential for the homogeneous Abelian gluon field in the presence of an external strong electromagnetic field was evaluated. The structure of extrema of the potential as a function of the angles between chromoelectric, chromomagnetic, and electromagnetic fields was analyzed. In this setup, the electromagnetic field is considered as an external one while the gluon field represents domain structured nonperturbative gluon configurations related to the QCD vacuum in the confinement phase. Two particularly interesting gluon configurations, (anti-)self-dual and crossed orthogonal chromomagnetic and chromoelectric fields, were discussed specifically. Within this simplified framework it was shown that the strong electromagnetic fields can play a catalyzing role for a deconfinement transition. At the qualitative level, the present consideration can be seen as a highly simplified study of an impact of the electromagnetic fields generated in relativistic heavy ion collisions on the strongly interacting hadronic matter.

1 Introduction

The purpose of papers [1, 2] was to study of a domain wall formation in the QCD vacuum and a potential influence of the strong electromagnetic fields, $eH \simeq \Lambda_{QCD}^2$, on the QCD vacuum structure. Electromagnetic fields with the strength of this order can emerge in relativistic heavy ion collisions. Before proceeding, we have to decode our understanding of the stock phrase "QCD vacuum structure". In pure gluodynamics a physical vacuum can be characterized, first of all, by two invariants composed of gauge field: scalar gluon condensate $\langle g^2 F^2 \rangle$ and pseudoscalar condensate $\langle g^2 F\tilde{F} \rangle$ (for instance see discussion in [3]). Since parity is not broken in strong interactions, the pseudoscalar condensate must be zero. Significance of the composite field $g^2 F\tilde{F}$ becomes manifest in terms of topological susceptibility. In QCD with quarks another condensate $\langle m\bar{\psi}\psi \rangle$ comes into consideration. Identification of gauge field configurations which are carriers of condensates and the method of their incorporation into the formalism of quantum field theory can be seen as the most fundamental step towards understanding the mechanisms of confinement, chiral

symmetry breaking and hadronization in QCD. This statement can be perceived as a kind of platitude since implicitly this step has to be assumed in all approaches dealing with configurations like center vortices, monopoles, instantons, etc. However, the feeling of having just a commonplace here relaxes if one identifies explicitly the point in the formalism where relevant condensates can be allowed or denied to be nonzero. As has been emphasized in a recent paper [4], this point can be recognized in the choice of a functional space of the gauge fields to be integrated over in the QCD functional integral. In the Euclidean functional integral approach to quantization of the pure YM theory one starts with a symbol

$$Z = N \int_{\mathcal{F}} DA \exp\{-S[A]\},$$

where the functional space $\mathcal{F}$ of fields is subject to certain conditions, which can disable, in particular, the gluon condensate (requirement of finite classical action $S[A]$, for instance) or enable it and restrict the type of fields which can contribute to the condensates. The character of fields in $\mathcal{F}$ has to be defined self-consistently on the basis of quantum effective action. Enabling the gluon condensate means that gauge fields A_μ^a should satisfy (for more details see [5])

$$\mathcal{F} = \{A : \lim_{V \to \infty} \frac{1}{V} \int_V d^4x \, g^2 F_{\mu\nu}^a(x) F_{\mu\nu}^a(x) = B^2\}. \tag{1}$$

First of all, the requirement of nonzero condensate $B^2 \neq 0$ singles out fields B_μ^a with the strength which is constant almost everywhere in R^4, i.e. the part of R^4 where the field is inhomogeneous has measure (4-volume) zero. The rest of deviations from homogeneity can be treated as fluctuations in the background of B_μ^a. Separation of the long range modes B_μ^a responsible for gluon condensate and the local fluctuations Q_μ^a in the background B_μ^a, must be supplemented by the gauge fixing condition. The background gauge condition $D(B)Q = 0$ is the most natural choice. At the formal level, the separation can be achieved by the insertion of identity

$$1 = \int_{\mathcal{B}} DB\Phi[A,B] \int_{\mathcal{Q}} DQ \int_{\Omega} D\omega \delta[A^\omega - Q^\omega - B^\omega]$$

$$\times \delta[D(B^\omega)Q^\omega], \tag{2}$$

$$A_\mu^a = B_\mu^a + Q_\mu^a, \tag{3}$$

where Q are fluctuations of the gluon field with zero gluon condensate: $Q \in \mathcal{Q}$. Fields B_μ^a are long range field configurations with, in general, the nonzero condensate: $B \in \mathcal{B}$. Functional $\Phi[A,B]$ is defined by Eq.(2) itself and relates to the Faddeev-Popov determinant, and Ω is the gauge group with corresponding Haar measure $d\omega$. Performing the standard Faddeev-Popov procedure one arrives at

$$Z = N' \int_{\mathcal{B}} DB \int_{\mathcal{Q}} DQ \det[D(B)D(B+Q)]$$

$$\times \delta[D(B)Q] \exp\{-S[B+Q]\}.$$

The character of long-range fields has yet to be identified by the dynamics of fluctuations Q. At the formal level, integral over Q defines an effective action for the long range part of the gluon field

$$Z = N' \int_{\mathcal{B}} DB \exp\{-S_{\text{eff}}[B]\}.$$

Gluon fields B_μ^a, which correspond to the global minima of $S_{\text{eff}}[B]$, dominate over the integral in the thermodynamic limit $V \to \infty$ and define the phase structure of the system. First of all, one has to take a look at fields with just constant strength. There are two different kinds of this type of fields: Abelian covariantly constant fields $B_\mu^a = -\frac{1}{2}n^a B_{\mu\nu} x_\nu$ and non-Abelian constant vector potentials $B_\mu^a = \text{const}$. Unlike the former, non-Abelian fields are unstable against small perturbations Q_μ^a (for comprehensive discussion of the effective potential in pure Yang-Mills theory see [6, 7]). Pagels and Tomboulis studied an effective action for these fields within the context of scale anomaly [8] , Woloshyn and Trottier attempted lattice calculation [9]. All these calculations indicated a minimum of the effective action at nonzero Abelian (anti-)self-dual field. Recently, the effective potential was calculated within the functional RG [10]. The result has also indicated a minimum of the effective action at the nonzero Abelian (anti-)self-dual field. In [1], the Landau-Ginsburg Lagrangian for pure Yang-Mills gauge fields invariant under the standard space-time and local gauge $SU(3)$ transformations was considered. It has been demonstrated that for $N_c = 3$ a set of twelve degenerated minima of the action density exists as soon as a nonzero gluon condensate is postulated in the action. The minima are connected to each other by the Weyl group transformations associated with the color $su(3)$ algebra and parity transformation. The presence of degenerated discrete minima in the Lagrangian leads to the solutions of the effective equations of motion in the form of the kink-like gauge field configurations interpolating between different minima. The homogeneous field with a kink defect is the simplest example of gluon configurations which are homogeneous almost everywhere in R^4 and satisfy the basic condition Eq.(1). The spectrum of covariant derivative squared D^2 in the presence of the simplest solution, which interpolates between self-dual and anti-self-dual Abelian homogeneous fields, was estimated. This kink configuration can be seen as a domain wall defect separating the regions with self-dual and anti-self-dual Abelian gauge field. On the domain wall the gluon field is Abelian with orthogonal to each other chromomagnetic and chromoelectric fields. For the aims of the present study it is important that the spectrum of D^2 or $\slashed{D}$ in the (anti-)self-dual field is purely discrete with bound state type eigenfunctions while for the crossed orthogonal fields the spectrum is continuous with the Landau level structure and the corresponding wave eigen functions.

The eigenvalues and the square integrable eigenfunctions of D^2 for the (anti-)self-dual field are

$$
\begin{aligned}
\lambda_r &= 4B\,(r+1) \\
\phi_{nmkl}(x) &= C_{nmkl}\left(\beta_+^+\right)^k \left(\beta_-^+\right)^l \left(\gamma_+^+\right)^n \left(\gamma_-^+\right)^m \phi_0(x), \\
\phi_0(x) &= e^{-\frac{1}{2}Bx^2}, \quad C_{nmkl} = \frac{1}{\sqrt{n!m!k!l!\pi^2}},
\end{aligned}
$$

where $r = k + n$ for the self-dual field, $r = l + n$ for the anti-self-dual field, $\beta_\pm^\pm$ and $\gamma_\pm^\pm$ are related to a set of creation and annihilation operators (details can be found in [1]). The spectrum is discrete. In this background no color charged waves are enabled, and there are no charged particle degrees of freedom. This is understood below as confinement of dynamical charged fields. This treatment follows the concept that confinement of dynamical quarks means that the quark field does not have corresponding asymptotic field. This should be manifest in the character of the eigen modes of the quark field. In the confinement regime they correspond to pure fluctuations localized in space and time, but not to any kind of waves. The character of eigenmodes is reflected in the analytical properties of the quark propagator which ensure that the colorless state can not decay into charged elementary particles [7, 11, 24, 25, 26, 5]. At the same time the proper QCD short distance limit is ensured as well.

Inside the infinitely thin domain wall placed at $x_1 = 0$ with the chromomagnetic field directed along the x_2 axis and the chromoelectric field along the x_3 axis the charged scalar field displays a continuous spectrum similar to the Landau levels. The eigen functions square integrable over x_3 take the form

$$\phi_n(p_2, p_4 | x_2, x_3, x_4) = \exp(-ip_4 x_4 - ip_2 x_2)\chi_n(p_4|x_3),$$

where the functions χ_n are

$$\chi_n(p_4|x_3) = \exp\left\{-2\sqrt{2}B\left(x_3 + \frac{p_4}{4B}\right)^2\right\}$$
$$\times H_n\left(2^{3/4}\sqrt{B}\left(x_3 + \frac{p_4}{4B}\right)\right).$$

The eigenvalues look like

$$\lambda_n(p_2^2, p_4^2) = 2\sqrt{2}B(2n+1) + p_2^2 + p_4^2,$$

and correspond to the color charged quasiparticles with mass $m_n^2 = 2\sqrt{2}B(2n+1)$ freely moving along the chromomagnetic field:

$$p_0^2 = p_2^2 + m_n^2. \tag{4}$$

The purely discrete spectrum and bound state (four-dimensional oscillator) eigen functions can be treated as confinement of color charged fields in the (anti-)self-dual homogeneous field (in the bulk of R^4). Landau levels and wave eigenfunctions indicate the absence of confinement at the domain wall. In other words, charged particles are localized at the wall.

The idea of the dominance of the gluon fields which are (anti-)self-dual Abelian almost everywhere turned out to be phenomenologically efficient. The model of confinement, chiral symmetry breaking and hadronization based on the ensemble of Abelian (anti-)self-dual fields was developed in a series of papers [5, 24, 25, 26]. In the model, the direction of the gauge field in space and color space, and the duality of the field are random parameters of the domains as well as positions of domain centers. All configurations of this type are summed up in the partition function. The domain model

exhibits confinement of static (square law) and dynamical quarks (absence of poles in the propagators of color charged fields, discrete spectrum of the corresponding differential operator), spontaneous breaking of the flavor chiral symmetry, $U_A(1)$ symmetry is broken due to the axial anomaly, strong CP violation is absent in the model. With a minimal set of parameters (meson masses, gauge coupling constant, gluon condensate and mean domain size) the model gives rather accurate results for meson masses from all different parts of the spectrum: light mesons including excited states, heavy-light mesons, heavy quarkonia). The decay constants and some form factors were also calculated within the model. The above mentioned kink configurations have not been yet incorporated into the domain model directly but strongly motivate it.
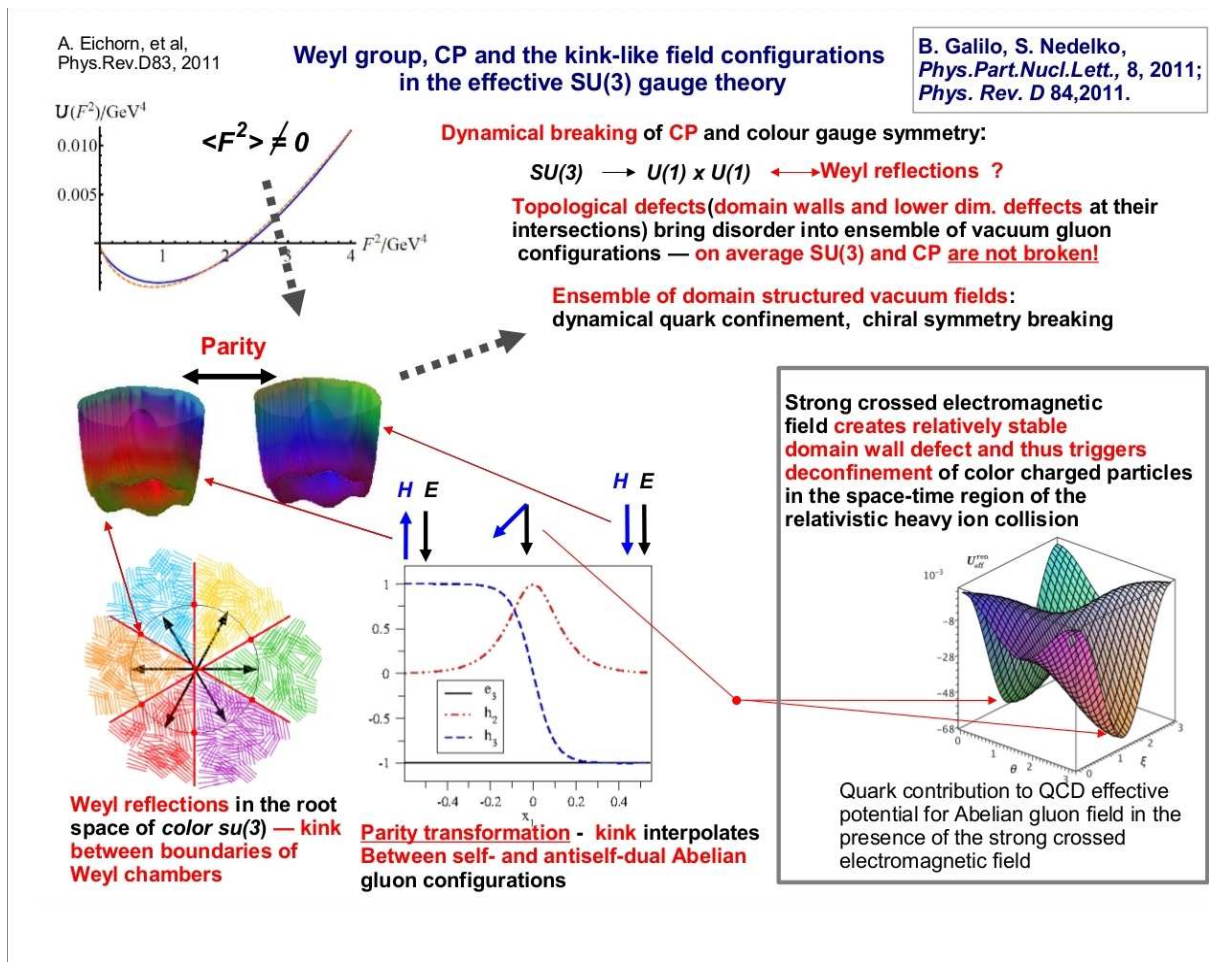

Figure 1: A mechanizm of domain wall formation due to a nonzero vacuum value of gluon condensate $\langle g^2 F^2 \rangle$ is illustrated at this scheme. Quark contribution to the QCD effective potential in the crossed external electromagnetic field is minimal for a crossed gluon field (right bottom corner) which is treated as catalyzing role of electromagnetic field for deconfinement.

In paper [2], we studied an impact of the strong electromagnetic field on strong interactions in the context of lumpy or domain structured gluon fields. The one-loop quark contribution to the QCD effective potential for the homogeneous Abelian gluon fields in the presence of homogeneous electromagnetic field is evaluated. Extrema of the potential as a function of angles between chromoelectric, chromomagnetic and crossed orthogonal electromagnetic fields are analyzed. In this setup the electromagnetic field is considered as an external one while the Abelian part of the gluon field represents domain structured nonperturbative gluon configurations related to QCD in the confinement phase. It is shown that the quark contribution is minimal for the crossed chromoelectric and chromomagnetic fields orthogonal to each other, which can be treated as a catalyzing impact of strong electromagnetic fields on deconfinement in hadronic matter. The present simplified calculation can play an instructive role for more realistic consideration. The main qualitative result of [2] is an observation that strong electromagnetic field could trigger a deconfinement transition in QCD.

[1] B.V. Galilo and S.N. Nedelko, Phys. Part. Nucl. Lett., **8** (2011) 67 [arXiv:hep-ph/1006.0248v2].

[2] B.V. Galilo and S.N. Nedelko, Phys. Rev. D84 (2011) 094017.

[3] P. Minkowski, Nucl. Phys. B**177** (1981) 203.

[4] L. D. Faddeev, [arXiv:0911.1013 [math-ph]].

[5] A.C. Kalloniatis and S.N. Nedelko, Phys. Rev. D **73** (2006) 034006.

[6] P. Minkowski, Phys. Lett. B 76 (1978) 439.

[7] H. Leutwyler, Phys. Lett. B96 (1980) 154; *ibid* Nucl. Phys. B **179** (1981) 129.

[8] H. Pagels, and E. Tomboulis, Nucl. Phys. B **143** (1978) 485.

[9] H. D. Trottier and R. M. Woloshyn, Phys. Rev. Lett. **70** (1993) 2053.

[10] A. Eichhorn, H. Gies and J. M. Pawlowski, Phys. Rev. D **83**, 045014 (2011) [Erratum-ibid. D **83**, 069903 (2011)] [arXiv:1010.2153 [hep-ph]].

[11] G.V. Efimov and M.A. Ivanov, The quark confinement model of hadrons, Institute of Physics Pub., 1993.

[12] Y.M. Cho Phys. Rev. Lett. **44** (1980) 1115.

[13] Y. M. Cho, J. H. Kim and D. G. Pak, Mod. Phys. Lett. A **21** (2006) 2789.

[14] Y.M. Cho, and D.G. Pak, Phys. Rev. Lett. **86** (2001) 1947.

[15] S.V. Shabanov, J. Math. Phys. **43** (2002) 4127 [hep-th/0202146].

[16] S. V. Shabanov, Phys. Rept. **326** (2000) 1 [arXiv:hep-th/0002043]; S. V. Shabanov and J. R. Klauder, Phys. Lett. B **456** (1999) 38. L. V. Prokhorov Yad. Fiz., **35** (1982) 229.

[17] L. D. Faddeev, A. J. Niemi, Nucl. Phys. B **776** (2007); *ibid*, Phys. Lett. B **449** (1999) 214.

[18] Kei-Ichi Kondo, Toru Shinohara, Takeharu Murakami, Prog. Theor. Phys. **120** (2008) 1 [arXiv:0803.0176 [hep-th]].

[19] P. J. Moran and D. B. Leinweber arXiv:0805.4246 [hep-lat].

[20] *P. J. Moran and D. B. Leinweber* PoS **LAT2007** (2007) 383 [arXiv:0710.2380 [hep-lat]].

[21] Ph. de Forcrand, A. Kurkela and A. Vuorinen Phys. Rev. D **77** (2008) 125014.

[22] P. de Forcrand AIP Conf. Proc. 892 (2007) 29 [arXiv:hep-lat/0611034].

[23] E. M. Ilgenfritz, *et al*, PoS **LAT2007** (2007) 311 [arXiv:0710.2607 [hep-lat]].

[24] G.V. Efimov, and S.N. Nedelko, Phys. Rev. D **51** (1995) 176; J. .V. Burdanov, G. V. Efimov, S. N. Nedelko, S. A. Solunin, Phys. Rev. D **54** (1996) 4483.

[25] A.C. Kalloniatis and S.N. Nedelko, Phys. Rev. D **64** (2001) 114025;

[26] A.C. Kalloniatis and S.N. Nedelko, Phys. Rev. D **66** (2002) 074020; *ibid*, Phys. Rev. D **69** (2004) 074029; *Erratum-ibid.* Phys. Rev. D **70** (2004) 119903; *ibid*, Phys. Rev. D **71** (2005) 054002;

[27] D. E. Kharzeev, L. D. McLerran, and H. J. Warringa, Nucl. Phys. A **803 227** (2008)

[28] V. Voronyuk, V. D. Toneev, W. Cassing, E. L. Bratkovskaya, V. P. Konchakovski and S. A. Voloshin, arXiv:1103.4239 [nucl-th].

[29] V. Skokov, A. Y. Illarionov and V. Toneev, Int. J. Mod. Phys. A **24** (2009) 5925 [arXiv:0907.1396 [nucl-th]].

[30] D. E. Kharzeev and D. T. Son, Phys. Rev. Lett. **106**, 062301 (2011) [arXiv:1010.0038 [hep-ph]].

Journal Publications

1. Kh.U. Abraamyan, S.V. Afanasiev, V.S. Alfeev, N. Anfimov, D. Arkhipkin, P.Zh. Aslanyan, V.A. Babkin, M.I. Baznat, S.N. Bazylev, D. Blaschke, D.A. Bliznyuk, D.N. Bogoslovsky, I.V. В и др., The MPD detector at the NICA heavy-ion collider at JINR, Nuclear Instruments and Methods in Physics Research Section A: 628, 1, 99-102, 2011.

2. C. Adolph, ... A. Efremov, ... [COMPASS Collaboration], Transverse spin effects in hadron-pair production from semi-inclusive deep inelastic scattering, Physics Letters B, 713, 1, 10-16.

3. C. Adolph, ... A.Efremov, ... et al. [COMPASS collaboration], Measurement of the Cross Section for High-pT Hadron Production in Scattering of 160 GeV/c Muons off Nucleons, Physical Rewier Letters, 2012, ISSN:0031-9007 (print)

4. C. Adolph, ..., A. Efremov, ... et al. [COMPASS Collab.], Measurement of the Cross Section for High-p_T Hadron Production in Scattering of 160 GeV/c Muons off Nucleons, 1-10, original paper, Submited to Physics Letters B, 2012.

5. C. Adolph, ... A. Efremov, et al. [COMPASS Collaboration], D* and D Meson Production in Muon Nucleon Interactions at 160 GeV/c, European Physical Journal C , ISSN:1434-6044, 2012.

6. C. Adolph, ... A. Efremov... et al. [COMPASS collab.], Exclusive ρ0 muoproduction on transversely polarised protons and deuterons, Nuclear Physics B, 865, 1, 1-20, 2012.

7. C. Adolph, ... A. Efremov, ... et al. [COMPASS Collaboration], Experimental investigation of transverse spin asymmetries in μ-p SIDIS processes: Collins asymmetries, Physics Letters B, 717, 4,5, 376-382, 2012.

8. C. Adolph, ... A. Efremov, ... et al [COMPASS Collaboration], Experimental investigation of transverse spin asymmetries in muon-p SIDIS processes: Sivers asymmetries, Physics Letters B, 717, 4,5, 383–389, 2012.

9. C. Adolph, ... A. Efremov, ... et al. [COMPASS collaborations], First Measurement of Chiral Dynamics in pi⁻ gamma - > pi⁻ pi⁻ pi⁺, Physical Review Letters, 108, 19, 192001.1-6, 2012.

10. S. Albino, P. Bolzoni, B.A. Kniehl, A. Kotikov, Fully double-logarithm-resummed cross sections., Nuclear Physics B, 851, 86-103, 2011.

11. S. Albino, P. Bolzoni, B.A. Kniehl, A.V. Kotikov, Timelike Single-logarithm-resummed Splitting Functions., Nuclear Physics B, 855, 801-814, 2012.

12. S.Albeverio and M.V.Altaisky, A remark on gauge invariance in wavelet-based quantum field theory, New Advances in Physics, 5, 1, 1-8, 2011.

12. M.V.Altaisky, N.E. Kaputkina, On discrete symmetries and relic radiation anisotropy, New Advances in Physics, 6, 2, 43-52, 2012.

13. A. B. Arbuzov, E. A. Kuraev and M. K. Volkov, Processes e+ e- --- > pi0 (pi0-prime) gamma in extended NJL model, The European Physical Journal A, 49, 9, 103-106, 2011.

14. A.B. Arbuzov, E.A. Kuraev, M.K. Volkov, Production of omega-p0 pair in electron-positron annihilation, Physical Review C - Nuclear Physics, ISSN:0556-2813, 83, 048201, brief reports, 2011.

15. A.B. Arbuzov, E.A. Kuraev, M.K. Volkov, Electromagnetic interactions of radially excited mesons pi^0 -prime, rho^0 -prime, omega-prime and production of pi^0 -prime at lepton colliders, Nucl. Phys., 74, 5, 752-757, 2011.

16. A.B. Arbuzov, E.A. Kuraev, M.K. Volkov, Production of omega-p0 pair in electron-positron annihilation, Physical Review C 83, 048201, 1-4, 2011.

17. A.B. Arbuzov, E.A. Kuraev, M.K. Volkov, Electromagnetic interactions of radially excited mesons pi^0 -prime, rho^0 -prime, omega-prime and production of pi^0 -prime at lepton colliders, Nuclear Physics, 74, 5, 752-757, 2011.

18. A.B. Arbuzov and M.K. Volkov, Two-photon decays and photoproduction on electrons of eta(550), eta(958), eta(1295), and eta(1475) mesons, Physical Review C, 84, 5, 058201(1)-058201(4), 2011.

19. M.V.Altaisky, N.E.Kaputkina, On the corrections to the Casimir effect depending on the resolution of measurement, Journal of Experimental and Theoretical Physics, 94, 5, 371-373, 2011.

20. I.V.Anikin, A.Besse, D.Yu.Ivanov, B.Pire, L.Szymanowski, S.Wallon, A phenomenological study of helicity amplitudes of high energy exclusive leptoproduction of the rho meson, Physical Review D, 84, 054004, 2011.

21. I. V. Anikin, R. S. Pasechnik, B. Pire, O. V. Teryaev, Gauge invariance of DVCS off an arbitrary spin hadron: the deuteron target case, arXiv:1112.1849v2 [hep-ph], 2011.

22. A.I.Ahmadov, Yu.M.Bystritskiy, E.A.Kuraev, Peripherical processes 2 o 3 and 2 o 4 in QED and QCD in p(p)p high energy collisions, Journal of Experimental and Theoretical Physics, 140, 4 (10), 732-740, 2011.

23. A.I.Ahmadov, E.A.Kuraev, M.K.Volkov, Generalizes polarzability of neutral pions of the process e$^-$ e$^+$ in the NJL model, International Journal of Modern Physics A, 26, 20, 3337-3346, 2011.

24. A. I. Ahmadov, E. A. Kuraev, M. K. Volkov, Production of π^0 π^0 pair in electron-positron annihilation in the Nambu-Jona-Lasinio model, Physics of Elementary Particles and Atomic Nuclei, Letters, 9, 6-7 (176-177), 756-760, 2012.

25. A.I.Ahmadov, B.A.Kniehl, E.A.Kuraev, E.S.Scherbakova, Production of one or two vector mesons in peripheral high-energy collisions of heavy ions, Physical Reviev C, 86, 045203, 2012.

26. Altaisky M.V. and Kaputkina N.E., Quantum hierarchic models for information processing, International Journal of Quantum Information, 10, 2, 1250026-1-11, 2012.

27. A. I. Ahmadov, E. A. Kuraev, M. K. Volkov, Production of π^0 π^0 pair in electron-positron annihilation in the Nambu-Jona-Lasinio model, Physics of Elementary Particles and Atomic Nuclei, Letters, 9, 6-7 (176-177), 756-760, 2012.

28. A.I.Ahmadov, Yu.M.Bystritskiy, A.N.Ilyichev, E.A.Kuraev, V.A.Zykunov, One-loop chiral amplitudes of Moller scattering process, The European Physical Journal C - Particles and Fields, 72, 1977, 2012.

29. A.I.Ahmadov, Yu.M.Bystritskiy, E.A.Kuraev, Peripherical processes 2-- > 3 and 2-- > 4 in QED and QCD in p̃(p)p high energy aollisions. Azimuthal correlation of gluon jets., Nuclear Physics B (Proc. Suppl.), 219-220, 229-234, 2011.

30. A.I.Ahmadov, Yu.M.Bystritskiy, E.A.Kuraev, A.N.Ilyichev, Charge-odd correlation of lepton and pion pair production in electron-proton scattering, J.Phys. G: Nucl.Part.Phys, 38, 1, 035005, 2011.

31. A.I.Ahmadov, E.A.Kuraev, M.K.Volkov, Generalized polarizability of neutral pions of the process $e^- e^+$ in the NJL model, International Journal of Modern Physics A, 26, 20, 3337-3346, 2011.

32. A.A. Bagaev, A.V. Bednyakov, A.F. Pikelner, V.N. Velizhanin, The 16th moment of the three loop anomalous dimension of the non-singlet transversity operator in QCD., Physics Letters B, B714, 76-79, 2012.

33. D. Bakalov, V.I. Korobov, S. Schiller, Magnetic field effects in the transitions of the HD^+ molecular ion and precision spectroscopy, Journal of Physics B, 44, 2, 025003(1-11), 2011.

34. A. P. Bakulev, S. V. Mikhailov, A. V. Pimikov, N. G. Stefanis, Comparing antithetic trends of data for the pion-photon transition form factor, Physical Review D, 83, 3, 031501-031504, 2012.

35. A. P. Bakulev, S. V. Mikhailov, A. V. Pimikov, N. G. Stefanis, Pion-photon transition form factor using light-cone sum rules: theoretical results, expectations, and a global-data fit, Nuclear Physics B - Proceedings Supplements, 219-220, 133--140, 2011.

36. A. P. Bakulev1, S. V. Mikhailov1, A. V. Pimikov1, N. G. Stefanis, Pion-photon transition: The new QCD frontier, Physical Review D, 84, 3, 034014/1-11, 2011.

37. A. P. Bakulev, Irina V. Potapova, Resummation Approach in QCD Analytic Perturbation Theory, Nuclear Physics B - Proceedings Supplements, 219--220, 193--200, 2011.

38. Yu.O.Belyakova, A.V.Nesterenko, A nonperturbative model for the strong running coupling within potential approach, International Journal of Modern Physics A. , 26, 6, 981-993, 2011.

39. A.V. Bednyakov, A.F. Pikelner, V.N.Velizhanin,Anomalous dimensions of gauge fields and gauge coupling beta-functions in the Standard Model at three loops, Journal of High Energy Physics, 17, 1-23, 2012.

40. C. Beskidt, W. de Boer, D.I. Kazakov, F. Ratnikov, E. Ziebarth, V. Zhukov., Constraints from the decay B0s- > mu+mu- and LHC limits on Supersymmetry., Physics Letters B, B 705, 493-497, 2011.

41. A.V.Bednyakov, D. I. Kazakov, S. H. Tanyildizi, SUSY Enhancement of Heavy Higgs Production, International Journal of Modern Physics A, 26, 24, 4187-4202, 2011.

42. A.K. Bekbaev, V.I. Korobov, M. Dineykhan, Variational calculations of the HT^+ ro-vibrational energies, Physical review. A, 83, 4, 044501(1-3), Rapid Communication, 2011.

43. A. K. Bekbaev, V. I. Korobov, and M. Dineykhan, Variational calculations of the HT+ rovibrational energies, Physical review A, 83, 4, 1-3, 2011.

44. C. Beskidt, W. de Boer, D.I. Kazakov, F. Ratnikov, *Where is SUSY?*, Journal of High Energy Physics, 1205, 094, 2012.

45. C. Beskidt, W. de Boer, D.I. Kazakov, F. Ratnikov., Constraints on Supersymmetry from LHC data on SUSY searches and Higgs bosons combined with cosmology and direct darkmatter searches, European Journal of Physics, C72, 2166, 2012.

46. C.Beskidt, W. de Boer, T. Hanisch, E. Ziebarth, D.I.Kazakov and V. Zhukov,Constraints on Supersymmetry from Relic Density compared with future Higgs Searches at the LHC, Physics Letters B, 695, 143, 2011.

47. D. Blaschke, M. Buballa, A.E. Radzhabov, M. K. Volkov, Nonlocal PNJL model beyond mean field, Nucl. Phys A, 75, 6, 788–790, 2012.

48. L.V.Bork, D.I.Kazakov, G.S.Vartanov, On form factors in N=4 SYM, Journal of High Energy Physics, 1102, 063, 2011.

49. L.V. Bork, D.I. Kazakov, G.S. Vartanov., On MHV Form Factors in Superspace for n=4 SYM Theory, Journal of High Energy Physics, 1110, 133, 2011.

50. L.V. Bork, D.I. Kazakov, G.S. Vartanov, A.V. Zhiboedov, Infrared finite observables in $N = 8$ supergravity, Trudy V.A. Steklov MI RAS, 2011, Vol. 272, pp. 46–53. 2011.

51. L.V. Bork, D.I. Kazakov, G.S. Vartanov, From amplitudes to form factors in the N=4 SYM theory, Teor. Mat. Fiz., Vol. 169, No. 1, 2011.

52. W. Broniowski, A.E. Dorokhov, E. Ruiz Arriola, Transversity Form Factors and Generalized Parton Distributions of the Pion in Chiral QuarkModels, Few Body Systems, 52, 295-300, 2012.

53. P. Bydzovsky, Yu.S. Surovtsev, R. Kaminski, M. Nagy, Resonances in the isovector P wave of pi pi scattering, International Journal of Modern Physics A, 26, 3&4, 634-635, 2011.

54. I.O. Cherednikov, T. Mertens, F.F. Van der Veken, Evolution of cusped lightlike Wilson loops and geometry of the loop space, Physical Review D, 86, 085035(1-7), 2012.

55. I.O. Cherednikov, Layout of Wilson lines and light-cone peculiarities of transverse-momentum dependent PDFs, Proceedings of Science, 061(1-6), 2012.

56. B.V. Galilo, S. N. Nedelko, Impact of the strong electromagnetic field on the QCD effective potential for homogeneous Abelian gluon field configurations
Physical Review D, 84, 9, 094017, 2011

57. B.V. Galilo, S. N. Nedelko, Weyl group, CP and the kink-like field configurations in the effective SU(3) gauge theory,PEPAN Lett., 8, 2, 118-127, 2011

58. I.O. Cherednikov, N.G. Stefanis, On correlations in high-energy hadronic processes and the CMS ridge: A manifestation of quantum entanglement?, International Journal of Modern Physics A. Particles and Fields. Gravitation. Cosmology. Nuclear Physics., 27, 1250008(1-14), 2012.

59. I.O. Cherednikov, N.G. Stefanis, Taming singularities in transverse-momentum-dependent parton densities, AIP Conference Proceedings, 1350, 325-328, 2011.

60. G. Cvetic, A. V. Kotikov, Analogs of Noninteger Powers in General Analytic QCD., Journal of Physics G: Nuclear and Particle Physics, 39, 065005, 2012.

61. A. E. Dorokhov, Sergey V. Esaybegyan,Bound states in modified action for light quarks in instanton vacuum model, Physics Letters B, 712, 4-5, 381-385, 2012.

62. A.E. Dorokhov, Wojciech Broniowski, Enrique Ruiz Arriola, Generalized Quark Transversity Distribution of the Pion in Chiral Quark Models, Phys. Rev. D, D84, 7, 074015-1-17, статья, 2011.

63. A.E. Dorokhov, A.E. Radzhabov, A.S. Zhevlakov, The light-by-light contribution to the muon (g-2) from lightest pseudoscalar and scalar mesons within nonlocal chiral quark model, European

Physical Journal C , 72, 2227-1-12, 2012.

64. A.E. Dorokhov, A.E. Radzhabov, A.S. Zhevlakov, The pseudoscalar hadronic channel contribution of the light-by-light process to the muon (g-2)$_\mu$ within the nonlocal chiral quark model, Eur. Phys. J. C, 71, 1702-1-12, 2011.

65. S. Dubnicka, A.Z.Dubnickova, M.A.Ivanov, J.G.Korner, P.Santorelli, G.G.Saidullaeva, One-photon decay of the tetraquark state X(3872) in a relativistic constituent quark model with infrared confinement, Physical Review D, 84, 1, 014006, 2011.

66. B. El-Bennich, M.A. Ivanov, C.D. Roberts, Strong D* - > D+pi and B* - > B+pi couplings., Physical Review C, 83, 2, 025205 (5 pages), 2011.

67. A.V.Efremov, P.Schweitzer, O.V.Teryaev, P.Zavada, The relation between TMDs and PDFs in the covariant parton model approach, Physical Review D, 83, 5, 054025.1-8, original paper, 2011.

68. D.V. Fursaev, Entanglement Rényi entropies in conformal field theories and holography, Journal of High Energy Physics, 1205, 080, 2012.

69. G.Ganbold, Infrared-Finite Behavior of QCD Coupling, Physics of Particles and Nuclei Letters, 43, 1, pp 79-105, 2011.

70. G. Ganbold, Meson Spectra and Infrared-Finite Behavior of QCD Running Coupling, Physics of Elementary Particles and Atomic Nuclei, (PEPAN), 43, 1, 156-207, 2012.

71. S.V. Goloskokov, Generelized Parton Distributions in light meson production., Nuclear Physics B (Proc. Suppl.), 219-220, 1, 185–192, 2011.

72. S.V. Goloskokov, P. Kroll, Transversity in hard exclusive electroproduction of pseudoscalar mesons, The European Physical Journal A, A47, 9, 112-128, 2011.

73. A A Gusev, O Chuluunbaatar, L L Hai, S I Vinitsky, E M Kazaryan, H A Sarkisyan and V L Derbov, Spectral and optical characteristics of spheroidal quantum dots, Journal of Physics: conference series, 393, 012011-1-9, 2012.

74. A.A. Gusev, S.I. Vinitsky, O. Chuluunbaatar, V.P. Gerdt, V.A. Rostovtsev, Symbolic-numerical algorithms to solve the quantum tunneling problem for a coupled pair of ions, Lecture Notes in Computer Science, 6885, 175--191, article, 2011.

75. A. Gusev, S. Vinitsky, O. Chuluunbaatar, V. Gerdt, L.L. Hai, V. Rostovtsev, Symbolic-Numerical Calculations of High-|m| Rydberg States and Decay Rates in Strong Magnetic Fields, Lecture Notes in Computer Science, 7442, 155-171, 2012.

76. T. Gutsche, M. A. Ivanov, J. G. Korner, V. E. Lyubovitskij and P. Santorelli, Light baryons and their electromagnetic interactions in the covariant constituent quark model, Physical Review D - Particles, Fields, Gravitation and Cosmology, D, 86, 7, 074013 (1-15), 2012.

77. A.Yu. Illarionov, A.V. Kotikov, S.S. Parzycki, D.V. Peshekhonov, New type of parametrizations for parton distributions., Physical Review D, particles, fields, gravitation, and cosmology, 83, 034014, 2011.

78. A. Yu. Illarionov, Bernd A. Kniehl, Anatoly V. Kotikov, Ultrahigh-energy neutrino-nucleon deep-inelastic scattering and the Froissart bound., Physical Review Letters, 106, 231802, 2011.

79. A.Yu. Illarionov, A.V. Kotikov, Fc2 at low x., Yadernaya Fizika, 75, 10, 1234 1239, 2012.

80. M. A. Ivanov, J. G. Korner, S. G. Kovalenko, P. Santorelli and G. G. Saidullaeva, Form factors for semileptonic, nonleptonic and rare B(Bs) meson decays., Physical Review D, 85, 034004, 2012

81. M.A. Ivanov, M. Schmid,, Integrating out the heaviest quark in N-flavour ChPT, The European Physical Journal C, 71, 9, 1732 (1-11), 2011.

82. A. L. Kataev, S. V. Mikhailov, New perturbation theory representation of the conformal symmetry breaking effects in gauge quantum field theory models, Teoreticheskaya i Matematicheskaya Fizika, Vol. 170, No. 2, pp. 174–187, 2012.

83. J.-Ph. Karr, L. Hilico, and V. I. Korobov, Theoretical progress in the H_2^+ molecular ion: towards electron to proton mass ratio determination, Canadian Journal of Physics, 89, 1, 103-107, 2011.

84. V.L. Khandramai, O.P. Solovtsova, Analysis of the nucleon spin sum rules within the frame of analytic approach in QCD, Nonlinear phenomena in complex systems, 15, 3, 283–291, 2012.

85. V.L. Khandramai, R.S. Pasechnik, D.V. Shirkov, O.P. Solovtsova, O.V. Teryaev, Four–loop QCD analysis of the Bjorken sum rule, Physics Letters B, 706, 340-344, 2012.

86. Y.N. Klopot, Armen G. Oganesian, Oleg V. Teryaev, Axial anomaly and mixing: From real to highly virtual photons., Physical Review D, 84, 5, 051901, 2011.

87. Y. N. Klopot, Armen G. Oganesian, Oleg V. Teryaev, Axial anomaly as a collective effect of meson spectrum, Physics Letters B, 695 (2011) 130 135, 2011.

88. Y. Klopot, Oganesian A., Teryaev O., Quark-hadron duality, axial anomaly and mixing, Journal of Experimental and Theoretical Physics, 94, 10, 791-795, 2011.

89. B.A. Kniehl, Anatoly V. Kotikov, Counting master integrals: integration-by-parts procedure with effective mass., Physics Letters B, 712, 233-234, 2012.

90. V.I. Korobov and Zhen-Xiang Zhong, Bethe Logarithm for the H_2^+ and HD^+ molecular ions, Phys. Rev. A, 86, 4, 044501(1-5), regular article, 2012.

91. V.I. Korobov, Calculation of the nonrelativistic Bethe logarithm in the velocity gauge, Phys. Rev. A, 85, 4, 042514(1-9), regular article, 2012.

92. A.V. Kotikov, On the Critical Behavior of (2+1)-Dimensional QED., Physics of atomic nuclei, 75, 7, 890-892, 2012.

93. A. V. Kotikov, The Property of Maximal Transcendentality of Anomalous Dimensions of the Wilson Operators in the N = 4 SYM, Nucl. Phys, 74, 6, 961-968, 2011.

94. G.A. Kozlov, Correlations of two photons at hadron colliders, Modern Physics Letters A, 26, 26, 1943-1952, 2011.

95. G.A. Kozlov, I.N. Gorbunov, Dilaton Decays Into Unparticles and A Single Photon, International Journal of Modern Physics A. Particles and Fields. Gravitation. Cosmology. Nuclear Physics., 26, 3987-3996, 2011.

96. G.A. Kozlov and I.N. Gorbunov, On decays of Z` into Unparticle Stuff, Advances in High Energy Physics, 2011, 1-10, 2011.

97. A.V. Kotikov, V.G. Krivokhizhin, B.G. Shaikhatdenov, Analytic and "frozen" QCD coupling constants up to NNLO from DIS data., Physics of atomic nuclei, 75, 4, 507-524, 2012.

98. E.A. Kuraev, S. Bakmaev, E.S. Kokoulina, Azimuthal correlation of gluon jets created in pp, p̃p and e+e- collisions, Nuclear Physics B, B851, 3, 551-564, 2011.

99. Lashkevich V.I., Solovtsova O.P., Role of Target Mass Corrections to the Longitudinal Structure Function F_L, Nonlinear phenomena in complex systems, 14, 2, 184–189, 2011.

100. E. Leader, A. V. Sidorov, D. B. Stamenov, A Possible Resolution of the Strange Quark Polarization Puzzle?, Phys. Rev. D, D4, 014002, 2011.

101. V.A. Naumov, Solar neutrinos. Astrophysical aspects., pepan letters , 8, 7, 683-703, Physics of Particles and Nuclei Letters, Vol. 8, No. 7 (2011) pp. 683–703 2011.

102. H.-P. Pavel, SU(2) Dirac-Yang-Mills quantum mechanics of spatially constant quark and gluon fields, Physics Letters B, 700, 265-276, 2011.

103. H.-P. Pavel, A novel strong coupling expansion of the QCD Hamiltonian,Physics of atomic nuclei, 75, 729-731, 2012.

104. A.E. Radzhabov, D. Blaschke, M. Buballa, M.K. Volkov, Nonlocal PNJL model beyond mean field and the QCD phase transition, Physical review. D, 83, 116004, 1-16, 2011.

105. O.V. Selyugin, GPDs of the nucleons and elastic scattering at high energies, Eur. Phys. J. C, 72, 2073-2081, 2012.

106. O.V. Selyugin, Gravitation interaction with extra dimension and periodic structure of the hadron scattering amplitude, Modern Physics Letters A (MPLA), 26, 28, 2109-2117, 2011.

107. O.V. Selyugin, The effects of the small t properties of hadronic scattering amplitude on the determination its real part, Modern Physics Letters A (MPLA), 27, 20, 125013-125022, 2012.

108. Yu.S.Surovtsev, P.Bydz, R.Kamin´ski, V.E.Lyubovitskij, M.Nagy, Can parameters of f_0-mesons be determined correctly analyzing only scattering?, Physical review. D,, 86, 116002, 2012.

109. Yu.S.Surovtsev, P.Bydzovsky, V.E.Lyubovitskij, Nature of the scalar-isoscalar mesons in the uniformizing-variable method based on analyticity and unitarity, Physical Review D, 85, 3, 036002-1--18, 2012.

110. Yu.S. Surovtsev, P. Bydzovsky, T. Gutsche, V.E. Lyubovitskij, On scalar mesons from the combined analysis of multi-channel ⎕⎕ scattering and J/psi decays, International Journal of Modern Physics A, 26, 3 & 4, 610–612 2011.

111. M.K. Volkov, A.B. Arbuzov, D.G. Kostunin, Decay tau -- > pi omega nu in the extended NJL model, Physical Review D, 86, 057301, 1-4, статья, 2012.

112. M.K. Volkov, D. G. Kostunin, Decays ro -- > eta pi and tau -- > eta(eta□) pi nu in the Nambu–Jona-Lasinio model, Physical Review D, 86, 013005, 1-4, 2012.

113. M. K. Volkov, D. G. Kostunin, Processes e+e--> pi pi (pi-prime) in the extended Nambu-Jona-Lasinio model, Physical Review C, Nuclear Physics, 86, 025202, 1-4, 2012.

114. M.K. Volkov, D.G. Kostunin, tau- -- > pi- pi 0 nu tau decay in the extended NJL model, Physics of Elementary Particles and Atomic Nuclei, Letters, 10, 178, 18-23, 2012.

115. A.S. Zhevlakov, A.E. Dorokhov, A.E. Radzhabov, Calculation of hadronic contribution to the anomalous magnetic momentum of muon (g-2)(mu) from light by light scattering diagram in nonlocal chiral quark model, Physics of Particles and Nuclei Letters, 8, 7, 768-771, 2011.

Proceedings

1. M.V. Altaisky, N.E. Kaputkina, Scale-dependent corrections to Casimir effect 11-14, IEEE, Proceedings of the International conference "Days on Diffraction 2011", 978-1-4577-1577-8, 2011.

2. Ayryan E.A., Egorov A.A., Sevastyanov L.A., Lovetskiy K.P. and Sevastyanov A.L., Mathematical Modeling of Irregular Integrated Optical Waveguides., International Conference on Mathematical Modeling and Computational Physics (MMCP 2011)., JINR Dubna; IEP SAS, UPJS, TU Kosice, Stara Lesna, Slovakia,.L., 136-147, Springer-Verlag Berlin Heidelberg, Mathematical Modeling and Computational Science. International Conference, MMCP 2011. Revised Selected Papers. ISBN 978-3-642-28212-6, 2012.

3. H Avakian (Jefferson Lab), A V Efremov (Dubna, JINR), P Schweitzer (Connecticut U.), 1-6, Schpringer, TMDs in the Bag Model, ADVANCED STUDIES INSTITUTE, Карлов Унив., ОИЯИ, Прага, Чехия, The European Physical Journal Special Topics (EJP ST) Series (to be published), Reported at Spin Symposium 2010, Juelich, Germany and at Advanced Studies Institute on Symmetries and Spin (SPIN-Praha-2011), 2011.

4. A. P. Bakulev, S. V. Mikhailov, A. V. Pimikov, N. G. Stefanis,Pion-Photon Transition Form Factor and Pion Distribution Amplitude in QCD: Facing the Enigmatic Behavior of the BaBar Data., International Workshop on e+e- collisions from Phi to Psi, ИЯФ СО РАН, Новосибирск, Россия, 146–150, Nuclear Physics B - Proceedings Supplements, ISSN:0920-5632, eISSN:1873-3832, Изд:Elsevier Science Limited, 225–227, 2012.

5. A. P. Bakulev, S. V. Mikhailov, A. V. Pimikov, N. G. Stefanis, Pion-photon transition form factor in light-cone sum rules., QCD@Work 2012: International Workshop on QCD Theory and Experiment - VI Edition (QCD @ Work), Bari U., Lecce, Italy, 134-138, American Institute of Physics, 1492, 1551-7616, 2012.

6. A.P. Bakulev, S.V. Mikhailov, A.V. Pimikov, N.G. Stefanis, Pion-photon transition form factor using light-cone sum rules: theoretical results,expectations, and a global-data fit, Hadron Structure`11, Institute of Physics, SAS (Bratislava, Slovakia); St. Petersburg Nuclear Physics Institute of RAS (Gatchina, Russia); Ministry of Education, Science, Research and Sport of the Slovak Republic (Slovakia); Comenius University (Bratislava, Slovakia); Institute of Experimental Physics, SAS(Ko&352;af&353;ice, Slovakia); Slovak Physical Society (Slovakia), Tatranska Strba, Slovakia, 133-140, Elsevier, Nuclear Physics B Proceedings Supplement, 219-220, Talk presented by the second and third authors at the 5th

joint International HADRON STRUCTURE '11 Conference, Tatranska Strba (Slovak Republic),June 27--July 1, 2011, 2011.

7. M. Dineykhan, M.A. Ivanov , G.G. Saidullaeva, Exotic states and rare B/s-decays in the covariant quark model., Физика элементарных частиц и атомного ядра, ISSN:0367-2026, eISSN:1814-7445, Изд:ОИЯИ, 43, 749-782, 2012.

8. B. El-Bennich, C. D. Roberts and M. A. Ivanov, Heavy-quark symmetries in the light of nonperturbative QCD approaches, International Workshop On QCD Green`s Functions, Confinement, And Phenomenology (QCD-TNT-II), , Trento, Italy, 1-13, Proceedings of Sciemce, SISSA, 2012.

9. S.M. Eliseev, Finite Formation Time of Hadrons: the QGP Signatures, Physics of atomic nuclei , ISSN:1063-7788 , eISSN:1562-692X, Изд:MAIK Nauka/Interperiodica, Pleiades Publishing, Ltd, 75, 7, 879–881, российские, 2012.

10. A.V. Efremov, J. Soffer, An analytic review of DSPIN-11,
XIV Международное рабочее совещание по спиновой физике при высоких энергиях, 20-24.09.2011, ОИЯИ, Дубна, Россия, 407-410, Joint Institute for Nuclear Research, 2012, XIV Advanced Research Workshop on High Energy Spin Physics (DSPIN-11), Proceedings, Ed. A.V. Efremov and S.V. Goloskokov, 1, ISBN:978-5-9530-0315-5, Published: Joint Institute for Nuclear Research, 2012 XIV Advanced Research Workshop on High Energy Spin Physics (DSPIN-11), Proceedings, Ed. A.V. Efremov and S.V. Goloskokov, pp.407-410, 2011.

11. A.V. Efremov, J. Soffer, An analytic review of DSPIN-11,
The 20-th INTERNATIONAL SYMPOSIUM on Spin Physics (SPIN2012),, JINR, Dubna, Дубна, Россия, To be published in Journal Physics of Elementary Particles and Atomic Nuclei.(special review), 2012.

12. Ефимов Г.В., Стационарное уравнение Шредингера нерелятивистской квантовой механики и функциональный интеграл, Теоретическая и Математическая физика, ISSN:0564-6162, Изд:МАИК НАУКА, 171, 3, 452-474, 2012.

13. A.V. Efremov, I.F. Ginzburg, A.V. Radyushkin, Regge trajectories in QCD, International Workshop on Diffraction in High-Energy Physics (Diffraction-2012), Instituto de F&243;rica UAM/CSIC (SPAIN) Universidad Autónoma de Madrid (SPAIN) Istituto Nazionale di Fisica Nucleare (ITALY), VIK Hotel San Antonio, Puerto del Carmen, Lanzarote, Canary Islands, Spain, Испания, 1-4, American Institute of Physics., Diffraction 2012 is the seventh biennial Workshop dedicated to theoretical and experimental progress in diffractive hadronic collisions at high energies. The previous events took place at Cetraro (2000), Alushta (2002), Cala Gonone (2004), Milos (2006), La Londe-les-Maures (2008), Otranto (2010)., 2012.

14. G. Ganbold, Spectra of Light and Heavy Mesons, Glueball and QCD Effective Coupling, XIV International Conference on Hadron Spectroscopy "Hadron2011" (TUV Munich, Germany, 12-17 June 2011), XIV International Conference on Hadron Spectroscopy "Hadron2011" (TUV Munich, Germany, 12-17 June 2011), 2011.

15. S.B.Gerasimov, Towards inquiring about the non-quark-antiquark-admixture in light meson multiplet structure., Russian Academy of Sciences, Institute of Nuclear Research, Proceedings of the XIII International Seminar on Elecromagnetic Interactions of Nuclei, EMIN-2012, Moscow, September 20-23,2012, Generalized schemes are considered of meson state-vectors mixing within two lowest mass nonets in each J^PC -sector of the spin zero mesons with the objetives to

single out possible exotic non-quark-antiquark states in the considered resonance-mass interval and provide their experimental investigation., 2012.

16. S.B. Gerasimov, On possible role of scalar glueball-quarkonia mixing in the f(0) (1370;1500;1710) resonances produced in J/psi radiative decays, PoS, The next to lowest mass scalar multiplet is treated as the q-q, P-wave, non-radial-excited nonet, mixed withthe JPC =0++ -glueball. The generalized Schwinger-type mass-formulas are used to derive and discuss the quark-gluon configuration structure of the obtained meson states which used then to obtain the relations between their decay modes into the pair of the lowest mass pseudoscalar mesons (pp, K-K,hh, etc.), 2012.

17. S.B.Gerasimov, Why the study of the polarized photonuclear absorption reactions could be interesting? 236-243, Dubna, 2011, Relativistic Nuclear Physics and Quantum Chromodynamics. Proceedings of the XX International Baldin Seminar on High Energy hysics Problems. Dubna, October 4-9,2010, vol.1, ISBN-978-5-9530-0308-7, It was shown, in particular, that the measurements of the photoabsorption of the circularly-polarized photons on polarized Li-6 or Li-7 nuclei could discriminate between different models of the interference of nucleon resonances in the 2nd-resonance region., 2011.

18. S. V. Goloskokov, Polarized and transversity GPDs in kaon leptoproduction, The 20-th INTERNATIONAL SYMPOSIUM on Spin Physics (SPIN2012),, JINR, Dubna, Дубна, Россия, 1-4, arxiv.org, 4 pages, 4 figures. Talk at the 20th International Symposium on Spin Physics (SPIN2012) JINR, Dubna, Russia September 17 - 22, 2012. To be publish in Proceedings, 2012.

22. S.V.Goloskokov, Generelized Parton Distributions in light meson production, Hadron Structure`11, Institute of Physics, SAS (Bratislava, Slovakia); St. Petersburg Nuclear Physics Institute of RAS (Gatchina, Russia); Ministry of Education, Science, Research and Sport of the Slovak Republic (Slovakia); Comenius University (Bratislava, Slovakia); Institute of Experimental Physics, SAS (Ko&352;af&353;ice, Slovakia); Slovak Physical Society (Slovakia), Tatranska Strba, Slovakia, 1-14, 14 pages, Presented at the 5th joint International HADRON STRUCTURE '11 Conference, June 27- July 1, 2011, Tatranska Strba (Slovak Republic), 2011.

19. S.V. Goloskokov, HARD MESON ELECTROPRODUCTION AND TWIST-3 EFFECTS., XIVth International Workshop onHigh Energy Spin Physics, JINR, Dubna, Russia, 71-77, JINR, XIV Advanced Research Workshop on High Energy Spin Physics, 6 pages, report at XIV Workshop on High Energy Spin Physics Dubna, Russia, September 20 - 24, 2011, 2012.

20. S. V. Goloskokov, What can we lean about GPDs from light meson leptoproduction experiments, Advanced Studies Institute Symmetries and Spin (SPIN PRAHA 2011), Prague 02.05.2011 09.05.2011, Charles University in Prague, Faculty of Mathematics and Physics, Prague, Czech Republic, 1-8, 8 pages, talk at conference "Symmetries and Spin", May 2 - 9, Prague, Czech Republic, 2011.

21. S. V. Goloskokov, Polarized GPDs in pions and kaons electroproduction. Tranversity effects, ADVANCED STUDIES INSTITUTE SYMMETRIES AND SPIN(SPIN-Praha-2012)Prague, July 1 - 8, 2012, Charls University, Praha, Chech Republic, 1-8, arxiv.org, 8 pages, 12 figures, talk at the International Conference "Advanced Studies Institute Symmetries And Spin" (SPIN-Praha-2012) Prague, July 1 - 8, 2012, 2012.

22. A. A. Gusev, O. Chuluunbaatar, S.I. Vinitsky, K.G. Dvoyan, E.M. Kazaryan, H.A. Sarkisyan, V.L. Derbov, A.S. Klombotskaya and V. V. Serov, Adiabatic Description of Nonspherical Quantum Dot Models, Ядерная Физика, ISSN:0044-0027, eISSN:1562-692X /

1063-7788(eng), Изд:МАИК Наука/Интерпериодика, Pleiades Publishing Inc., 75, 10, 1281-1297, 2012.

23. А.А. Гусев, В.А. Ростовцев, С.И. Виницкий,, Применение метода Канторовича для компьютерного анализа моделей квантоворазмерных наноструктур, Системный анализ в науке и образовании, Изд:Международный университет природы, общества и человека, 02, 01-14, 2012.

24. A.L. Kataev, S.V. Mikhailov, Conformal symmetry breaking effects in gauge theories: new perturbative expressions,An international Workshop HSQCD`2010, Hadron Structure and QCD: from LOW to HIGH energies Gatchina, Russia, July 5 – July 9, 2010, St. Petersburg Nuclear Physics Institute of Russian Academy of Sciences, St. Petersburg State University, V.A. Fock Institute of Physics, St. Petersburg Scientific Center of Russian Academy of Sciences, Гатчина, Россия, 160--173, PNPI Publishing, Proceedings of Int. "Workshop Hadron Structure and QCD: HSQCD-2010", Gatchina, July 5--9, 2011, 978-5-86763-296-0, Talk gived by the first author at international Workshop HSQCD`2010, Hadron Structure and QCD: from LOW to HIGH energies Gatchina, Russia, July 5 – July 9, 2010, 2011.

25. Y. Klopot, Armen Oganesian, Oleg Teryaev, Anomaly, mixing and transtition form factors of pseudoscalar mesons, Hadron Structure`11, Institute of Physics, SAS (Bratislava, Slovakia); St. Petersburg Nuclear Physics Institute of RAS (Gatchina, Russia); Ministry of Education, Science, Research and Sport of the Slovak Republic (Slovakia); Comenius University (Bratislava, Slovakia); Institute of Experimental Physics, SAS (Ko&352;af&353;ice, Slovakia); Slovak Physical Society (Slovakia), Tatranska Strba, Slovakia, Yaroslav, 141-144, Elsevier, Nuclear Physycs B (Proc. Suppl.), 219-220 (2011), 0920-5632, 2011.

26. Y. Klopot, Armen Oganesian, Oleg Teryaev, Anomaly, quark-hadron duality and transition form factors, 11-я международная "Байкальская Школа по Физике Элементарных Частиц и Астрофизике", Иркутский Государственный Университет и Объединенный Институт Ядерных Исследований (Дубна), Большие Коты, Россия, 2011.

27. Коробов В.И., Antiprotonic Helium Spectroscopy. Toward better than 10 digit precision, 2012. COMBINED ANALYSIS OF PROCESSES PION-PION -- > PION-PION, K-antiK, ETA_ETA AND J/PSI DECAYS AND PARAMETERS OF SCALAR MESONS, XXI International Baldin Seminar on High Energy Physics Problems, JINR, Dubna, Russia,

28. E.A.Kuraev, M.K.Volkov, Tau lepton decays and peripheral processes in the framework of the NJL model, CMS Workshop "Perspectives on Physics and on CMS at Very High Luminosity, HL-LHC", CMS Collaboration, Алушта, Украина, 1-11, -, 2012.

29. E.A.Kuraev, M.K.Volkov, Tau lepton decays and peripheral processes in the framework of the NJL model, CMS Workshop "Perspectives on Physics and on CMS at Very High Luminosity, HL-LHC", CMS Collaboration, Алушта, Украина, 1-11, 2012.

30. Лашкевич В.И., Соловцова О.П., Новый подход к учету поправок на массу мишени в структурных функциях нуклона, 2077-8708, Гомельский научный семинар по теоретической физике, ГГУ, Гомель, Беларусь, 38-42, УО «Гомельский государственный университет им. Ф. Скорины», Проблемы физики, математики и техники, 2, 7, 2077-8708, Проблемы физики, математики и техники. – 2011.– № 2(7), С. 38-42., 2011.

31. E. Leader, A.V. Sidorov, D.B. Stamenov, Importance of Fragmentation Functions in Determining Polarized Parton Densities., The 20-th INTERNATIONAL SYMPOSIUM on Spin Physics (SPIN2012),, JINR, Dubna, Дубна, Россия, 1-4, to be published, 2012.

32. E. Leader, A.V. Sidorov, D.B. Stamenov, The role of semi inclusive DIS data in determining polarized PDFs.,ISSN 1742-658819-th International Spin Physics Symposium, September 27 - October 02 (2010), Juelich, Germany, 1-6, Издано в J.Phys.Conf.Ser.295:012054, 2011.

33. E. Leader, A.V. Sidorov, D.B. Stamenov, THE STRANGE QUARK POLARIZATION PUZZLE, XIVth International Workshop onHigh Energy Spin Physics, JINR, Dubna, Russia, 139-144, Издательский отдел ОИЯИ, XIV рабочее совещпние по физике спина при высоких энеогиях. E1,2-2012-9, 2012.

34. A.V.Nesterenko, The effects due to hadronization in the inclusive tau lepton decay, Eleventh Workshop on Nonperturbative Quantum Chromodynamics, Institut Astrophysique de Paris, Duke University, Brown University, Paris, France, 23, SLAC eConf, C1106064, 2011.

35. V.A Naumov., Neutrino velocity anomalies. A resolution without a revolution, Advances in Quantum Field Theory, JINR, Dubna, Russia, 2011.

36. H.-P. Pavel, QCD in terms of gauge invariant variables, 10th International Conference on Quark Confinement and the Hadron Spectrum, Technical University Munich, Munich, Germany, 2012.

37. Ю.В. Попов, С.А. Зайцев, С.И. Виницкий, J-матричный метод вычисления трёхчастичных кулоновских волновых функций и сечений физических процессов, Физика элементарных частиц и атомного ядра, ISSN:0367-2026, eISSN:1814-7445, Изд:ОИЯИ, 42, 5, 1311-1370, 2011.

38. O.V. Selyugin, Fiatures of high energy pp and pA elastic scattering at small t, The 5th APCTP-BLTP JINR Joint WorkshopFrontiers in Nuclear Physics at Dubna, JINR (Dubna), Dubna, Russia, 2011.

39. O.V. Selyugin, The size of the slope of the hadron spin-flip amplitude, XIVth International Workshop onHigh Energy Spin Physics, JINR, Dubna, Russia, 125-128, Proceedings, Dubna, 2012, pp. 125-128, 2011.

40. O.V. Selyugin, The structure of nucleons and the description of the electromagnetic form factors, The 20-th INTERNATIONAL SYMPOSIUM on Spin Physics (SPIN2012),, JINR, Dubna, Дубна, Россия, 2012.

41. O.V. Selyugin, Generalized hadron structure and elastic scattering, ADVANCED STUDIES INSTITUTE SYMMETRIES AND SPIN(SPIN-Praha-2012)Prague, July 1 - 8, 2012, Charls University, Praha, Chech Republic, 2012.

42. O.V. Selyugin, Fiatures of high energy pp and pA elastic scattering at small t, The 5th APCTP-BLTP JINR Joint WorkshopFrontiers in Nuclear Physics at Dubna, JINR (Dubna), Dubna, Russia, 2011.

43. D.V. Shirkov, O.P. Solovtsova, O.V. Teryaev, Perturbative and nonperturbative QCD to the Bjorken sum rule up to four loops, The XXth International WorkshopHigh Energy Physics and Quantum Field Theory (QFTHEP`2011), НИИЯФ МГУ, Сочи, Россия, 1-7, SISSA, PoS QFTHEP2011, 1824-8039, 2011.

44. Yu.S.Surovtsev, P.Bydzovsky, R.Kaminski, V.E.Lyubovitskij, M.Nagy, 120, Dubna, JINR, 2012, Book of Abstracts of the XX1 International Baldin Seminar on High Energy Physics Problems "Relativistic Nuclear Physics and Quantum Chromodynamics" (Dubna, Russia,

September 10--15, 2012), ISBN 978-5-9530-0341-4, 2012.

45. Yu.S.Surovtsev, P.Bydzovsky, R.Kaminski, V.E.Lyubovitskij, M.Nagy Parameters of scalar resonances from the combined analysis of data on processes pion-pion -- > pion-pion, K-antiK, eta-eta and J/psi decays, International Conference "Hadron Structure and QCD: from LOW to HIGH energies", , Gatchina, Russia,, 2012.

46. Yu.S. Surovtsev, P. Bydzovsky, R. Kaminski, M. Nagy, The f_2- and rho_3-Mesons in Multi-Channel Pion-Pion Scattering, 244-250, JINR, Relativistic Nuclear Physics and Quantum Chromodynamics: Proc. of the XX Intern. Baldin Seminar on High Energy Physics Problems (Dubna, Russia, October 4-9, 2010), I, ISBN (vol.I): 978-5-9530-0308-7, 2011.

47. Yu.S.Surovtsev, P.Bydzovsky, T.Gutsche, R.Kaminski, V.E.Lyubovitskij, M.Nagy, Parameters of scalar resonances from the combined analysis of pion-pion scattering and coupled-channel data, Poster at the Internatuonal Workshop "MESON'2010" (Krakow, Poland, 31 May - 5 June 2012), 2012.

48. Yu.S.Surovtsev, P.Bydzovsky, T.Gutsche, V.E.Lyubovitskij, R.Kaminski, M.Nagy,Parameters of scalar resonances from the combined analysis of pi-pi scattering and \ coupled-channel data,12th International Workshop on Meson Production, Properties and Interaction, , KRAKÓW, POLAND, 09036, Published online: 6 December 2012 DOI: http://dx.doi.org/10.1051/epjconf/20123709036; Eds. A. Wro\'nska, R. Skibi\'nski, C. Guaraldo, St. Kistryn and H. Stroeher, EPJ Web of Conferences, 37, 2012.